

The dynamics of ontogenescence: Modelling age trajectories of feto-infant mortality

Jonas Schöley

Thesis submitted to
University of Southern Denmark

in partial fulfillment for the award of the degree of

DOCTOR OF PHILOSOPHY

Faculty of Health Sciences
Department of Public Health
Interdisciplinary Centre on Population Dynamics

Odense, Denmark

June 2020

Academic Advisors

Professor **James W. Vaupel**, Ph.D.

Interdisciplinary Centre on Population Dynamics
University of Southern Denmark

Associate Professor **James Oeppen**, M.A.

Interdisciplinary Centre on Population Dynamics
University of Southern Denmark

Professor **Rune Lindahl-Jacobsen**, Ph.D.

Interdisciplinary Centre on Population Dynamics
University of Southern Denmark

Assessment Committee

Professor **Michel Guillot**, Ph.D.

Department of Sociology & Population Studies Center
University of Pennsylvania

Professor **Laust Hvas Mortensen**, Ph.D.

Department of Public Health
University of Copenhagen

Professor **Jesper Lier Boldsen**, Ph.D.

Institute of Forensic Medicine
University of Southern Denmark

Dedicated to Hans Richter

Contents

Preface	i
English summary	ii
Dansk resumé	iv
List of manuscripts	vi
I Thesis summary	1
II A parametric family of hazard trajectories for infant mortality	29
III The impact of population heterogeneity on the age trajectory of neonatal mortality	63
IV The gestational age pattern of feto-infant mortality	91

Preface

My maternal grandfather was the optometrist in a small village close to what used to be the international border separating east and west Germany. Long retired, his home-office still looks very much like I remember it from my childhood days. Amongst his library of books, one can find old medical scales, a human skull, geological samples, ancient arrow tips found in the field, a star chart, a lunar globe, a microscope, and other instruments which would not look out of place in a reimagination of Victorian-era science. His scientific ambitions, however, remained unfulfilled. In the “German Democratic Republic” a person’s aptitude for science was not the most important requirement for the *permission* to engage in doctoral studies. Opa, your ongoing curiosity has been an inspiration to me. I dedicate this thesis to you – but not without thanking Grandmother as well – Oma, wasn’t it you who paid the rent while Opa was studying for his diploma?

The academic ambitions of one person tend to affect the whole family. I’ve finished this thesis during the Corona pandemic, at home with my wife Anja and my son Linus. Anja, not only did you allow me to write under rather unusual circumstances, but you’ve also given me perspective whenever I needed it, i.e., constantly; and so did you Linus: you’ve grown faster than my thesis and having you was the best decision I’ve ever made. Also, going through an elaborate good-night ritual with you Linus was a welcome distraction during the final writing stage.

Jim, you’ve recruited me into the Ph.D. program, set me up with a big research question, and gave me the freedom not only to approach the topic on my own but also to do so while being with my family. For all that, I thank you. The range of research and teaching activities I was allowed to engage in have given me the experience I would have never gained under a more restrictive supervisor.

I thank my co-supervisors Jim Oeppen and Rune Lindahl-Jacobsen for their support and for always promptly commenting on the drafts I sent them.

I thank Roland Rau, who taught me the joy of programming; Frans Willekens and Trifon Missov, who prompted me to start my Ph.D. journey; Steffi, who was a fantastic room-mate; Catalina, with whom I’ve had such honest conversations; Marius, who made everything look so easy; Rita, who selflessly helped me out; Anthony, who more than once shared his wisdom with me; Tim, who gave me plenty opportunities to build a research profile; Ilya, with whom I engaged in incredibly productive procrastination; my ThinkPad, which has been a reliable tool for the last five years; all my friends from EDSD, with whom I spent an incredible time in Warsaw; and my parents, who never questioned the path I’ve taken.

English summary

Even before our lives begin, we are on an escape trajectory from death. It has been estimated that out of 100 conceptions around 66 do not survive until the clinical recognition of pregnancy. The risk of in-utero death then declines until the third trimester, yet for some, the struggle of labor acts as a barrier of entry to life with most infant deaths in the U.S. nowadays occurring within the first seven days following birth. From there on, survival prospects improve continuously until the onset of adolescence.

The pattern of declining death rates before maturity has been observed all across nature, and, as the mirror image of the senescent increase in mortality later in life, the phenomenon has been coined *ontogenescence*.

What drives ontogenescence? Despite its potentially deep evolutionary roots, there are three more immediate explanations: 1) *acquired robustness* due to continued growth and development of the fetus and infant, 2) *mortality selection* leading to declining death rates on the cohort level as those with the highest individual risk of death tend to die early, and 3) *transitional timing*, meaning the clustering of risky transitions early in life.

This thesis aims to separate the three explanations by defining measurements for each and applying them to detailed data on fetal and infant survival for the United States. I contribute to the demographic study of age trajectories of mortality by proposing and validating a general family of hazard models for infant mortality, connecting this family to frailty and shock theory, explicitly testing the mortality selection hypothesis by considering the observed distribution of risk among neonates and presenting the phenomenon of the “birth hump” in the context of mortality over the age of gestation.

In the first paper, it is shown that many of the parametric models commonly used to describe the age trajectory of infant mortality are part of a class of probability distributions I call the power-exponential hazard family. I demonstrate that the family can conveniently be fitted within the framework of Generalized Linear Models and provide evidence that the trajectory of infant mortality in the United States, measured over days of age, is extremely well captured by said hazard. Interpreted as a “frailty model”, the power-exponential hazard has a natural connection to the hypothesis of mortality selection, which I explore, while interpreted as the description of a “thinned Poisson process”, the hazard points towards the transitional timing hypothesis. In both cases, the component of acquired robustness is reflected in an individual level exponentially declining hazard with a “rate of ontogenescence” around one percent per day of age.

In paper two, the mortality selection hypothesis is put to the test by explicitly considering the level and shape of neonatal hazard trajectories across 252 mutually exclusive population strata. Surprisingly, despite mortality levels among a population of newborns spanning five orders of magnitude, I find no evidence for the age-trajectory of infant mortality being shaped by selective dropout. The reason for that lies within a remarkable mortality convergence of extremely frail newborns towards the population average: Hazard trajectories in the days following birth are strikingly non-proportional as survival prospects among even the most vulnerable newborns improve drastically once the first day of life has passed.

Having cast doubt on the selection hypothesis, I consider the transitional shock of birth in greater detail. A natural timescale for studying the effect of labor on the survival of a cohort is the age of gestation measured in weeks since the last menses of the mother. Unlike chronological age, the gestational time scale allows for existence before infancy, thereby making it possible to study birth as a transition. On the aggregate level, this transition appears as a “hump” in an otherwise exponentially declining hazard of death for a cohort of fetuses as we follow them on their way into life. I study this gestational age pattern across multiple populations with a particular focus on describing the phenomenon of the “birth hump”.

Dansk resumé

Allerede inden vores liv begynder, befinder vi os i en flugt fra døden. Det er blevet estimeret, at 66 ud af 100 undfangelser ikke når til den kliniske anerkendelse af graviditet. Risikoen for død i livmoderen falder derefter indtil tredje trimester, men for nogle fungerer arbejdskampen som en barriere for adgangen til livet med de fleste spædbørnsdødsfald i USA i dag, der forekommer inden for de første 7 dage efter fødslen. Derfra forbedres udsigterne til at overleve kontinuerligt indtil ungdomsårenes begyndelse.

Mønsteret med faldende dødsrater inden modenhed er blevet observeret overalt i naturen, og som et spejlbillede af den aldersbetingede stigning i dødelighed senere i livet, er fænomenet blevet betegnet *ontogenescence*.

Hvad driver ontogenescence? På trods af de potentielt dybe evolutionære rødder er der yderligere tre mere umiddelbare forklaringer: 1) *acquired robustness* på grund af fortsat vækst og udvikling af fosteret og spædbarnet, 2) *mortality selection* der fører til faldende dødsrater på cohorte-niveau, da dem med den højeste individuelle døds-risiko har tendens til at dø tidlige, og 3) *transitional timing* hvilket angiver klyngen af risikable overgange tidligt i livet.

Formålet med denne afhandling er at adskille de tre forklaringer ved at definere målinger for hver og at anvende dem med de detaljerede data om føtal- og spædbarnsoverlevelse, der er tilgængelige for USA. Jeg bidrager til den demografiske undersøgelse af aldersbaner omkring dødelighed ved at foreslå og validere en generel familie af hazard-modeller til spædbørnsdødelighed og ved at forbinde denne familie til *frailty* og *shock theory*. Og ved eksplisit at afprøve hypotesen til valg af dødelighed ved at overveje observeret fordeling af risiko blandt nyfødte og præsentation af fænomenet “birth hump” i sammenhæng med dødelighed i forhold til svangerskabsalderen.

I den første artikel vises det, at mange af de parametriske modeller, der ofte bruges til at beskrive aldersbanen for spædbørnsdødelighed, er en del af en klasse med sandsynlighedsfordelinger, jeg kalder *power-exponential hazard family*. Jeg demonstrerer, at familien bekvemt kan tilpasses inden for rammerne af *Generalized Linear Models* og give bevis for, at banen for spædbørnsdødelighed i USA, målt i alder i dage, er ekstremt godt beskrevet af den nævnte *hazard*. Tolket som en *frailty model* har *power-exponential hazard* en naturlig forbindelse til hypotesen om *mortality selection*, som jeg udforsker, mens den fortolkes som beskrivelsen af en *thinned Poisson process*, farepunkterne for *transitional timing* hypotese. I begge tilfælde afspejles komponenten i *acquired robustness* i et individuelt niveau eksponentielt faldende fare med en *rate of ontogenescence* omkring 1% pr. dag.

I anden artikel bliver hypotesen om *mortality selection* testet ved eksplisit at overveje niveauet og formen for neonatale *hazard trajectories* i 252 isolerede befolkningslag. Selvom dødelighedsniveauer blandt en population af nyfødte, der spænder over fem forskellige størrelsesordener, finder jeg overraskende nok ingen beviser for, at aldersbanen for spædbørnsdødelighed er formet af selektive frafald. Årsagen hertil ligger inden for en bemærkelsesværdig dødelighedskonvergens af ekstremt skrøbelige nyfødte over for befolkningsgennemsnittet: Farebaner i dagene efter fødslen er slænde ikke-proportionelle, da overlevelsudsigterne blandt de mest sårbare nyfødte forbedres drastisk, når den første dag i livet er overstået.

Efter at have rejst tvivl om selektionshypotesen betragter jeg *transitional shock* ved fødsel mere detaljeret. En naturlig tidsskala til undersøgelse af arbejdseffekten på en kohortes overlevelse er svangerskabsalderen målt i uger siden moderens sidste menstruation. I modsætning til kronologisk alder giver svangerskabets tidsskala mulighed for en eksistens før den tidlige barndom, hvilket gør det muligt at studere fødsel som en overgang. På det samlede niveau fremstår denne overgang som et “hump” i en ellers eksponentielt faldende fare for at dø før en kohorte af fostre, når vi følger dem på vej ind i livet. Jeg studerer dette svangerskabsaldersmønster på tværs af flere populationer med et specielt fokus på at beskrive fænomenet “birth hump”.

List of manuscripts

This thesis is based upon three papers:

- Paper 1: Schöley. *A parametric family of hazard trajectories for infant mortality.* Under review by Demographic Research.
- Paper 2: Schöley. *The impact of population heterogeneity on the age trajectory of neonatal mortality.* In preparation for submission to Demography.
- Paper 3: Schöley. *The gestational age pattern of feto-infant mortality.* Manuscript.

Other publications I contributed to over the course of my Ph.D. studies which are not included in the thesis:

- Schöley (2020). *The centered ternary balance scheme: A technique to visualize surfaces of unbalanced three part compositions.* Demographic Research. Forthcoming.
- Mattsson, Lindhart, Schöley, Friis-Hansen & Herrstedt (2019). *Patient self-testing of white blood cell count and differentiation: A study of feasibility and measurement performance in a population of Danish cancer patients.* European Journal of Cancer Care. DOI 10.1111/ecc.13189.
- Conde, Stärk, Colchero, da Silva, Schöley et al. (2019). *Data gaps and opportunities for comparative and conservation biology.* PNAS. DOI 10.1073/pnas.1816367116.
- Schöley & Kashnitsky (2019). *But Why? Design choices made while creating “Regional population structures at a glance”.* New Generations in Demography. DOI 10.18267/pu.2019.fis.2302.6.
- Pascariu, Danko, Schöley, Rizzi (2018). *ungroup: An R package for efficient estimation of smooth distributions from coarsely binned data.* Journal of Open Source Software. DOI 10.21105/joss.00937.
- Schöley, Pascariu, Villavicencio, Danko (2017). *pash: An R package for pace-shape analysis of life-tables.* github.com/jschoeley/pash.
- Riffe, Schöley & Villavicencio (2017). *A unified framework of demographic time.* Genus. DOI 10.1186/s41118-017-0024-4.
- Schöley & Willekens (2017). *Visualizing compositional data on the Lexis surface.* Demographic Research. DOI 10.4054/DemRes.2017.36.21.
- Colchero et al. (2016). *The emergence of longevous populations.* PNAS. DOI 10.1073/pnas.1612191113.

Chapter I

Thesis summary

1. Introduction and research questions

Making our way into this world, we face a string of challenges: the conceptus must implant in the uterus and within the next nine months develop into a fetus strong enough to survive the struggle of birth and the separation from the mother's organism. Having made this transition, the newborn's resilience against death continues to be tested: it needs to learn to fight infections, to digest food, and to communicate basic needs while remaining entirely dependent on appropriate care. But each challenge overcome is rewarded by a better prospect of future survival. From conception until maturity, the hazard of death declines continuously – only disrupted by the event of birth. While human life has famously been characterized as a “*being-toward-death*” (Heidegger 1962), the situation initially is reversed: With each additional day of survival, the child moves further away from death.

The phenomenon of declining rates of mortality between conception and maturity has been coined “*ontogenescence*” (Levitis 2011)¹. This thesis concerns its quantification.

The changing risk of death early in life has been an object of study long before the phenomenon was honored with a neologism. Motivated by the prospect of formulating a “law” of mortality across the whole life, actuaries began to include data on death during infancy and childhood into their graduation efforts (Oppermann 1870; Thiele 1871; Wittstein and Bumsted 1883; Steffensen 1930; Harper 1936). The method of fitting curves to infant life tables was creatively employed by Bourgeois-Pichat (1951), who estimated the number of infant deaths due to exogenous versus endogenous causes from the age distribution of deaths alone. While the universality of the relationship uncovered by Bourgeois-Pichat has been questioned, his method continues to be used in historical demography contexts where data are scarce (Knodel and Kintner 1977; Wrigley et al. 1997; Galley and Woods 1999). Other demographic applications that rely on some measure of ontogenescence are life expectancy calculations, which require data on the exact timing of infant death within the first year of life (Chiang 1979), and the monitoring of the continued progress towards lower infant and childhood mortality, where knowledge about the age pattern of mortality acts as a check on data quality, aids in forecasting and provides insight into the specific groups that need to be targeted for further progress (Mahy 2003; Rao et al. 2011; Guillot et al. 2012; Mejía-Guevara et al. 2019).

The study of fetal and infant mortality over the so-called “gestational age,” the approximate time since conception, is a prime concern of perinatal epidemiology. Here the phenomenon of ontogenescence is twofold as it describes both the decline of the risk of fetal death throughout pregnancy and the decline in infant mortality following birth. The relevance of both gestational and chronological age when it comes to the survival prospects of a newborn child and the obstetric balancing act between stillbirth and neonatal death (Trudell et al. 2014) informs questions about the optimal timing of delivery and has lead to a range of indicators of perinatal mortality (Yudkin et al. 1987; Feldman 1992; Platt et al.

¹ The word is a combination of *ontogenesis*, i.e., the development of an individual organism, and *senescence*, i.e., deterioration with age.

2004; Joseph 2007). The importance of studying the measurement of ontogenescence is reflected in the extensive debates about the best way to estimate the changing risk of fetal death over the course of a pregnancy (Smith 2005; Joseph 2004; Joseph and Kramer 2017).

What drives ontogenescence?

The realization that ontogenescence occurs in many species has led to speculation regarding its evolutionary roots. Hamilton (1966) argued that the concentration of deaths early in life (or even before birth) is “advantageous” as it increases the time that the parents have to “replace” the lost offspring and decreases the parental resources spent on what ultimately will have been a failed attempt at reproduction. Various authors have refined this argument without, however, explaining why ontogenescence continues to be observed in some species long after the offspring becomes fully independent from the parents (Levitis 2011). A proposed evolutionary trade-off between the current rate of growth and the current survival of an organism solves this paradox: Juvenile organisms who invest in fast-growth momentarily worsen their survival chances with the prospect of increasing their adult survival once they have grown large (Chu et al. 2008).

Ontogenescence and the growth of an organism can, of course, be linked without invoking the theory of evolution. A striking example of size-dependent mortality is given with the palm tree *Euterpe globosa*: Out of 1,000 seeds, most will fail to germinate, and only one will have survived the ten years it takes to develop into a young tree. In order to mature, the young tree again has to beat the odds of 1000:1, but once aged 60 years, and grown to a height of 20 meters, mortality remains at an exceptionally low level (Valen 1975; discussed in Berrut et al. 2016). Levitis (2011) summarizes hypothesis linking an organism’s growth and maturity to its survival prospects under the term *acquired robustness*, a concept reflected in the parametric mortality models by Siler (1979)², Heligman and Pollard (1980)³ and Bourgeois-Pichat (1951)⁴.

Increasing robustness can hardly explain the drastic shift in the risk of death over the first hours and days of an infant’s life. Taking into account the event of birth itself leads to the *transitional timing* hypothesis, which states that risky physiological and environmental transitions tend to be concentrated early in life, thus increasing early mortality (Levitis 2011).

While the aforementioned hypotheses imply that not only cohorts but also individuals are subject to ontogenescence, this need not be the case when *mortality selection* is considered: Even if mortality for individuals is constant over age, one would observe an age-decline in aggregate death rates given heterogeneous mortality levels among population subgroups. Over time, the proportion of the group with lower mortality would rise, thus lowering population average mortality. Here we connect back to demographic theory, which offers

² “While the most common use of this decreasing hazard would be to account for the hazard due to immaturity, it can also be used [...] for other hazards to which an animal adjusts successfully” Siler (1979).

³ “C measures the rate of mortality decline in childhood (the rate at which a child adapts to its environment” Heligman and Pollard (1980).

⁴ He proposed an expression linking his mortality curve to infant growth curves (via Woods 2009, p. 40f.).

methods of quantifying this discrepancy between individual and population-level mortality (Vaupel et al. 1979; Vaupel 1983; Vaupel and Canudas-Romo 2002; Vaupel 2010a; Steinsaltz and Wachter 2006; Missov and Vaupel 2015).

This thesis concerns the description of patterns of ontogenescence in fetal and infant populations and the potential for learning about the mechanisms of ontogenescence from population data alone. Following the terminology in Levitis (2011), I will investigate ontogenescence in a large sample of births, infant and fetal deaths registered in the U.S. from 1989–2012 under three different premises: *acquired robustness*, *mortality selection*, and *transitional timing*. To that end, the following research questions are addressed:

- *Paper 1. A parametric family of hazard trajectories for infant mortality:* Is it possible to find a parsimonious, well-fitting, parametric survival model that provides a mechanistic explanation for the phenomenon of ontogenescence rather than just a phenomenological description of the data?
- *Paper 2. The impact of population heterogeneity on the age trajectory of neonatal mortality:* Does mortality selection explain the rapid decline in mortality following birth?
- *Paper 3. The gestational age pattern of feto-infant mortality:* How does the risk of death evolve over gestational age in a cohort of fetuses transitioning into infancy?

2. Data and Methods

In this section, I give an overview of the data and the techniques used in the three papers constituting the core of this thesis. Readers familiar with survival analysis, mixture distributions, mortality selection, and frailty models may safely skip the methods description.

2.1 United States registry data on births, fetal and infant death

The vital statistics of the United States is perhaps the most extensive publicly available data source on age trajectories of fetal and infant mortality. The “Birth Cohort Linked Birth-Infant Death Data Files” (National Center for Health Statistics 2016a) contain most of the information available on a newborn’s birth certificate and, where applicable, the death certificate starting with birth cohort 1983, whereas the “Fetal Death Data Files” (National Center for Health Statistics 2016b) cover all fetal deaths registered in the United States since 1982.

By making use of this registry data, I can compare patterns of ontogenescence across diverse population strata, and, for example, inquire how conditions upon birth affect the subsequent mortality trajectory, or how the event of birth itself shapes ontogenescence. The public availability of the data furthermore ensures the reproducibility of my results. Despite these advantages, it is clear that the topic of ontogenescence is much broader than any single data source can capture. As stated in the first paper, and equally true for the thesis as a whole:

“[. . .] without further study, the results of this paper can not be generalized to populations other than present-day U.S. infants. While similar results for countries with similar overall levels of infant mortality (implying a similar level of development) are to be expected, it would be foolish to assume the same age pattern of infant mortality in pre-20th century populations or present populations suffering under a crisis: Historically the age-pattern of infant mortality was very much shaped by the interaction of seasonality effects, improper substitutes for breastfeeding, and deadly infectious diseases (Knodel and Kintner 1977; Huck 1995), factors which have lost relevance in the U.S. over the course of the 20th century. Likewise, an analysis of 21st century U.S. infant mortality yields little insight into the characteristics of infant death in parts of the world suffering from humanitarian crises and violent conflicts.”

2.2 Basic survival analysis

The numerous techniques employed in this thesis are unified under the label “Survival Analysis.” On a technical level, survival analysis is nothing but inference about the distribution of a non-negative random variable X . Interpreting this variable as the “time

until death” transforms simple probability calculations into statements about the survival of a cohort.

The function

$$S(x) = \text{P}(X > x)$$

is commonly called a *survival curve* and gives the probability of survival to age x . Conversely

$$F(x) = 1 - S(x) = \text{P}(X \leq x)$$

is the *cumulative distribution function* of lifetimes interpreted as the probability of dying before or at age x . The *density of deaths* is given by the derivative

$$f(x) = \frac{dF(x)}{dx} = \frac{-dS(x)}{dx}.$$

Much of this thesis concerns inference about the *hazard of death*, a.k.a. force of mortality, hazard function, hazard rate, defined as

$$h(x) = \frac{f(x)}{S(x)} = \lim_{\delta \rightarrow 0} \frac{\text{P}(x < X \leq x + \delta | X > x)}{\delta}.$$

The hazard function operationalizes a particularly intriguing concept: the instantaneous risk of death among the survivors of a cohort at age x . Changes in this risk of death over age qualify the type of “aging” a cohort experiences. If $h(x)$ increases, the cohort experiences *senescence*, for decreasing $h(x)$, we use the term *ontogenesence*, and “constant hazards” indicate the absence of aging in a statistical sense. It is the exponential increase of $h(x)$ with age that generations of demographers, actuaries and evolutionary biologists attempted to explain; it is $h(x)$ that forms the basis for one of the most widely employed biostatistical models (Cox 1972); it is $h(x)$ that Vaupel et al. (1979) builds his theory of frailty upon; it is $h(x)$ which cuts across 200 years of statistical methodology from the cohort life table to the Poisson regression and the piecewise exponential survival model (Holford 1980), and it is $h(x)$ which, by definition, reflects the *dynamics of ontogenesence* in a cohort of fetuses or infants (Levitis 2011).

The hazard function and the survival curve are connected via the identity

$$S(x) = \exp \left(- \int_0^x h(s) ds \right),$$

where

$$H(x) = \int_0^x h(s) ds$$

is known as the *cumulative hazard*.

2.3 Censoring and truncation

In the study of fetal and infant mortality, the age at death x , by definition, is incompletely observed. Infants cease to be part of the sample once they survived to their first birthday, and the study of fetal death ends either with birth or with induced abortion. In both cases, observations on the age at death are *right censored*. In the infant case, the censoring is deterministic, i.e., it occurs 366 days following birth due to the study design, whereas in the fetal case, the censoring is random as both the timing of birth and of induced abortion vary from case to case. A usual assumption in survival analysis is that the age at censoring and the age at death are independent. This is clearly not the case when it comes to the study of fetal death given that fetal conditions that increase the risk of fetal death, such as congenital malformations, also increase the risk of induced abortion and early delivery. In the third paper, I discuss some of the implications of this dependence.

Interval censoring describes a situation where the age at death is only known to fall within an interval $[x, x + \delta]$, but the exact timing is unknown. To a degree, this is always the case as the ages are only ever known up to some unit of observation, being it weeks, as in fetal mortality, or days/hours, as in infant mortality. In paper three, where the intervals are rather large relative to the total time under investigation, I take special care to account for this type of censoring.

A death is said to be *left truncated* if it occurred before some truncation age, and, as a consequence, one neither learns about the death nor about the existence of the deceased subject. Left truncation is a significant challenge for the study of fetal mortality. In the U.S., most states only require the reporting of a fetal death starting at 20 weeks of gestation. This puts a lower limit on the left truncation age. In practice, however, under-registration of fetal deaths also occurs at later ages of gestation and depends on the individual circumstances of the pregnancy. Therefore the left truncation age is not well defined. In my analysis of fetal mortality, I only consider fetuses that survived until 24 weeks of gestation, limiting the influence of left truncation due to under-registration and of right censoring due to induced abortions on the estimates of fetal mortality.

2.4 Estimation of survival quantities

Cohort life tables

A century-old tool of demographic analysis, the *cohort life table* may be regarded as one of the first big data methods in statistics as it reduces the survival of millions of individuals down to a manageable number of cells in a table. With tens of millions of individual-level observations on fetuses and infants, such an aggregation continues to be useful, and hence I employ the cohort life table method before fitting the actual models of interest to the now aggregated data. Estimates of mortality and survival derived from the cohort life table serve as a baseline against which I compare the fit of other models.

The construction of a cohort life table starts with N individuals at age $x = 0$, which are followed for ω units of time. The total follow up time is cut into $j = 1, \dots, J$ age intervals $[x_j, x_j + n_j)$ of width n_j and a tally is kept on the number of observed deaths D_j and

censorings C_j within an age interval j , the total population at risk N_j at the start of the age interval, and the total person-time lived over the age interval E_j . To calculate E_j , one can either use available information on the exact timing of censorings and deaths within an age group or assume that events occur uniformly over the interval (mid-point assumption).

Availability of D_j and E_j allows to calculate an *occurrence-exposure rate* $m_j = \frac{D_j}{E_j}$ giving the expected number of deaths in interval j per unit of person-time exposure. For a cohort of newborns, m_j is the life table estimate of the age-specific infant mortality rate.

By defining a piecewise constant hazard function $h(x) = m_j$ if $x_j \leq x < x_{j+1}$ the cohort life table connects back to the basic survival analysis framework outlined in section 2.2. As a constant hazard function is characteristic of the exponential distribution, this model is also referred to as piecewise exponential. It is assumed that the ages at death within each age interval j follow an exponential distribution with rate parameter $h(x_j)$. See Holford (1980) for the equivalence of piecewise-defined occurrence-exposure rates and a piecewise exponential survival model.

The simple cohort life table may of course be stratified over any number of subpopulations simply by adding an index k to the aforementioned quantities, e.g., $m_{jk} = \frac{D_{jk}}{E_{jk}}$ for the mortality rate in stratum k . This way one can capture “observed” heterogeneity in the risk of death between population strata. Note that the stratum specific mortality rates give rise to the overall mortality rate m_j via the weighted average $m_j = \sum_k m_{jk} \pi_{jk}$, where $\pi_{jk} = \frac{E_{jk}}{\sum_k E_{jk}}$ is the stratum specific relative exposure. This relationship can be exploited to estimate the effect of mortality selection on changes in m_j over age.

The analysis of mortality during the period surrounding birth in paper three necessitates the distinction between fetal, neonatal, and postneonatal populations. To that end, the cohort life table can be extended such that it takes into account, for each age group j , the number of transitions between the fetal, neonate, post neonate states, the number of survivors and population exposures in each state, and the number of deaths from each state. This is called an *increment-decrement life table* as the risk population in state s , N_j^s , is allowed to increase as well as decrease.

While the calculation of (increment-decrement) cohort life tables from individual-level data is straightforward, it may become quite a memory-intensive operation if the usual approach of episode splitting is employed whereby the size of the whole data set of individual-level observations is multiplied by the number of age groups j before the aggregation takes place. To speed up the aggregation process, I have implemented an algorithm that does not necessitate any episode splitting: `nosplit` aggregates individual level transitions between multiple states into state-specific transition counts, risk populations, and exposure times allowing for arbitrarily defined age groups. The code is reproduced in the appendix of the third paper.

Survival analysis via Poisson regression

For estimation and inference, one may assume that the age and stratum specific fetal and infant death counts D_{jk} given exposure times E_{jk} are realizations from the Poisson distribution

$$D_{jk} \sim \text{Pois}(\lambda_{jk} E_{jk}).$$

The rate parameter λ_{jk} can be linked to a vector of co-variates \mathbf{x}'_{jk} via

$$\lambda_{jk} = \exp(\beta_0 + \mathbf{x}'_{jk} \boldsymbol{\beta}),$$

ensuring that the product $\lambda_{jk} E_{jk}$ is positive. As shown by Holford (1980), λ_{jk} can be interpreted as the value for a stratum specific piecewise constant hazard function $h_k(x) = \lambda_j$ where $x_{jk} \leq x < x_{j+1,k}$. This equivalence allows one to estimate the survival quantities introduced in section 2.2 by employing the flexible and efficient apparatus of Generalized Linear Models (GLMs, McCullagh and Nelder 1989), specifically, log-linear Poisson regression. Advantages of the GLM approach to survival analysis are a stable estimation of parameters without the need to specify starting values, the ability to work with pre-aggregated data which vastly reduces memory requirements and computation time, and the easy inclusion of random effects terms which I employ in paper two to estimate neonatal life tables and hazard trajectories for extremely sparse subpopulations which may only consist of a few dozen observations.

The Poisson approach to survival analysis predicts a piecewise constant hazard function over age with one parameter per age group. However, large parts of demography are formulated in the continuous language of calculus and require the hazard to be differentiable. As demonstrated by, e.g., Aitkin and Clayton (1980) and Currie (2016), common continuous survival distributions such as the Weibull or the Gompertz may fit within the Poisson regression framework via the inclusion of transformed age variables into the regression equation. In the first paper, I show how this technique can be extended to fit a wide range of parametric distributions to infant life tables.

In the case of fetal mortality, the age intervals are wide enough as to warrant the use of an interval censored likelihood function when fitting a parametric survival model to the data. Details on this procedure are given in the appendix of paper three.

2.5 Heterogeneity, mortality selection, and Frailty models

The “mortality selection” hypothesis for ontogenescence may be formalized by considering the survival curve for a cohort of infants stratified into κ subpopulations $k = 1, \dots, \kappa$,

$$S(x) = \text{P}(X > x) = \sum_k S(x|k) \text{P}(K = k),$$

where $\text{P}(K = k)$ is the probability to be born into stratum k , and $S(x|k)$ is the corresponding conditional survival curve.

Given that $S(x|k)$ varies between strata the composition of the cohort along subgroups changes according to

$$P(k|X > x) = \frac{S(x|k)P(k)}{S(x)}.$$

Over age, the proportion of subgroups with good survival prospects will increase at the expense of subgroups with a worse outlook. This compositional shift affects the average mortality observed in the population, which will be less and less influenced by the high-mortality subgroups, due to their selective disappearance. This mechanism is evident in the age derivative of the population hazard

$$h(x) = \sum_k h(x|k)P(k|X > x),$$

which yields the Vaupel-Zhang equality (Vaupel and Zhang 2010),

$$\dot{\bar{h}}(x) = \bar{h}(x) - \sigma_h^2(x),$$

stating that cohort level ontogenescence, $\dot{\bar{h}}(x)$, i.e., the derivative in the hazard over age as observed for a cohort of infants, is a function of the average ontogenescence observed over subgroups of the cohort, $\bar{h}(x)$, compounded by the variance of hazard levels within the cohort, $\sigma_h^2(x)$. Even in the complete absence of ontogenescence on the individual or subpopulation level, one will observe it on the cohort level as long as the risk of death is heterogeneous.

In the second paper, the expressions above are employed to, for the first time, test the mortality selection hypothesis of infant mortality on the grounds of actually observed population heterogeneity. See Vaupel and Yashin (1983), Vaupel and Zhang (2010), Vaupel and Missov (2014), and the appendix of paper two for details and proofs regarding the stated equalities.

If $h(x)$ is only observed on the population level, one may estimate the level of population heterogeneity and mortality selection via a “frailty model.” Vaupel et al. (1979) assume that each individual in a cohort is subjected to a hazard of death given by

$$h(x|z) = zh_0(x),$$

where $h_0(x)$ is the *baseline hazard* common to all cohort members, and z is the realization of a continuous, strictly positive random variable Z called *frailty* and thus varies between individuals.

Integrating with respect to age yields the conditional cumulative hazard

$$H(x|z) = zH_0(x),$$

and corresponding conditional survival function

$$S(x|z) = e^{-zH_0(x)}.$$

This conditional survival function can be linked to the survival of the complete cohort by integrating over the density of z

$$S(x) = \int_0^\infty e^{-zH_0(x)} f_Z(z) dz,$$

which, as noted by Hougaard (1984), is the Laplace transform of Z evaluated at $H_0(x)$,

$$S(x) = \mathcal{L}_Z\{H_0(x)\},$$

a connection, which simplifies the construction of frailty models from distributions with known Laplace transform.

Placing distributional assumptions on H_0 and f_Z then yield an expression for $S(x)$, and, via the survival identities, $h(x)$, which can be fitted to the cohort level data. Different measures of population heterogeneity may then be derived from that fit, such as the variance of Z .

Applied to the study of ontogenescence, frailty models allow quantifying the amount of heterogeneity and mortality selection needed to reproduce the observed cohort level survival pattern, given that the distributional assumptions are correct. In papers one and two, I evaluate the capability of frailty models to reproduce the observed pattern of ontogenescence in cohorts of U.S. born infants and discuss the implications of that fit for the mortality selection hypothesis.

2.6 Decomposition analysis

The Kitagawa decomposition (Kitagawa 1955) allows expressing differences between weighted averages in terms of differences in the weights and differences in the weighted component. In paper two, I use this method to assess how changes in the composition of a cohort of newborns over age impact the cohorts age trajectory of mortality. Additionally, I show how changes in the distribution of mortality risk over the first few days following birth can be decomposed into a mortality convergence and a mortality selection component. In paper three, Kitagawa's method allows me to show how the hazard trajectory of a cohort of fetuses, as they pass into infancy, is shaped by compositional shifts.

The Horiuchi decomposition (Horiuchi et al. 2008) is employed in paper three to assess how the shape of the feto-infant hazard trajectory impacts the observed differences in the probability of fetal and infant death between different population strata.

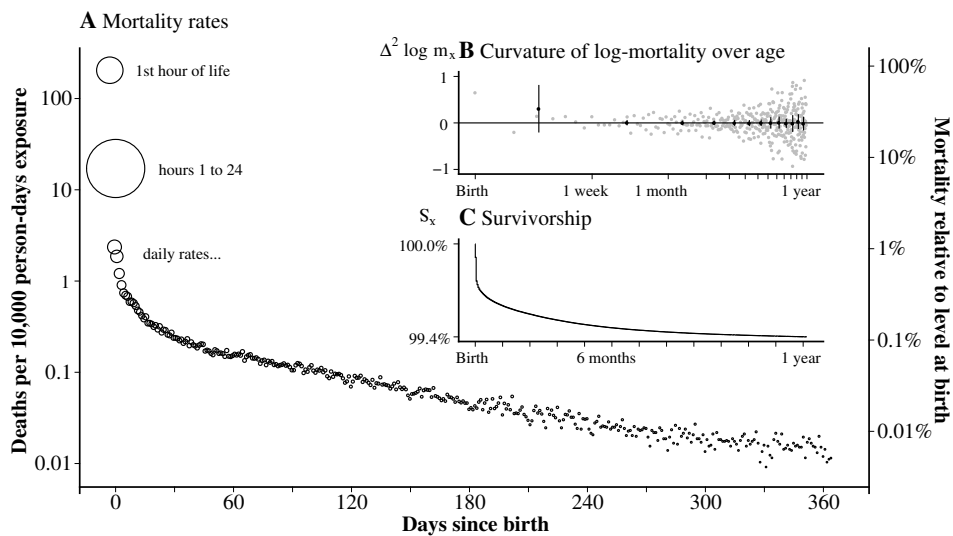
3. Summary of results

3.1 Paper 1: A parametric family of hazard trajectories for infant mortality

Parametric probability distributions tell origin stories: The Weibull distribution of lifetimes arises whenever the failing of a “weakest link” in a chain of connected systems determines the eventual timing of death, a similar derivation holds for the Gompertz distribution, a favorite among Demographers and a standard model for human senescence. Mortality selection arises as a consequence of mixtures of distributions, such as the Gamma-Gompertz, which fits the apparent mortality deceleration at older ages, and whenever the hazard function of a distribution is represented as a sum of terms, competing risks are supposedly at work.

Three potential origins of ontogenescence are “mortality selection,” “acquired robustness,” and the “shock of birth.” Is it possible to find a probability distribution for the age at infant death reflecting these origin stories while fitting the data well?

Figure 1: Ontogenescence, as observed in the U.S. 2005-2009 birth cohort.



During the five years from 2005 to 2009, 25,143,288 births have been registered in the United States, resulting in 162,541 infant deaths. When plotted over day-of-age, the life table mortality rate estimates for this quinquennial birth cohort reveal a rather simple pattern: The relative rate of infant mortality decline is highest right after birth and over the first month of life approaches a constant value of around 0.5-1 percent per additional day of life (Figure 1). Clearly, any probability distribution fitting such a pattern must feature a hazard function that smoothly transitions into an exponential tail. A convenient choice for the rapidly declining early part of the curve is a power of age as this leads to a

hazard which may easily be fitted to counts of deaths within the framework of Generalized Linear Models.

The power-exponential hazard family of probability distributions reflects the aforementioned features of age-specific infant mortality. Its hazard function is given by

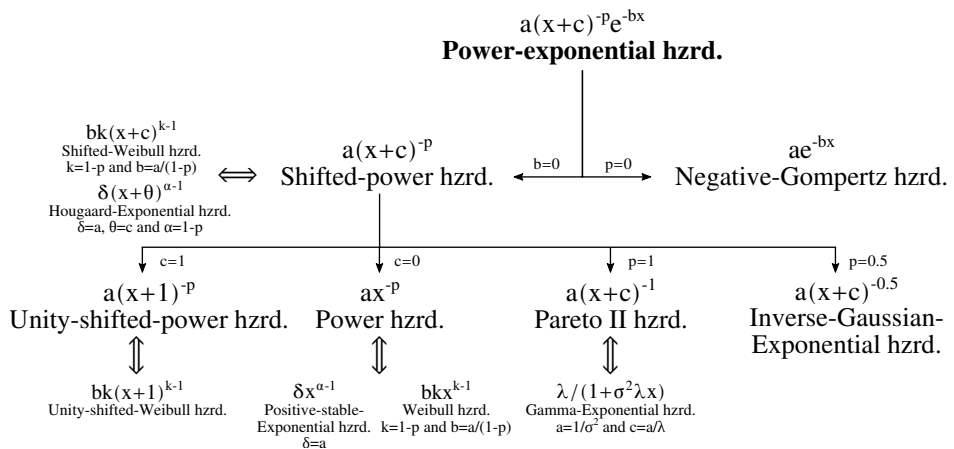
$$h(x) = a(x + c)^{-p} e^{-bx},$$

with corresponding survival function

$$S_{PE}(x) = e^{ab^{p-1} e^{bc} (\Gamma[1-p, b(c+x)] - \Gamma[1-p, bc])},$$

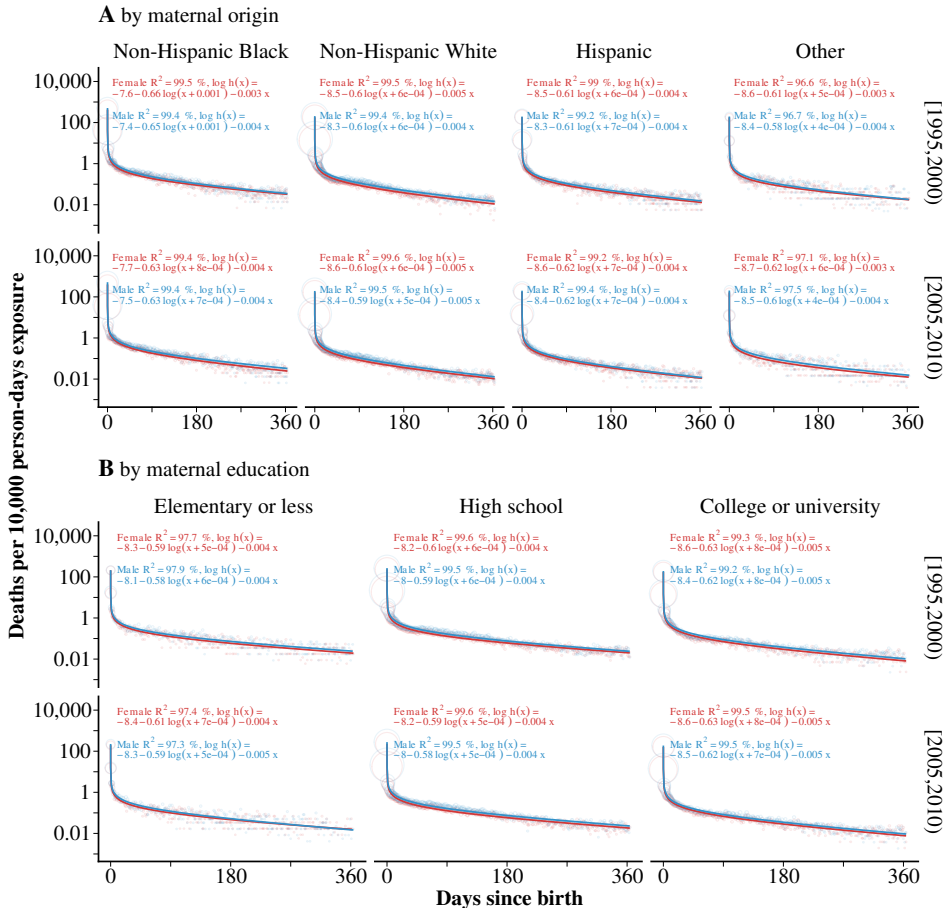
The family contains many of the distributions that have previously been used in the survival analysis of infant mortality (Figure 2).

Figure 2: The power-exponential hazard family of probability distributions generalizes many distributions commonly used to model infant mortality and permits multiple frailty interpretations.



Testing the power-exponential hazard across a range of populations, I find strong evidence for the exponential tail behavior (Figure 3). Such a pattern is consistent with the hypothesis of mortality selection under acquired robustness on the individual level: While mortality rates for each individual decline exponentially over time due to the continuous adaptation of the organisms to the extrauterine environment, the *level* of mortality varies proportionally between individuals according to some “frailty” distribution. Thus, the initial power-law decline in the risk of death shortly after birth is a population-level phenomenon induced by the early death of extremely frail newborns, while the effect of acquired robustness on the individual level can be seen in the more homogeneous population of infants that survived into the postneonatal period. Simply put, the steeper the mortality decline over the first few days of life as measured by the power parameter p , the more heterogeneous the population of infants is at birth.

Figure 3: Patterns of ontogenesence are well described by the power-exponential family of probability distributions.



Under such a frailty interpretation, most of the observed cohort level mortality decline over infancy is due to mortality selection. While the hazard of death for the 2005–2009 cohort of newborns in the U.S. drops by a factor of more than 10,000 over the first year of life, individual members of the cohort are only expected to experience a decline in mortality by a factor of 4.3 over the same period. Such a high degree of mortality selection would necessitate an extremely skewed frailty distribution. But what could this distribution be? The power-exponential hazard is closely related to the so-called Hougaard-Gompertz frailty model, a multiplicative frailty model with an extremely flexible mixing distribution that smoothly interpolates among the Gamma, the inverse Gaussian and the positive-stable (in increasing order of positive skewness). Both the power-exponential hazard model and the Hougaard-Gompertz model fit the data equally well and lead to similar conclusions regarding the role of mortality selection.

However, mortality selection is not the only “origin story” of the power-exponential hazard. Another possible interpretation is that of the rate function of a non-homogeneous thinned Poisson process where each infant upon birth is subjected to “shocks” to their health arriving with rate $\lambda(x)$, each shock leading to death with a probability $p(x)$. In such a model, the shocks would plausibly be associated with the event of birth, and thus the corresponding arrival rate is expected to fall off quickly over the first few days of life – as modeled with the power-law term – whereas the probability of a shock leading to death depends on the maturity of the infant and declines more gradually with age – as modeled with the rather slow exponential decline. Under this interpretation, the power-exponential hazard connects directly to the transitional timing and the acquired robustness hypotheses of ontogenescence.

With the power-exponential hazard, I have proposed a family of probability distributions that

1. exhibits a close and parsimonious fit to the observed age trajectory of infant mortality in the current-day U.S. across a range of sub-populations,
2. can be fit within the extremely well-developed apparatus of Generalized Linear Models,
3. generalizes a wide range of probability distributions commonly used to fit infant mortality,
4. features parameters with a clear phenomenological interpretation (e.g., the hazard of death around birth, the hazard’s elasticity around birth, the rate of postneonatal mortality decline), and
5. can be interpreted as either a frailty model or a shock model with a corresponding change in the meaning of the parameters.

The last point is crucial concerning any investigation into ontogenescence: Quite different assumptions about the process giving rise to the hazard of death can lead to statistically indistinguishable lifetime distributions. While this indeterminacy has long been realized in the context of modeling old-age mortality (Beard 1959; Yashin et al. 1994), I demonstrated that the very same problem applies to the study of ontogenescence and its central concepts of mortality selection, acquired robustness and the timing of transitional shocks.

Thus, deciding which process actually gives rise to the remarkably regular and simple pattern of ontogenescence requires different inference strategies. This realization is the origin of papers two and three of this thesis, the former facing the mortality selection hypothesis head-on by estimating the observed distribution of risk in a population of newborns and the latter addressing the transitional timing hypothesis by looking what “mark” the event of birth leaves on a cohort as they transition into life.

3.2 Paper 2: The impact of population heterogeneity on the age trajectory of neonatal mortality

How much of the observed population-level decline in the hazard of death throughout the first month of life arises from individual-level ontogenescence, and how much is due to population heterogeneity? The answer to this question directly addresses the *mortality selection* hypothesis of ontogenesis, and it requires some knowledge about the individuals in a population.

The hazard of death for an individual at some point in time is always a latent variable, as it can not be measured directly. A person is either alive or dead, and the risk to move from one state to the other must be estimated via some model. One ingenious approach to this modeling problem is to assume some functional form for the individual level hazard trajectory and some family of distributions for the distribution of risks between individuals and then, putting the strong assumptions to work, infer the most likely individual level hazard trajectory from the observed distribution of lifetimes in a cohort. These frailty models allow maximum inference from minimal data via a multitude of assumptions, which has lead to some skepticism regarding their usefulness regarding the test of hypothesis involving population heterogeneity:

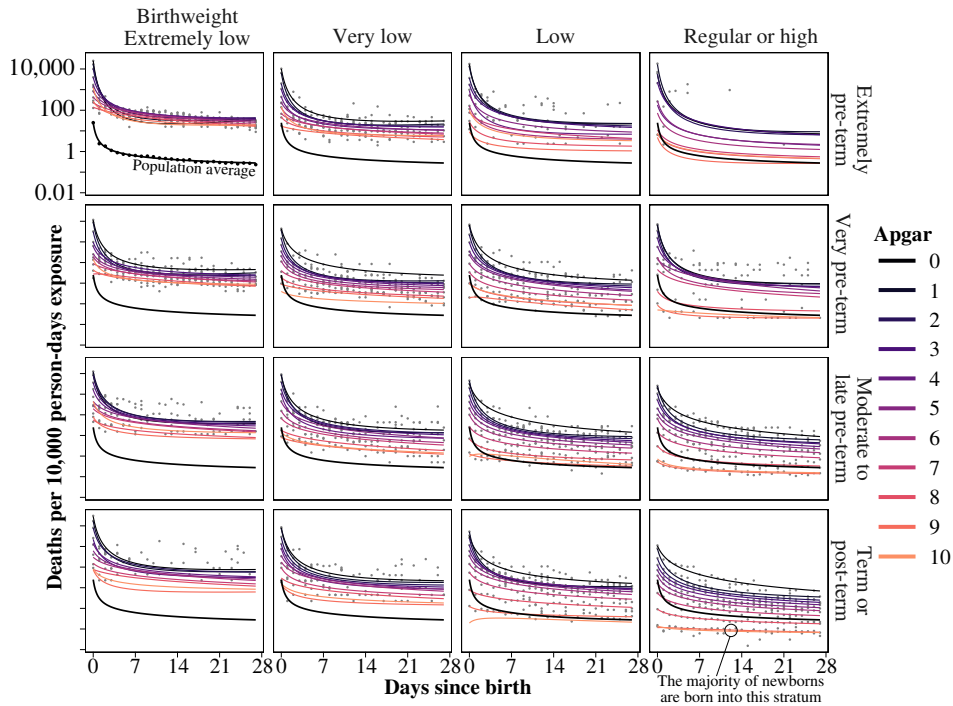
“Individual random effects (frailties), whenever detected, can be made to disappear by elementary model transformation. In consequence, unless we are to take some model form as unassailable, beyond challenge and carved in stone, and if we are to understand the term ‘frailty’ as referring to individual random effects, then frailty models have no value.” (O’Quigley and Stare 2002)

“The statistician who chooses $S(t|X, Z)$ will conclude that heterogeneity is clearly evident. The statistician who decides for $S(t|X)$ will come to the opposite conclusion.” (Wienke 2011)

To circumvent the identifiability issues, I turn the frailty modeling framework on its head: Instead of asking how much unobserved heterogeneity would be needed to produce an observed population hazard, I ask how much of the curvature of the observed population hazard is explained by the heterogeneity we can actually observe in the population.

Observable characteristics of a neonate’s “frailty” are the Apgar score, the birthweight, and the gestation at birth. For each of the 252 population strata defined by the intersection of the three frailty dimensions, I estimate the heterogeneity in level and shape of ontogenescence.

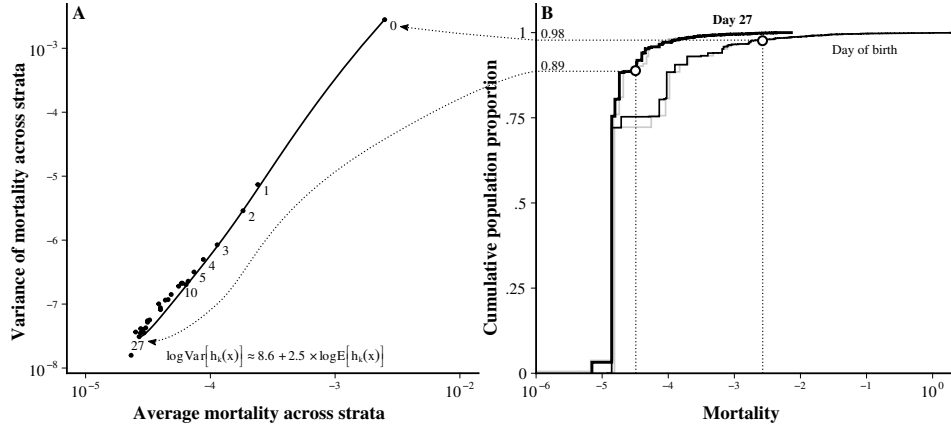
Figure 4: Estimated neonatal hazard trajectories for the 2008–2012 U.S. birth cohort by condition upon birth.



As shown in Figure 4, the variation in the risk of death is substantial between strata, with the hazard rates at birth stretching across more than five orders of magnitude. Most of the newborns, however, are part of a stratum with a nearly flat mortality trajectory. Thus, the cohort-level pattern of ontogenescence does not reflect the reality for the majority of the cohort's members. Early in life, the distribution of hazards is indeed so skewed, that the average loses any meaning as a measure of centrality: Upon birth, 98 percent of infants are part of a stratum with below-average mortality. Over the next 27 days of life, the risk distribution compresses somewhat but remains positively skewed (Figure 5B).

I find a near-perfect log-linear correlation between the average risk of death and the between stratum mortality variance (Figure 5A). Such a correlation is characteristic for the family of Hougaard probability distributions, which, in paper one, I suggested as the basis for a frailty model for infant mortality.

Figure 5: Mean-variance relationship over day-of-age (A) and distribution function (B) of the mortality/hazard rates in the 2008–2012 U.S. birth cohort across observed frailty strata. The points in (A) mark mean and variance of the life table mortality rates, whereas the smooth line is predicted from a model fit to stratum specific mortality. In plot (B), the gray lines refer to the life table estimates and the black lines to the model predictions.



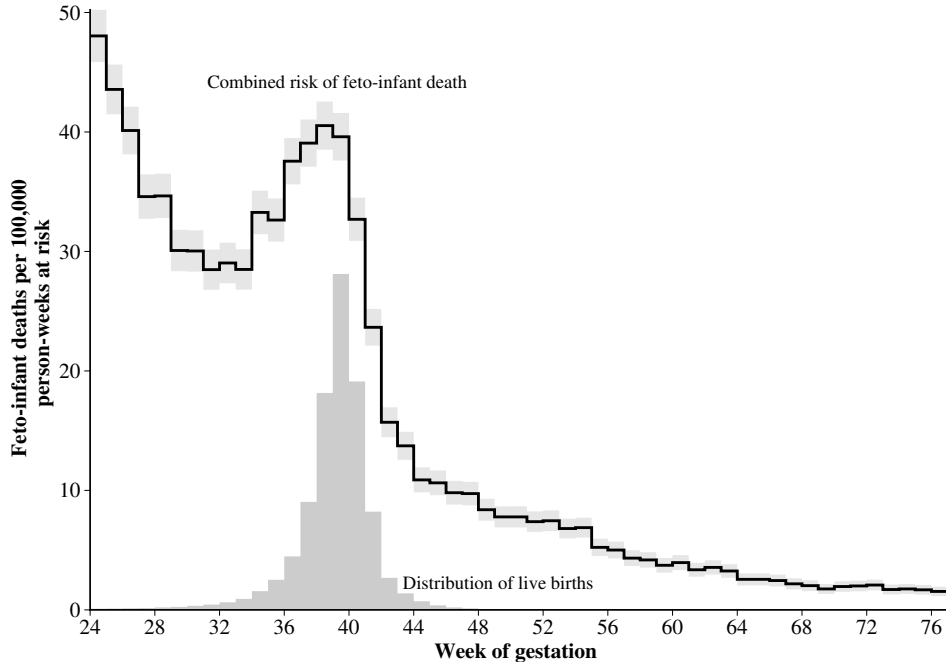
Perhaps surprisingly, the data at hand does not support the *mortality selection* hypothesis for ontogenescence. As shown by extensive analysis of the 252 population strata, mortality selection neither explains the day-to-day change in life table mortality rates, nor the slope of the population hazard trajectory, nor the compression of the distribution of mortality over age, nor the convergence between average mortality low frailty mortality. While selective dropout plays some role in all of these phenomena, they are mostly explained by converging stratum-specific mortality and hazard rates over the neonatal period.

3.3 Paper 3: The gestational age pattern of feto-infant mortality

Given the lack of evidence for the mortality selection hypothesis of ontogenescence, I turn my attention towards the role of the birth transition. As any transition divides time into “before” and “after,” it seems ignorant only to consider mortality *following* birth, so instead, I investigate “the gestational age pattern of feto-infant mortality.”

The decline in the risk of death does not start with birth. In fact, by the time a child is born, the risk of death may be orders of magnitude smaller than the hazard shortly after conception. Consequently, Levitis (2011) defines ontogenescence as “*a population-level phenomenon in which the death rate of each cohort tends to decrease with increasing age between conception and maturity.*”

Figure 6: The feto-infant mortality trajectory over gestational age for a U.S. cohort of fetuses conceived in 2009, surviving until fetal viability and followed over the next 52 weeks. The risk of feto-infant death among the survivors of the cohort declines exponentially over age interrupted only by a “birth hump.”



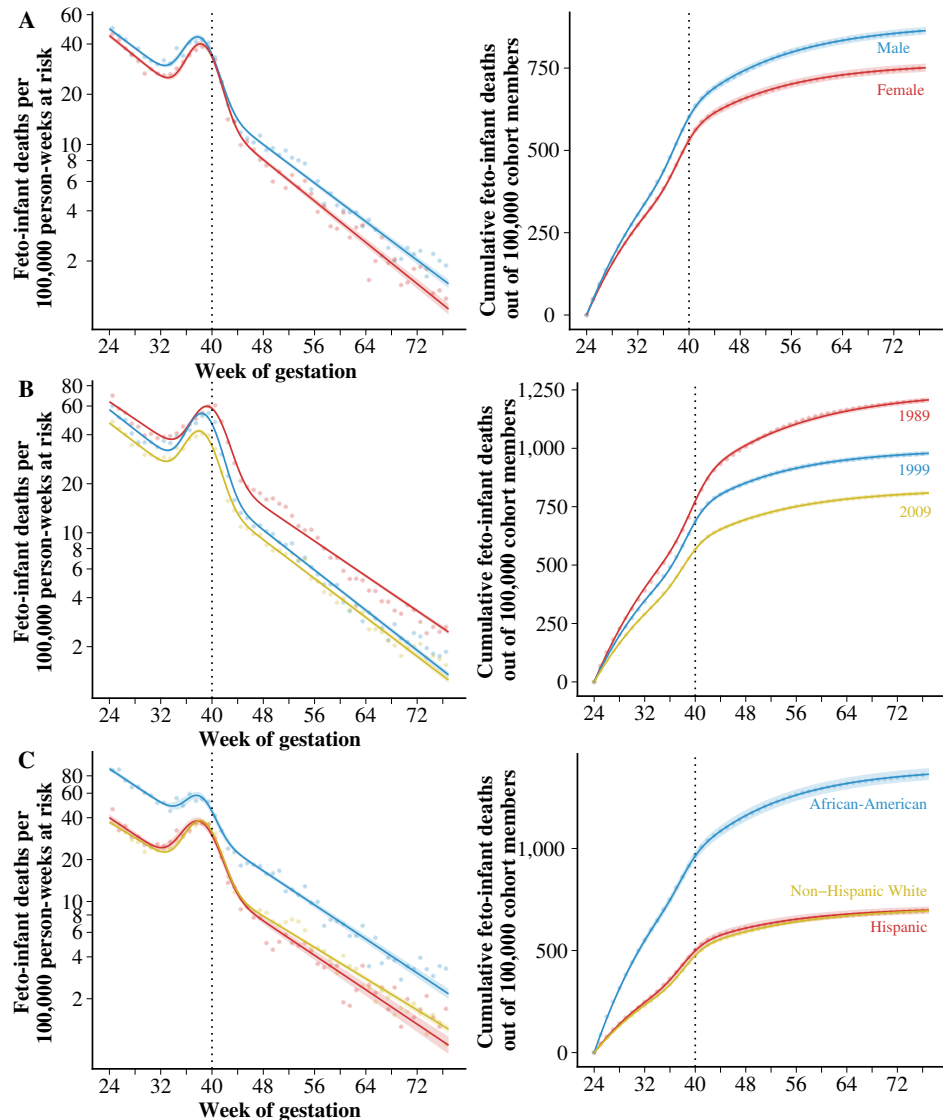
Discussing the *transitional timing hypothesis* Levitis (2011) argues that physiological, environmental, and genetic transitions bring about a momentary increase in the risk of death as the organism adapts to the new situation. While he proceeds to focus on the timing of genetic transcriptions, a much more visible transition is that of birth.

How does the risk of death evolve in a cohort of fetuses transitioning into infancy?

Using U.S. data on fetuses conceived in 2009, I found that the transition of birth leaves a mark in the form of a “birth hump” on an otherwise exponentially declining gestational age trajectory of feto-infant mortality (Figure 6). By performing a decomposition analysis, I show how the distinct mortality pattern arises from an interplay of

1. U-shaped mortality among the fetal population,
2. the lessening burden of prematurity with advancing age at delivery,
3. the changing likelihood of live birth over the length of a pregnancy, and
4. the sudden decline in mortality in the days following birth.

Figure 7: Age trajectories of feto-infant survival A) by sex for the U.S. conception cohort 2009, B) by U.S. conception cohort, C) by maternal origin for the U.S. conception cohort 2009. Fitted (lines) versus life table estimates (points).



As a summary measure of feto-infant mortality over gestational age, I propose the probability of a fetus alive at week 24 to die within the next year. While the incidence of adverse pregnancy outcomes as measured by this indicator has fallen from 1989 to 1999, and again to 2009, any lower limit is far away: out of 100,000 fetuses of African-American origin, one in 71–75 die within one year of fetal viability, roughly twice as many as observed in cohorts of Hispanic or White origin (Figure 7C). Pronounced differences in the magnitude of the “birth hump,” as it turns out, have only a minor effect on the probability of post-viability survival.

As an indicator of adverse pregnancy outcomes, the probability of death within a year following fetal viability is quite sensitive and, unlike the well-known perinatal mortality rate, embedded in a survival analysis framework. As concluded in paper 3:

“Would pregnancy come with the same warnings as prescription drugs, feto-infant death past the age of fetal viability would have to be labeled as a ‘common’ side effect according to the standards put forth in CIOMS Working Groups III and V (1999).”

4. Conclusion

The *demography of ontogenescence* presented in the preceding chapters is heavily inspired by the Vaupelian approach to the study of senescence. A central tenet of this school is the inquiry into simple mechanisms that can give rise to universally observed age patterns of mortality. I have shown that the mechanistic models which have been proposed for the study of mortality trajectories in old age – exponentially changing individual-level resilience towards death under mortality selection or varying rates of insults – also provide a close fit to infant life tables and lead to defendable, if somewhat simplistic, interpretations for ontogenescence.

Sir David Cox, when prompted by a reviewer to give a mechanistic explanation for his now eponymous survival model, cautions the reader against searching for physical processes in the mathematical formulation of survival models as “*The wide variety of possibilities serves to emphasize the difficulty of inferring an underlying mechanism indirectly from failure times alone rather than from direct study of the controlling physical processes*” (Cox 1972).

That different models describe the same phenomenon equally well is neither surprising nor in itself a problem but rather the starting point of empirical research. However, the constructs used in mechanistic formulations for the age trajectory of mortality have proved to be hard to operationalize: How do, e.g., individual-level hazards, frailty, and not further specified shocks to vitality connect to the world of observables?

The operationalization of the “frailty” concept in the context of ontogenescence among humans is a major contribution of this thesis. Separating a birth cohort of infants into hundreds of frailty levels based upon the condition at delivery allowed me to make progress on the initially posed question: “What drives ontogenescence?”

Despite decades of speculation to the contrary, mortality selection seems to play little role in explaining ontogenescence. As stated in the second paper:

“The average age trajectory of neonatal mortality is highly influenced by a small group of frail newborns and does not reflect the rather flat age effect estimated for the healthy majority of the birth cohort. While the risk decline over the first day of life is substantially influenced by mortality selection, the overall age trajectory is better explained by the convergence of high-risk towards low-risk population strata.”

In the introduction, I noted that physiological changes of the infant, i.e., *acquired robustness*, is an implausible explanation for the drastic change in the risk of death over the first few days of life. However, for the majority of the birth cohort – those born without complications – this drastic change is not observed. Instead, the hazard of death almost immediately after birth settles into a log-linear decline of less than one percent per day of age, a rate that is comparable to ongoing physiological development. Future research into the *acquired robustness* hypothesis thus may start with an inquiry into ontogenescence among the subset of those born healthy.

By tracing ontogenescence across the feto-infant gap, I contribute the phenomenon of a “birth hump” to the literature, which has implications for Levitis *transitional timing* hypothesis. As summarised by Levitis (2011) “*transcriptional, developmental and environmental transitions are dangerous, and these are concentrated early in life,*” thus cohort mortality should initially decline. The “birth hump,” however, is the existence proof for a transition that causes the average hazard for a cohort to increase. Further development of the *transitional timing* hypothesis may, therefore, distinguish between well-delineated physiological stages in the life-cycle of a developing organism, where each stage transition is expected to be accompanied by a “hump” shaped increase in cohort level mortality, and transitions which exhibit a monotonically declining incidence over time, such as the genetic mechanisms discussed by Levitis.

Hundreds of hypotheses on the origin of senescence are listed in Medvedev (1990). I doubt that future progress on the mirror phenomenon of ontogenescence will come from the construction of a similarly elaborate web of ideas. A better approach may be to confront a few broad explanations with a wide array of data. Levitis (2011) formulated five general hypotheses. Three have been considered in this thesis, one of which has been rejected on empirical grounds. Four more to go...

References

- M. Aitkin and D. Clayton. The fitting of exponential, Weibull and extreme value distributions to complex censored survival data using GLIM. *Journal of the Royal Statistical Society C*, 29(2):156–163, 1980. doi:10.2307/2986301.
- R. E. Beard. Appendix: Note on some mathematical mortality models. In G. E. W. Wolstenholme and M. O'Connor, editors, *The Lifespan of Animals. Ciba Foundation Colloquium on Ageing*, pages 802–811, Boston, 1959. Little, Brown. doi:10.1002/9780470715253.app1.
- S. Berrut, V. Pouillard, P. Richmond, and B. M. Roehner. Deciphering infant mortality. *Physica A: Statistical Mechanics and its Applications*, 463:400–426, 2016. doi:10.1016/j.physa.2016.07.031.
- J. Bourgeois-Pichat. La mesure de la mortalité infantile. II. les causes de décès. *Population*, 6(3):459–480, 1951. doi:10.2307/1523958.
- C. L. Chiang. Life table and mortality analysis. Technical report, 1979. URL <http://www.who.int/iris/handle/10665/62916>.
- C. Y. C. Chu, H.-K. Chien, and R. D. Lee. Explaining the optimality of u-shaped age-specific mortality. *Theoretical Population Biology*, 73(2):171–180, 2008. doi:10.1016/j.tpb.2007.11.005.
- CIOMS Working Groups III and V. Guidelines for preparing core clinical-safety information on drugs. Technical report, Geneva, 1999.
- D. R. Cox. Regression models and life-tables. *Journal of the Royal Statistical Society B*, 34(2):187–220, 1972. doi:10.1007/978-1-4612-4380-9_37.
- I. D. Currie. On fitting generalized linear and non-linear models of mortality. *Scandinavian Actuarial Journal*, 2016(4):356–383, 2016. doi:10.1080/03461238.2014.928230.
- G. B. Feldman. Prospective risk of stillbirth. *Obstetrics and Gynecology*, 79(4):547–553, 1992.
- C. Galley and R. Woods. On the distribution of deaths during the first year of life. *Population*, 11(1):35–60, 1999.
- M. Guillot, P. Gerland, F. Pelletier, and A. Saabneh. Child mortality estimation: a global overview of infant and child mortality age patterns in light of new empirical data. *PLoS medicine*, 9(8), 2012. doi:10.1371/journal.pmed.1001299.
- W. D. Hamilton. The moulding of senescence by natural selection. *Journal of Theoretical Biology*, 12(1):12–45, 1966. doi:10.1016/0022-5193(66)90184-6.
- F. S. Harper. An actuarial study of infant mortality. *Scandinavian Actuarial Journal*, 1936(3-4):234–270, 1936. doi:10.1080/03461238.1936.10405113.
- M. Heidegger. *Being and Time*. Harper and Row, New York, 1962. Translated from the German "Sein und Zeit".

- L. Heligman and J. H. Pollard. The age pattern of mortality. *Journal of the Institute of Actuaries*, 107(1):49–80, 1980. doi:10.1017/s0020268100040257.
- T. R. Holford. The analysis of rates and of survivorship using log-linear models. *Biometrics*, 36(2):299–305, 1980. doi:10.2307/2529982.
- S. Horiuchi, J. R. Wilmoth, and S. D. Pletcher. A decomposition method based on a model of continuous change. *Demography*, 45(4):785–801, 2008. doi:10.1353/dem.0.0033.
- P. Hougaard. Life table methods for heterogeneous populations: Distributions describing the heterogeneity. *Biometrika*, 71(1):75–83, 1984. doi:10.1093/biomet/71.1.75.
- P. Huck. Infant mortality and living standards of English workers during the industrial revolution. *The Journal of Economic History*, 55(3):528–550, 1995. doi:10.1017/s0022050700041620.
- K. Joseph. Incidence-based measures of birth, growth restriction, and death can free perinatal epidemiology from erroneous concepts of risk. *Journal of Clinical Epidemiology*, 57(9):889–897, 2004. doi:10.1016/j.jclinepi.2003.11.018.
- K. S. Joseph. Theory of obstetrics: An epidemiologic framework for justifying medically indicated early delivery. *BMC Pregnancy and Childbirth*, 7(1), 2007. doi:10.1186/1471-2393-7-4.
- K. S. Joseph and M. S. Kramer. The fetuses-at-risk approach: survival analysis from a fetal perspective. *Acta Obstetricia et Gynecologica Scandinavica*, 97(4):454–465, 2017. doi:10.1111/aogs.13194.
- E. M. Kitagawa. Components of a difference between two rates. *Journal of the American Statistical Association*, 50(272):1168–1194, 1955. doi:10.1080/01621459.1955.10501299.
- J. Knodel and H. Kintner. The impact of breast feeding patterns on the biometric analysis of infant mortality. *Demography*, 14(4):391–409, 1977. doi:10.2307/2060586.
- D. A. Levitis. Before senescence: the evolutionary demography of ontogenesis. *Proceedings of the Royal Society B*, 278(1707):801–809, 2011. doi:10.1098/rspb.2010.2190.
- M. Mahy. *Childhood mortality in the developing world: a review of evidence from the Demographic and Health Surveys*. Number 4 in DHS Comparative Reports. MEASURE DHS+, Calverton, Maryland, 2003.
- P. McCullagh and J. A. Nelder. *Generalized Linear Models*. Monographs on Statistics and Applied Probability. CRC Press, New York, 2nd edition, 1989. ISBN 9780412317606.
- Z. A. Medvedev. An attempt at a rational classification of theories of ageing. *Biological Reviews*, 65(3):375–398, 1990. doi:10.1111/j.1469-185x.1990.tb01428.x.
- I. Mejía-Guevara, W. Zuo, E. Bendavid, N. Li, and S. Tuljapurkar. Age distribution, trends, and forecasts of under-5 mortality in 31 sub-Saharan African countries: A modeling study. *PLoS medicine*, 16(3):e1002757, 2019. doi:10.1371/journal.pmed.1002757.

- T. I. Missov and J. W. Vaupel. Mortality implications of mortality plateaus. *SIAM Review*, 57(1):61–70, 2015. doi:10.1137/130912992.
- National Center for Health Statistics. Birth cohort linked birth-infant death data files (U.S. data), 2016a. URL ftp://ftp.cdc.gov/pub/Health_Statistics/NCHS/Datasets/DVS/cohortlinkedus/.
- National Center for Health Statistics. Fetal death data files (U.S. data), 2016b. URL ftp://ftp.cdc.gov/pub/Health_Statistics/NCHS/Datasets/DVS/fetaldeathus/.
- Oppermann. On the graduation of life tables, with special application to the rate of mortality in infancy and childhood. *Insurance Record*, page 42, Feb. 1870. Minutes from a meeting in the Institute of Actuaries.
- J. O’Quigley and J. Stare. Proportional hazards models with frailties and random effects. *Statistics in Medicine*, 21:3219–3233, 2002. doi:10.1002/sim.1259.
- R. W. Platt, K. S. Joseph, C. V. Ananth, J. Grondines, M. Abrahamowicz, and M. S. Kramer. A proportional hazards model with time-dependent covariates and time-varying effects for analysis of fetal and infant death. *American Journal of Epidemiology*, 160(3):199–206, 2004. doi:10.1093/aje/kwh201.
- C. Rao, T. Adair, and Y. Kinfu. Using historical vital statistics to predict the distribution of under-five mortality by cause. *Clinical medicine & research*, 9(2):66–74, Oct. 2011. doi:10.3121/cmr.2010.959.
- W. Siler. A competing-risk model for animal mortality. *Ecology*, 60(4):750–757, 1979. doi:10.2307/1936612.
- G. C. S. Smith. Estimating risks of perinatal death. *American Journal of Obstetrics and Gynecology*, 192(1):17–22, 2005. doi:10.1016/j.ajog.2004.08.014.
- J. F. Steffensen. Infantile mortality from an actuarial point of view. *Scandinavian Actuarial Journal*, 1930(2):272–286, 1930. doi:10.1080/03461238.1930.10416902.
- D. R. Steinsaltz and K. W. Wachter. Understanding mortality rate deceleration and heterogeneity. *Mathematical Population Studies*, 13(1):19–37, 2006. doi:10.1080/08898480500452117.
- T. N. Thiele. On a mathematical formula to express the rate of mortality throughout the whole of life, tested by a series of observations made use of by the Danish Life Insurance Company of 1871. *Journal of the Institute of Actuaries*, 16(5):313–329, 1871. doi:10.1017/s2046167400043688.
- A. S. Trudell, M. G. Tuuli, A. G. Cahill, G. A. Macones, and A. O. Odibo. Balancing the risks of stillbirth and neonatal death in the early preterm small-for-gestational-age fetus. *American Journal of Obstetrics and Gynecology*, 211(3):295–e1, 2014. doi:10.1016/j.ajog.2014.04.021.
- L. V. Valen. Life, death, and energy of a tree. *Biotropica*, 7(4):259, 1975. doi:10.2307/2989738.

- J. W. Vaupel and V. Canudas-Romo. Decomposing demographic change into direct vs. compositional components. *Demographic Research*, 7(1):1–14, 2002. doi:10.4054/DemRes.2002.7.1.
- J. W. Vaupel and T. I. Missov. Unobserved population heterogeneity: A review of formal relationships. *Demographic Research*, 31(1):659–686, 2014. doi:10.4054/DemRes.2014.31.22.
- J. W. Vaupel and A. I. Yashin. The deviant dynamics of death in heterogeneous populations. Technical report, Laxenburg, Austria, 1983. URL <http://user.demogr.mpg.de/jwv/pdf/IIASA-83-001.pdf>.
- J. W. Vaupel and Z. Zhang. Attrition in heterogeneous cohorts. *Demographic Research*, 23(26):737–748, 2010. doi:10.4054/DemRes.2010.23.26.
- J. W. Vaupel, K. G. Manton, and E. Stallard. The impact of heterogeneity in individual frailty on the dynamics of mortality. *Demography*, 16(3):439–54, 1979. doi:10.2307/2061224.
- A. Wienke. *Frailty Models in Survival Analysis*. Biostatistics Series. Chapman and Hall, Boca Raton, 2011. ISBN 978-1-4200-7388-1. doi:10.1111/j.1541-0420.2012.01769.x.
- T. Wittstein and D. A. Bumsted. The mathematical law of mortality. *Journal of the Institute of Actuaries and Assurance Magazine*, 24(3):153–173, 1883. doi:10.1017/s0020268100006260.
- R. Woods. *Death before Birth*. Oxford University Press, 2009. ISBN 978–0–19–954275–8. doi:10.1093/acprof:oso/9780199542758.001.0001.
- E. A. Wrigley, R. S. Davies, R. S. Schofield, and J. E. Oeppen. *English population history from family reconstitution 1580–1837*. Cambridge Studies in Population, Economy and Society in Past Time. Cambridge University Press, Cambridge, UK, 1997. ISBN 978-0-521-02238-5. doi:10.2307/4052836.
- A. I. Yashin, J. W. Vaupel, and I. A. Iachine. A duality in aging: the equivalence of mortality models based on radically different concepts. *Mechanisms of Ageing and Development*, 74(1-2):1–14, 1994. doi:10.1016/0047-6374(94)90094-9.
- P. L. Yudkin, L. Wood, and C. W. G. Redman. Risk of unexplained stillbirth at different gestational ages. *The Lancet*, 329(8543):1192–1194, 1987. doi:10.1016/S0140-6736(87)92154-4.

Chapter II

A parametric family of hazard trajectories for infant mortality

A parametric family of hazard trajectories for infant mortality

Jonas Schöley*

Abstract

Background While there is a consensus that the risk of death follows a Gompertz law over much of the adult age span, no such agreement exists about the parametric form of mortality at the very beginning of life with most literature on the topic suggesting either an exponential or various power-law expressions.

Objective I aim to identify a parsimonious, interpretable, and well-fitting model for the infant mortality age trajectory as observed in recent U.S. birth cohorts across a range of social and medical strata.

Results Age-specific infant mortality in the U.S. displays both power-law and exponential behavior and is better described by a product of those functions: a “power law with an exponential tail.” Across all infant populations under consideration, the age trajectory of mortality following birth is initially dominated by a power-law regime. Throughout infancy, it eventually approaches an exponential decline of less than a one percent reduction per additional day of age. The hazard of infant death varies in a highly non-proportional fashion by prematurity and the infant’s health upon birth.

Contribution The power-exponential hazard is a novel tool for the study of infant mortality being more parsimonious than smoothing-splines while providing interpretable parameters and an excellent fit over a range of diverse populations. The transition from a power-law dominated neonatal mortality schedule to an exponential post-neonatal hazard has not been noted before and suggests an underlying shock-recovery or mortality selection process.

*Interdisciplinary Centre on Population Dynamics, University of Southern Denmark. Correspondence: jschoeley@health.sdu.dk. During the writing of this article the author was a guest at the Max-Planck Institute for Demographic Research and funded by a grant from AXA Insurance.

1. Background

Since Benjamin Gompertz published his eponymous law of mortality for the adult ages, many suggestions were made for an expression of similar generality describing the age pattern of infant or childhood mortality. Perhaps the earliest attempt was published by Oppermann (1870; as stated by Thiele 1871) who proposed¹ $h(x) = ax^{-1/2} + b + cx^{1/2}$ for mortality prior to age 20. With a power law as the first term, this formula has the curious feature of predicting an infinite risk of death at the moment of birth, a property that reportedly was important to Oppermann though the reasons remain unclear (Steffensen 1930). One year later, Thiele (1871), motivated by the search for a mortality law covering the whole human life span, assumed $h(x) = ae^{-bx}$, the hazard of a negative-Gompertz distribution, for the changing risk of death before maturity. *These two expressions, a power-law and an exponential, constitute the functional basis for most parametric models of infant/childhood mortality employed thereafter.* Different power-law hazards have been used to describe the age pattern of infant mortality by Brillinger (1961), Choe (1981), de Beer and Janssen (2016), and Berrut et al. (2016); Gompertz-like exponential functions appeared as infant mortality terms in Siler (1979), Mode and Busby (1982), Rogers and Little (1994); and compositions of power- and exponential functions have been suggested by Wittstein and Bumsted (1883) and Heligman and Pollard (1980).

The mortality models above can be interpreted as describing an unspecified risk to which an infant adapts over time, resulting in a continuous decline in mortality as the child grows (as explicitly stated by Siler 1979; Heligman and Pollard 1980).² Levitis (2011) called this the “acquired robustness hypothesis.” A “competing-risks” explanation was proposed by Bourgeois-Pichat (1951), who hypothesized that the observed age pattern of mortality over the first year of life is the result of two separate processes: intrinsic mortality due to congenital disorders and extrinsic mortality due to accidents and maltreatment of the child. Bourgeois-Pichat noticed that the cumulative distribution of deaths during the post-neonatal period (> 1 month of age) is closely matched by a linear function of $\log_{10}(\text{days since birth} + 1)$ while neonatal deaths follow a different age trajectory. He then proposed that intrinsic and extrinsic mortality over age do not share the same functional form and that extrinsic mortality only starts to dominate over its intrinsic counterpart after the first month of life.

Some attempts have been made to express the parametric form of the infant hazard of death as a *frailty model* (Vaupel and Yashin 1983; Hougaard 1984; Vaupel and Yashin 1985). A valuable insight from these models is that in a population where individuals differ significantly in their risk of death the average mortality over age is determined not only by individual-level age effects but also by *mortality selection*, i.e., the changing composition of a cohort towards individuals with low frailty (Vaupel et al. 1979). It has been demonstrated that a *declining* infant mortality age trajectory may result from *constant* individual level hazards of different magnitudes (Vaupel and Yashin 1983, 1985). Hougaard (1984)

¹ Throughout the paper $h(x)$ denotes the force of mortality at age x .

² An exception is Oppermann (1870), who essentially proposed a competing risks model though the meaning Oppermann gave to the three components of his formula is unknown.

suggested that high mortality right after birth and the fast subsequent decline may be the result of substantial heterogeneity in individual frailties in the population of newborns.

In the presence of the ubiquitous semi-parametric Cox proportional hazards model (Cox 1972) and smoothing methods for count data such as penalized splines (Eilers and Marx 1996; Camarda et al. 2016) it may seem like an exercise in nostalgia to consider parametric hazard expressions as a basis for the analysis of the infant mortality age pattern. Nevertheless, a parametric treatment of deaths during the first year of life comes with unique advantages:

- 1) Successes in combating infant mortality over the past century made infant death an increasingly rare event in large parts of the world (World Health Organization 2006, 2015). The statistician thus is challenged to develop a methodology suited to inference from rare events, especially if the object of study is infant mortality over age, on the regional level, by season, in nations with a small population, by socio-economic group, by cause-of-death, or by any combination of those criteria. If correctly specified, parametric survival models alleviate the statistical challenge of small event counts. By imposing a tight structure on the distribution of life-times, one can gain insight from comparatively little data. Furthermore, a parametric specification of infant mortality expressed in terms of observable quantities (e.g., mortality at the day of birth, rate of post-neonatal mortality decline) facilitates the use of Bayesian methodology – a useful tool for working with sparse data – because informative prior distributions on the parameters are easily specified if the parameters are well understood.
- 2) Parametric models may allow insight into the mechanisms that determine the age distribution of infant deaths. This advantage is especially apparent with regard to the frailty model (Vaupel et al. 1979), which expresses the age-pattern of mortality on the population level as emerging from heterogeneous individual level hazards via selective mortality.
- 3) Information on the ages at death during infancy may only be available in broad age groups (e.g., birth to one day, one day to one week, one week to one month, months one to twelve). If the parametric form of the ages at death during the first year of life is known, this information can be used to graduate the grouped data. Demographers interested in a precise estimation of the “average age at death during infancy,” a relevant statistic for the construction of life tables, can make use of such graduation.

The advantages above depend on a parsimonious yet well-fitting expression of the age distribution of infant deaths. Validating such an expression requires a) data on the precise timing of each infant death in a birth cohort (ideally on a day-to-day basis); b) a cohort of infants large enough for a clear trend in the age trajectory of infant mortality rates to dominate over random variation; and c) data on multiple birth-cohorts, and subpopulations so that it is possible to check the generality of the parametric model. The individual-level data on millions of births and infant deaths provided by the National Center for Health

Statistics (2016) fit these requirements, and for this article, I confine the search for the shape of the hazard of infant death to the U.S. population.

After a brief description of the data, the methods, and the current day-to-day age pattern of infant mortality in the United States, I will present evidence for both power-law *and* exponential behavior of the age trajectory of infant death. Both types of models are then synthesized into a *power-exponential hazard*, a generalization of both the power law and negative-Gompertz hazards, whose fit is evaluated on life tables for various cohorts and subpopulations of U.S. infants. A discussion of the generative mechanisms which could give rise to a power-exponential hazard concludes the paper.

2. Data

The “NCHS Cohort Linked Birth – Infant Death Data Files” (National Center for Health Statistics 2016) contain a complete census of births and infant deaths on the territory of the United States³ and feature most fields present on the birth and infant death certificates. The size and detail of the data allow for the calculation of day-to-day infant life tables for various subpopulations.

I confine the analysis to the quinquennial birth cohorts 1995–1999 and 2005–2009 stratified by sex, prematurity, five-minute Apgar score (Apgar 1953), and social background of the mother. Those particular variables constitute major sources of heterogeneity in infant mortality along biological, medical, and social dimensions and are among the most reliably reported fields. In total, I analyze data on 277,004 infant deaths out of 40,727,055 births over the birth cohorts 1995–1999 and 2005–2009.

Female and male infant life tables are calculated for both birth cohorts, each life table stratified by either the five minute Apgar score (an ordinal measure of an infant’s vitality shortly after delivery discretized into three levels), prematurity (defined via the age of gestation upon delivery and discretized into four levels), mother’s education (three levels) or mother’s ethnicity (four levels). Those 56 life tables thus cover heterogeneity in the age trajectory of infant mortality across period, medical and social strata.

³ Available data on the overseas territories has been excluded due to compatibility issues.

3. Methods

To estimate the functional shape of infant mortality over the first year of life, I fit the power-exponential family of hazards to the day-to-day death counts and exposures for various populations of U.S. infants. Let $h(x)$ be the force of mortality (the hazard) at non-negative age x . The power-exponential family is given by the expression

$$h_{PE}(x) = a(x + c)^{-p} e^{-bx},$$

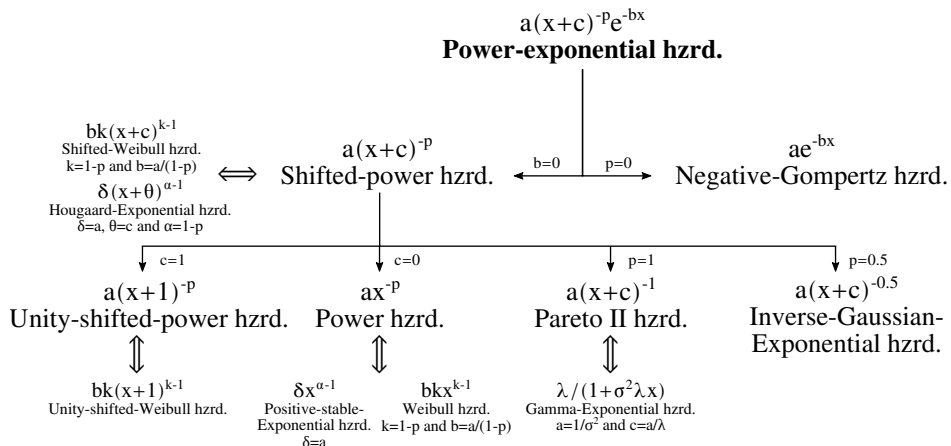
with $a \geq 0$, $p \geq 0$, $b \geq 0$, $c > 0$, and survivorship function

$$S_{PE}(x) = e^{ab^{p-1}e^{bc}(\Gamma[1-p,b(c+x)]-\Gamma[1-p,bc])},$$

where Γ is the incomplete Gamma function (Abramowitz and Stegun 1964, 6.5.3).

Many of the models proposed in the literature on infant mortality age trajectories are contained within the power-exponential family as special cases, such as the hazard functions of the negative-Gompertz (Lomax 1954; Marshall and Olkin 2007, pp. 368) and the Pareto II distribution (Lomax 1954; Marshall and Olkin 2007, pp. 400), the exponential-Gamma frailty parametrization of the Pareto II distribution (Clayton and Cuzick 1985; Wienke 2011, p. 78), (shifted)-power hazards and their (shifted)-Weibull parametrizations (Lehman 1963; Marshall and Olkin 2007, pp. 321), and the Hougaard-Exponential frailty model (Hougaard 1984). Having all these models nested in a single family (Figure 1 for a family tree) facilitates goodness-of-fit comparisons: A simpler model may be rejected in favor of a more complicated one on the grounds of significance test on the parameters, and the whole family of models can be rejected if the full expression fails to describe the data accurately.

Figure 1: The power-exponential family of hazards considered for the age trajectory of infant mortality. A range of distributions previously applied to the survival analysis of infant death appear as special cases.



Prior to fitting the power-exponential model to the data, I will discuss the respective properties and parameter interpretation of the nested power and negative-Gompertz hazards and demonstrate their fit (or lack thereof) to the observed death rates of the complete cohort of infants born in the U.S. 2005 to 2009. This procedure builds evidence that it takes both a power- and an exponential component to describe mortality over infancy adequately, a subtlety that, to my best knowledge, has remained unmentioned in the literature.

In a second analysis, I test the fit of the power-exponential hazard by birth cohort, sex, Apgar score, gestation at birth, maternal origin, and education. Confronting a mortality model with such a varied collection of life tables acts as a validity test and allows for the quantification of heterogeneous mortality trajectories via comparison of model coefficients across population strata. Particular attention will be paid to non-proportional variations of the hazard, the hazard's behavior during the neonatal period (the first month of life), and the post-neonatal period (months one to twelve of age).

All the models in this paper are fitted as generalized linear models (GLMs). Such an approach guarantees concave likelihood surfaces and consequently stable estimation of the model parameters while also capitalizing on the wide availability of software to fit and evaluate GLMs. By using suitable link functions and transformations of the age variable, a range of parametric hazard functions can be linearized and thus fitted to observed age-specific death counts and exposures via a Poisson GLM (Aitkin and Clayton 1980; Clayton 1983; Currie 2016).

The power-exponential family of hazards, and therefore the distributions shown in Figure 1, may be fit, after deciding on the value for c , as Poisson GLMs with a log-link. This is possible due to the log-linearity of $h_{PE}(x)$ given c :

$$\log h_{PE}(x) = \log(a) - p \log(x + c) - bx = \beta_0 + \beta_1 \log(x + c) + \beta_2 x,$$

with $a = \exp(\beta_0)$, $p = -\beta_1$ and $b = -\beta_2$. The non-linear c parameter is estimated by maximizing the *profile likelihood* (McCullagh and Nelder 1989, chapter 7.2.4) of c over a range of GLM fits⁴. Model evaluation is performed via the model deviances, LOESS-smoothed Pearson-residuals⁵, and McFadden's R^2 criterion (McFadden 1974). Confidence intervals around the parameter estimates of the power-exponential hazard are derived from 1,000 repeated fits of the model on 1,000 different parametric-bootstrap replicates of each life table. Unlike the asymptotic standard errors retrieved from the GLM fit, the bootstrap approach incorporates the uncertainty associated with the estimation of the non-linear c parameter.

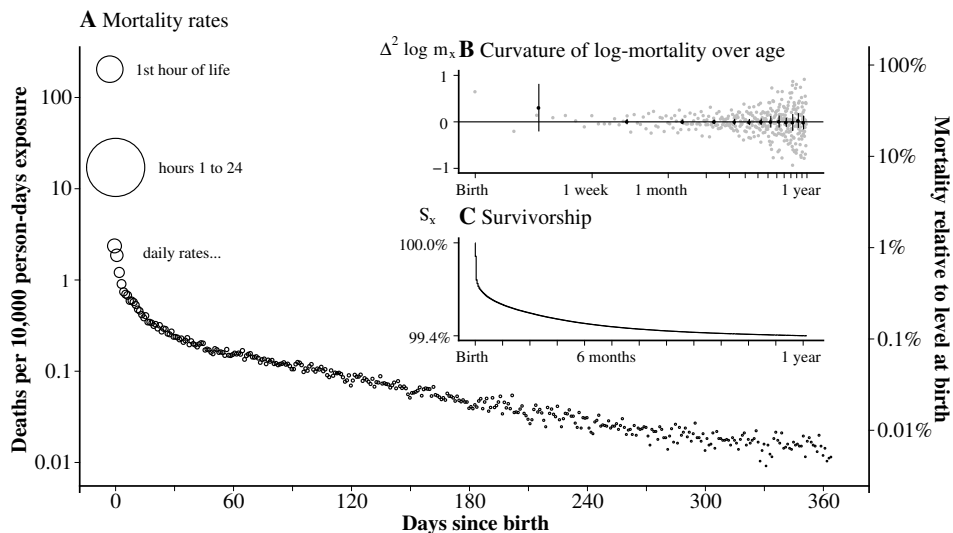
⁴ Let $L(\boldsymbol{\beta}, c)$ be the full likelihood of a GLM fit with coefficients $\boldsymbol{\beta}$ and age-offset c . The profile likelihood of c is given by $L_p(c) = \max_{\boldsymbol{\beta}} L(\boldsymbol{\beta}, c)$ and c is estimated as $\hat{c} = \arg \max_c [\max_{\boldsymbol{\beta}} L(\boldsymbol{\beta}, c)]$. I found $L_p(c)$ to be concave over c and the maximization was quick and stable. See also Rinne (2009), chapter 11.3.2.2 for the closely related strategy of using the profile likelihood to determine the location parameter of a three parameter Weibull distribution.

⁵ In order to smooth Pearson residuals over age x I use the `loess()` function implemented in R (R Core Team 2020) specified with quadratic polynomials, a tri-cubic weight function, Gaussian errors and a span of 0.4.

4. The age trajectory of U.S. infant mortality

The age trajectory of infant mortality, as observed in the U.S. birth cohort 2005-2009, is characterized by a peak at birth with a rapid decline thereafter (Figure 2A). While the mortality rate over the first hour following birth is around 200 deaths per 10,000 person-days of exposure, 24 hours later, the rate is at only 1.1 percent of its initial value and then again drops by a factor of ten over the next 29 days. Around one month after birth, mortality rates start to decline with a near-constant relative rate, approaching an exponential behavior. This log-linear trend is further illustrated by the second-differences of log-mortality rates over day-of-age, which have a mean close to zero for every month but the first (Figure 2C).

Figure 2: Infant life table measures for the U.S. birth cohort 2005-2009. A) Mortality rates drop rapidly during the neonatal period, after which the decline becomes exponential. Note that the area of the circles is proportional to the observed death counts. B) The exponential decline in mortality is further illustrated by the second differences in log-mortality over age clustering around zero. 95% CI via t-test of second differences aggregated over week one, weeks two to four and each of the following 11 months. C) As indicated by the survival curve, more than half of the infant deaths occur in the first few days following birth.

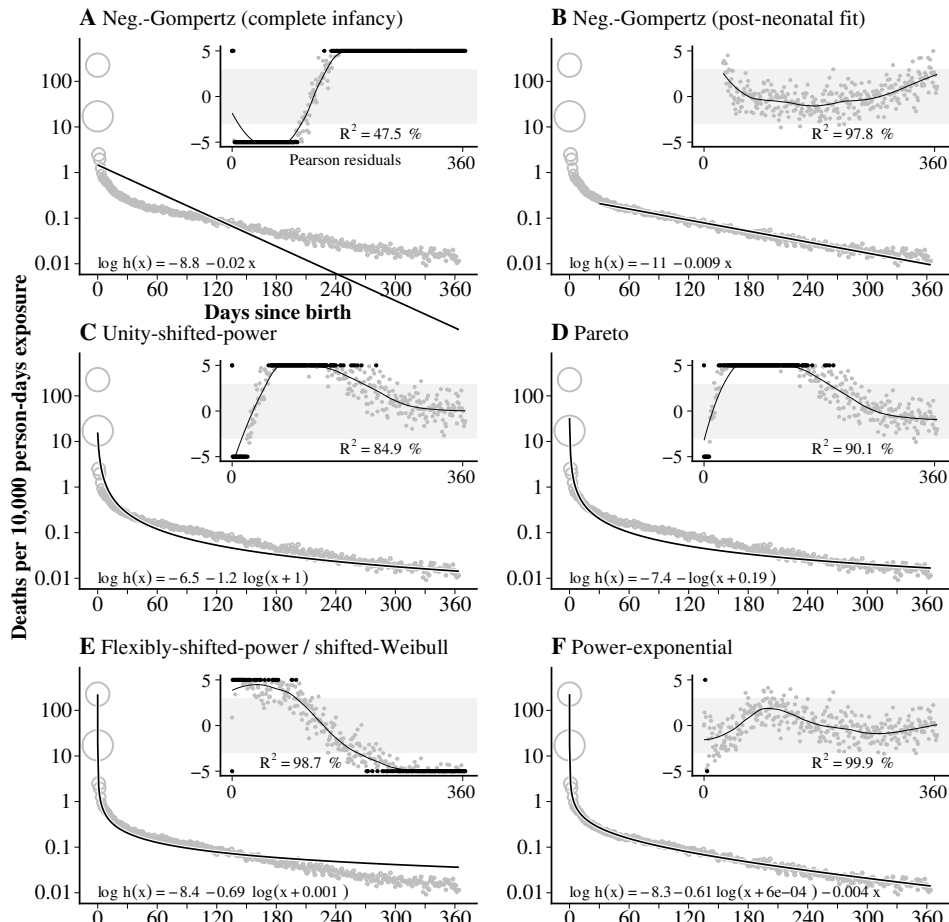


The pattern of a “super-exponential” decline in mortality during the neonatal period followed by an exponential tail over the remainder of the first year of life holds for girls and boys, irrespective of the social background of their mothers, the Apgar score upon birth, the gestation at birth or birth cohort (Figures 4 and 5).

Out of 162,541 infant deaths, 23,683 (14.5 percent) die during the first hour following birth and 81,506 (50.1 percent) before the age of 5 days. The overall probability of survival is 99.4 percent (Figure 2B).

5. Evidence for a power-exponential hazard

Figure 3: Fitted versus observed mortality over the first year of life for the U.S. birth cohort 2005–2009. Combining a power law (C, D, E) and a negative-Gompertz hazard (A, B) into the power-exponential model (F) accounts for the different behavior of the hazard in the neonatal and post-neonatal periods and achieves a close fit over the entire first year of life.



5.1 Negative-Gompertz hazard

In an early attempt to model mortality across the whole human lifespan, Thiele (1871) proposed to express the risk of death before maturity as an exponential function of age,

$$h_{\text{GP}}(x) = ae^{-bx},$$

with $a \geq 0$ and $b \geq 0$. This is the hazard function of a Gompertz distribution with a negative b parameter and therefore mirrors the shape of the hazard commonly assumed for adult humans. The simplicity of an exponential term for the hazard facilitates analytic treatment and gives the parameters a direct interpretation as important quantities in the study of infant mortality, $h_{\text{GP}}(0) = a$ being the hazard of death at the moment of birth and $-\frac{h'_{\text{GP}}(x)}{h_{\text{GP}}(x)} = b$ the instantaneous relative rate of mortality decline over age. The fact that the risk drops with a constant relative rate is the defining feature of the negative-Gompertz hazard. Related quantities are independent of age as well: the time t it takes for the hazard to drop by a factor k is the solution to equation $\frac{h_{\text{GP}}(x+t)}{h_{\text{GP}}(x)} = \frac{1}{k}$ given by $t_{1/k} = \frac{\log(k)}{b}$ and for each unit increase in age the hazard changes by a factor $\frac{h_{\text{GP}}(x+1)}{h_{\text{GP}}(x)} = \exp(-b)$.

The negative-Gompertz hazard can be expressed as a log-linear model with Poisson distributed age-specific death counts D_x as the outcome and age-specific exposure times E_x as a fixed offset⁶

$$\log E[D_x] = \beta_0 + \beta_1 x + \log E_x, \text{ with } D \sim \text{Poisson}.$$

From this fit the parameters of h_{GP} are recovered as $a = \exp(\beta_0)$ and $b = -\beta_1$.

The negative-Gompertz model of infant mortality is especially popular in biology due to the influential paper by Siler (1979), who included it as part of his “Competing-Risk Model for Animal Mortality.” In this model, a Gompertz term with negative b parameter is used “to account for the hazard due to immaturity” (Siler 1979). For life tables of human infants and children, however, the negative-Gompertz law has long been found to provide an insufficient fit (Thiele 1871, p. 326; Choe 1981; Gage and Dyke 1986).

Figure 3A clearly shows that the age trajectory of infant mortality for the 2005-2009 U.S. birth cohort deviates from a pure log-linear (i.e., exponential) form, ruling out the Gompertz hazard as a suitable model for the entire infant age range. Yet, a log-linear decline constitutes a near-perfect description of the mortality trajectory over the post-neonatal period (Figure 3B). The rate of death at day 30 after birth is around 2.03 per 100,000 person-days of exposure, with a subsequent decline of about 0.93 percent per additional day of age. Remarkably these two numbers explain 97.8 percent of the total deviance in the data during the post-neonatal period. Further investigating this result, I fit negative-Gompertz and power-law hazards to the post-neonatal life tables for each of the 60 monthly U.S. birth cohorts from January 2005 to December 2009 separate by sex. In most cases, the negative-Gompertz hazard provided a closer fit to the observed

⁶ Assuming that the width of each age group $j = 1, \dots, 366$ is small enough as not to introduce substantial aggregation bias. To simplify the notation I write D_x and E_x for total deaths and exposures in age groups with starting age x , where $x \in \{x_{j=1}, \dots, x_{j=366}\}$.

Table 1: Number of months over the five year period 2005-2009 a negative-Gompertz fit achieved a lower deviance on the post-neonatal cohort life tables compared to a given power-law fit.

Gompertz vs.	Female	Male
Pareto II	44/60 73.3%	54/60 90%
Unity-shifted power	59/60 98.3%	60/60 100%
Flexibly-shifted power	23/60 38.3%	41/60 68.3%

post-neonatal mortality trajectory than either of the alternative two or three-parameter power-law hazards (Table 1).

5.2 Power-law hazard

Various power-laws have been specified to characterize the age-specific hazard of infant death (Oppermann 1870; Brillinger 1961; Choe 1981; de Beer and Janssen 2016; Berrut et al. 2016) all of which are variations on the basic expression

$$h_{PW}(x) = ax^{-p},$$

with $a \geq 0$ and $p \geq 0$. Just like a negative-Gompertz hazard, a power-law hazard monotonically approaches 0 as $x \rightarrow \infty$; however, the relative rate of decline of a power hazard varies with age according to $-\frac{h'_{PW}(x)}{h_{PW}(x)} = \frac{p}{x}$, i.e., it is greatest right after birth and approaches 0 as age increases. It is this behavior that allows a power-law to initially decline faster than a Gompertz hazard, yet become slower for larger x , rendering it potentially useful for the description of the day-to-day age pattern of infant mortality.

Similar to the Gompertz case, the parameters of the power hazard can be interpreted in terms of mortality level and rate of change: The risk of death at age $x = 1$ is given by $h_{PW}(1) = a$ and the proportional change in mortality for change in age by proportion w is $\frac{h_{PW}(wx)}{h_{PW}(x)} = w^{-p}$. The proportional increase in age w needed for the hazard to drop by factor k is the solution to equation $\frac{h_{PW}(wx)}{h_{PW}(x)} = 1/k$ given by $t_{1/k} = k^{\frac{1}{p}}$. The power parameter p by itself represents the elasticity of the hazard, $\frac{d \log h_{PW}(x)}{d \log x} = -p$, i.e. for every infinitesimal proportional increase in age the hazard drops by proportion p . A convenient property of power-laws is that the elasticity is invariant to any rescaling of age in the form $x' = wx$. In practice this means that the units used for the age column of the infant life tables (e.g. hours, days, weeks) have no effect on the estimation of the exponent p .

Note that h_{PW} can be reparametrized into the hazard of the Weibull distribution $h_{UW}(x) = bkx^{k-1}$ by substituting $p = 1 - k$ and $a = bk$.

Berrut et al. (2016) fit h_{PW} to death rates starting shortly after birth for a range of human and non-human populations and identify power-law behavior in most populations⁷. Specifically, they identify a segmented power-law relationship between age and death rate

⁷ Note that while occurrence-exposure rates are used in this article, Berrut et al. (2016) use the total number of births in the denominator of their death-rates.

for a cohort of Swiss infants. The first segment starts one hour after birth and lasts for eight hours, while a different power coefficient is identified for the remainder of the first month of life.

Unity-shifted-power hazard

As x approaches 0, hazard h_{PW} approaches infinity. Due to this behavior, a pure power-law hazard can not be used to describe the age pattern of infant mortality starting from the moment of birth. Instead one can either choose to exclude the moment/hour/day of birth from the study period (as did Choe 1981; Berrut et al. 2016) or add a positive location parameter to h_{PW} , i.e. $h_{\text{PW}}(x + c)$. The offset can either be estimated from the data – allowing for additional model flexibility – or set to some constant. The latter option has the advantage that the resulting hazard can be written as a fully linear function of log-mortality. For mathematical convenience one may use a unity offset resulting in the *unity-shifted-power* expression

$$h_{\text{UP}}(x) = a(x + 1)^{-p},$$

with $a \geq 0$ and $p \geq 0$. Due to the unity offset, the risk of death at the moment of birth is $h_{\text{UP}}(0) = a$. The elasticity of $h_{\text{UP}}(x)$ approaches $-p$ as $x \rightarrow \infty$. In practice I found $-p$ to be a very close approximation to the true elasticity of $h_{\text{UP}}(x)$ for at least the post-neonatal period; thus one may safely interpret p as the approximate proportional drop in the hazard of infant death for an infinitesimal proportional change in age starting at day 30 after birth. The unity-shifted-power hazard can be fitted as the log-linear Poisson regression

$$\log E[D_x] = \beta_0 + \beta_1 \log(x + 1) + \log E_x,$$

with $a = \exp(\beta_0)$ and $p = -\beta_1$.

Note that h_{UP} can be translated into the unity-shifted Weibull hazard $h_{\text{UW}}(x) = bk(x+1)^{k-1}$ by substituting $k = 1 - p$ and $b = a/(1 - p)$.

While the unity-shifted-power law fits the 2005-2009 U.S. infant life table better than the Gompertz hazard, the Pearson residuals in Figure 3C still indicate systematic misspecification. Due to its very nature, the unity-shifted-power law can not capture the exponential portion of the hazard, and it also fails to adequately describe the swift drop in the risk of death over the first hours following birth.

Pareto hazard

In their model for the age pattern of human mortality de Beer and Janssen (2016) express the hazard of death during infancy and childhood as $h(x) = \frac{a}{c+x}$. This is the hazard function of a Pareto type II distribution (Lomax 1954; Marshall and Olkin 2007, pp. 400).

Rewriting the hazard reveals a shifted-power law with exponent -1 , scaling factor a and location offset c ,

$$h_{\text{PT}}(x) = a(x + c)^{-1},$$

where $a \geq 0$ and $c > 0$. While for the unity-shifted-power-law, the location offset is fixed, and the power exponent varies, the situation is reversed for the Pareto II hazard with a fixed power and a variable location offset. As $h_{\text{PT}}(x)$ is finite for $x > -c$ one may interpret the c parameter as the duration h_{PT} extends into the prenatal period. For such an interpretation to be justified the intrapartum death-rates (death during labor, i.e., at $x < 0$) have to follow the same functional form as the infant death rates and, given that $h(x + c)$ is declining with age, have to be higher than the mortality rates after birth. Of course the mortality at birth is $h_{\text{PT}}(0) = a/c$ with a being the hazard level at $x = 1 - c$. The elasticity of the Pareto hazard is $\frac{d \log h_{\text{PT}}(x)}{d \log x} = -\frac{x}{x+c}$ which approaches -1 as $x \rightarrow \infty$. Here a central characteristic of the Pareto hazard is implied: in the limit any proportional increase in age by factor w results in a proportional change of the hazard by $1/w$, e.g., doubling age halves the hazard. In practice, the estimated values for c are small enough for this limiting behavior to set in shortly after birth.

The Pareto hazard can be fitted via the Poisson regression

$$\log E[D_x] = \beta_0 - \log(x + c) + \log E_x,$$

an intercept-only model with additional offset $-\log(x + c)$ and $a = \exp(\beta_0)$. As described earlier c is estimated by maximizing its profile likelihood.

Vaupel and Yashin (1983) propose to describe the infant and childhood component of human mortality by a Gamma-Exponential frailty model with population hazard function $h_{\text{GE}}(x) = \lambda/(1 + \sigma^2 \lambda x)$, i.e., a mixture of constant baseline hazards (corresponding to an exponential baseline distribution of deaths) with Gamma distributed rate parameter λ . As noted by e.g. Wienke (2011) this model is equivalent to h_{PT} when $a = 1/\sigma^2$, i.e., the inverse of the variance parameter of the Gamma-Exponential frailty model, and $c = a/\lambda$. Therefore h_{PT} may be interpreted as the population hazard resulting from mortality selection among individuals with constant hazards of Gamma varying magnitudes.

The fit of the Pareto hazard to the 2005-2009 U.S. infant life tables is inadequate and similar to that of the shifted-power-law (Figure 3D).

Flexibly-shifted-power hazard

Adding a positive location offset c to h_{PW} results in the flexibly-shifted-power hazard

$$h_{\text{FP}}(x) = a(x + c)^{-p},$$

where $a \geq 0$, $b \geq 0$ and $c > 0$. This hazard shape contains the Pareto II hazard and the unity-shifted-power hazard as special cases. Note that h_{FP} can be interpreted as the

hazard function of the shifted Weibull distribution $h_{SW}(x) = bk(x + c)^{k-1}$ with $k = 1 - p$ and $b = a/(1 - p)$.

The elasticity of the flexibly-shifted-power hazard is $\frac{d \log h_{FP}(x)}{d \log x} = -\frac{px}{x+c}$ which approaches $-p$ as $x \rightarrow \infty$. Due to small estimates for c , this limiting behavior sets in shortly after birth, allowing an interpretation of the p parameter as the proportional drop in mortality for an infinitesimal proportional increase in age for all but the very first moments after birth. As for the Pareto II hazard, a is the hazard level at age $1 - c$, and c may be interpreted as the time that h_{FP} extends into the prenatal period.

The flexibly-shifted-power hazard can be fitted as a Poisson GLM of the form

$$\log E[D_x] = \beta_0 + \beta_1 \log(x + c) + \log E_x, \text{ with,}$$

with the original parameters recovered as $a = \exp(\beta_0)$ and $p = -\beta_1$. Again, c is estimated by maximizing its profile likelihood.

Substituting $a = \delta$, $c = \theta$ and $p = 1 - \alpha$ recovers the hazard of the Hougaard-Exponential distribution $h_{HE}(x) = \delta(x + \theta)^{\alpha-1}$, a continuous mixture of exponential distributions employed by Hougaard (1986) to describe the hazard in the days following myocardial infarction. The mixing distribution is flexible and contains the Gamma ($\alpha = 0$), the Inverse-Gaussian ($\alpha = 0.5$), and the positive-stable distribution ($\theta = 0$) as special cases. The Hougaard-Exponential hazard is a frailty model, albeit in a non-standard parametrization, with average frailty upon birth equal to $\delta\theta^{\alpha-1}$ and a baseline hazard fixed at unity (cp. Hougaard 1986, eq. 5.1). Because of the constant individual level hazard, all of the declining mortality observed on the population level is assumed to be due to mortality selection.

Allowing for both a free power parameter p and a free location offset c greatly improves the fit to the U.S. 2005-2009 infant life tables compared to the more restricted unity-shifted-power and Pareto hazards (Figure 3E). The estimate for c is 0.0012 (i.e. a location shift by ≈ 1.7 minutes of age) and for p equals 0.69, corresponding to an approximate drop in mortality by $(1 - 2^{-0.69}) \times 100 = 38$ percent for every doubling of age. While fitting better than the hazards discussed above, the Pearson residuals in Figure 3E still exhibit a clear trend signifying a systematic lack of fit.

5.3 Power-exponential hazard

Multiplying the flexibly-shifted-power law hazard h_{FP} with an exponential term results in the power-exponential expression

$$h_{PE}(x) = a(x + c)^{-p} e^{-bx},$$

with $a \geq 0$, $p \geq 0$, $b \geq 0$, and $c > 0$. This hazard contains all of the above models as special cases (Figure 1).

The power-exponential hazard smoothly transitions from power-law to exponential behavior: With increasing age h_{PE} approaches a constant relative rate of change and thus increasingly resembles a negative-Gompertz hazard, formally $\lim_{x \rightarrow \infty} \frac{h'_{PE}(x)}{h_{PE}(x)} = -b$.

The Poisson GLM form of the power-exponential hazard is

$$\log E[D_x] = \beta_0 + \beta_1 \log(x + c) + \beta_2 x + \log E_x,$$

where $a = \exp(\beta_0)$, $p = -\beta_1$, $b = -\beta_2$ and the non-linear coefficient c is estimated via profile likelihood maximization.

Adding the exponential term to h_{FP} significantly ($p < 0.001$ via deviance-ratio test, Table 2) improves the fit of the Poisson GLM to the 2005-2009 U.S. birth cohort and flattens the trend in the Pearson residuals over age (Figure 3F) albeit a hump-shaped curvature remains with a peak around 90 days of age. A likely source for this residual pattern is Sudden Infant Death, which exhibits an incidence-hump with a peak at around two to four months of age (Kinney and Thach 2009).

6. Evaluation of the power-exponential hazard

The power-exponential hazard achieves an excellent fit irrespective of cohort, sex, five minute Apgar score, gestational age at birth, maternal origin or education. The percentage of deviance explained by the model ranges from 94.5 to 99.6 percent in all life tables under consideration. For every single population, the inclusion of an exponential term in addition to the shifted-power term significantly ($p < 0.001$ via deviance-ratio test, Table 2) improves the fit, reducing the residual deviance by more than 50% on 43 out of the 56 populations.

The shape of the hazard function over age varies most strongly by Apgar score (Figure 4A) with the exponential behavior most pronounced among infants born with a score of nine or ten (the majority). Within two weeks after delivery, the initial mortality spike at birth transitions into a log-linear decline in mortality risk of around 0.7 percent per day. Conversely, the hazard trajectory for infants with a “low” Apgar score (indicating health problems of upon delivery), while still exponential in the tail, features a more gradual transition into log-linear behavior. The most considerable difference in the behavior of the hazard among the Apgar groups can be seen over the first week of life. While for Apgar group zero to five, the hazard drops by a factor of 1000 from the day of birth to an age of seven days, it only drops by a factor of nine or less for the other groups (Table 3). Thus hazards vary by Apgar score in a highly *non-proportional* fashion as can also be inferred from the varying power (p), exponential-rate (b), and offset (c) parameters of the fitted models. Non-proportional behavior, albeit less pronounced, is also evident when comparing hazards by prematurity, with higher values for the power parameter $p = -\beta_1$ for lower ages of gestation at birth (Figure 4B), a result also observed by Berrut et al. (2016) for Swiss and Norwegian infants after fitting a simple power-law to age-specific mortality rates.

Table 2: Percent reduction in residual deviance after multiplying the flexibly-shifted-power-law hazard with an exponential term. All results significant at $p < 0.001$ (via deviance-ratio tests).

		1995-1999		2005-2009	
		Female	Male	Female	Male
APGAR	Very low [0,5)	50.2	45.6	61.3	60.3
	Low [5,9)	20.6	27.9	49.5	49.7
	Regular 9+	86.8	86.4	89.8	92.0
Origin	Non-Hispanic Black	56.0	60.1	65.1	63.9
	Non-Hispanic White	76.3	74.2	81.9	79.6
	Hispanic	55.4	63.6	60.2	69.4
	Other	20.3	29.4	24.7	33.5
Prematurity	Extremely preterm <28w	67.4	67.1	74.1	75.7
	Very preterm [28,32)w	54.7	56.1	60.9	63.0
	Moderate to late preterm [32,37)w	58.2	60.0	71.0	70.2
	Term 37w+	79.8	78.1	83.7	80.9
Education	Elementary or less	38.6	41.9	30.5	40.9
	High school	76.9	74.7	79.9	77.3
	College or university	67.3	66.0	76.6	76.8

The relative rate of mortality decline during the post-neonatal period, as approximated by b , is higher for premature infants and infants with a low Apgar score compared to infants born at term or with a regular Apgar score, implying that the relative difference in mortality between very frail and less frail infants diminishes over age.

Hazards are mostly proportional by ethnicity of the mother (Figure 5B) with the risk of death during the later stages of infancy declining exponentially with a rate of 0.3 to 0.5 percent per day of age and the power parameter ranging from -0.51 to -0.55 across the life table strata. Notably, during the post-neonatal period mortality over age declines slower for children of African-American mothers compared to infants of white mothers⁸; taken together with the observation that the intercept of the hazard curve is highest among infants of African-American mothers, this puts the group at a double disadvantage. Along education strata, the hazards are proportional (Figure 5B).

There are no systematic differences in the age trajectory of infant mortality between the sexes, apart from a proportionally higher hazard for males than females. Similarly, the difference between the two birth cohorts is mostly proportional, with the younger cohort having a lower intercept β_0 (Figures 4 and 5).

⁸ Significant at $p < 0.05$ for female and male infants of either birth cohort (Table 5).

Figure 4: Age specific hazard of death as predicted by the power-exponential hazard contrasted with life table mortality rates by sex, birth cohort, and condition of the infant upon birth.

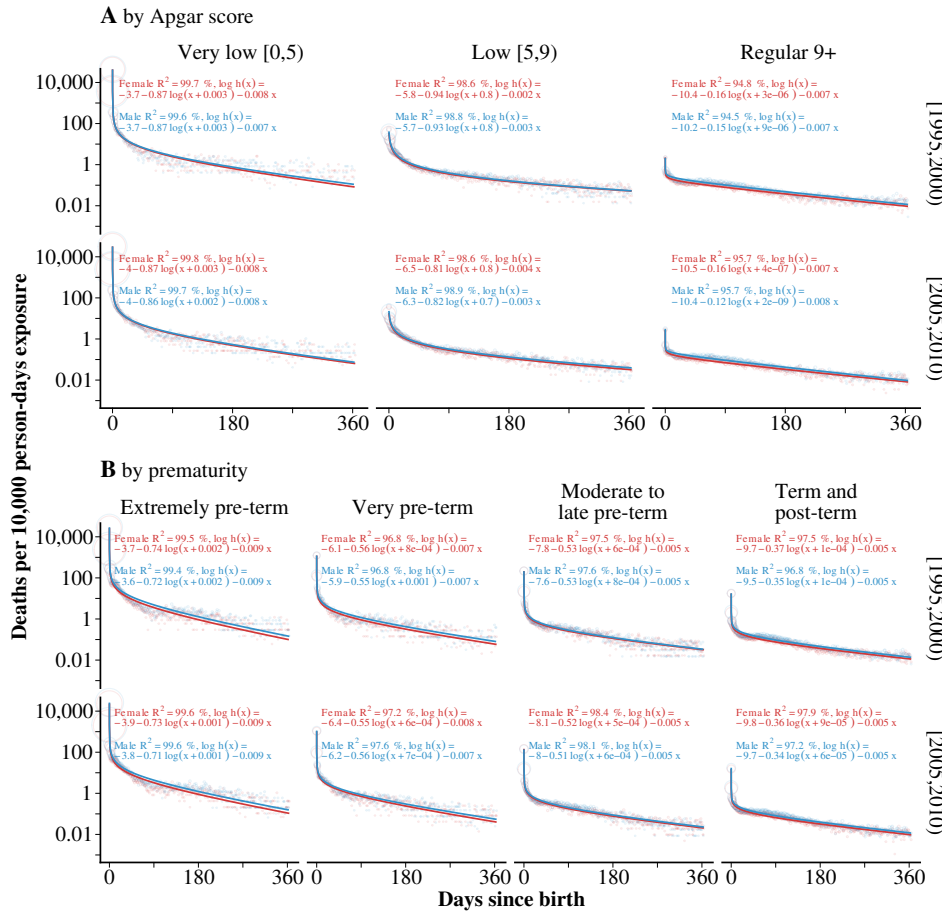
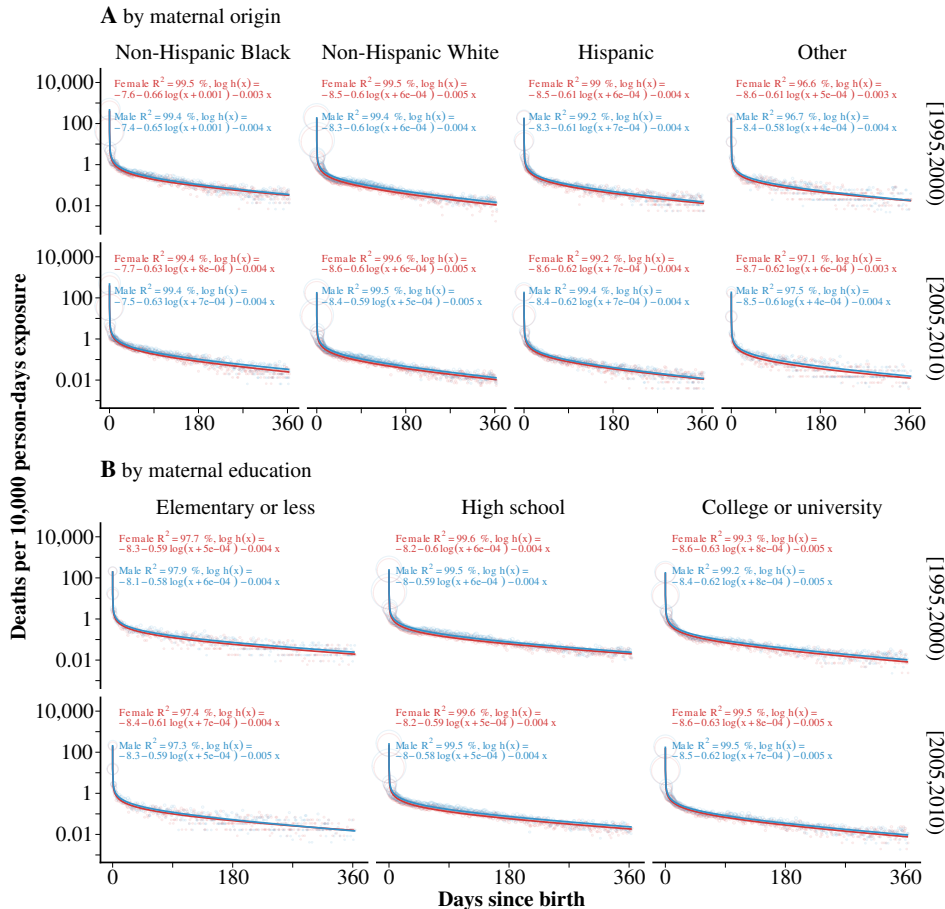


Figure 5: Age specific hazard of death as predicted by the power-exponential hazard contrasted with life table mortality rates by sex, birth cohort, and maternal background.



7. Interpretation of the exponential-power hazard

7.1 A shock-recovery process

The power-exponential product in the population hazard h_{PE} can be interpreted as a *non-homogeneous split Poisson process*, where *shocks* to an infant's health arrive with rate $\lambda(x)$ per unit person-time, each shock resulting in infant death with probability $p(x)$. Shock models in the context of human mortality have, for example, been studied by Strehler and Mildvan (1960), Finkelstein (2005), Cha and Finkelstein (2016). A similar explanation for the age trajectory of preadolescent mortality across species has been put forward by Levitis (2011) under the name "transitional timing hypothesis," stating that "*transcriptional, developmental and environmental transitions are dangerous, and these are concentrated early in life.*"

Let $N(x)$ be the number of infants alive at age x and let $E[Y]$ be the expected value of a Poisson distributed random variable Y with rate parameter $\int_x^{x+n} \lambda(s)N(s) ds$ representing the total number of *health-shocks* the population of infants is expected to experience over age interval $[x, x + n]$. If each shock leads to death with probability $p(x)$ then the number of deaths D over age interval $[x, x + n]$ follows a Poisson distribution with expected value

$$E[nD_x] = \int_x^{x+n} \lambda(s)p(s)N(s) ds,$$

see Prékopa (1958) for a proof. The hazard of death experienced by survivors N at time x is $h(x) = \lambda(x)p(x)$. If the rate of shocks $\lambda(x)$ varies over time according to a flexibly-shifted-power hazard and if the probability of a shock leading to death $p(x)$ is exponentially declining the power-exponential hazard is recovered. Note that neither the rate of shocks nor the probability of death following a shock are identified as this would require inferring the model $h(x) = a_1(x+c)^{-p} \times a_2 e^{-bx}$ from the fit $h(x) = a(x+c)^{-p} e^{-bx}$ – a problem with infinitely many solutions. However, the power and the exponential rate parameters p and b are completely identified. They can be interpreted as follows: For the extremely preterm female births of the U.S. birth cohort 1995-1999 (Figure 3F) the rate of shocks, $\lambda(x) \propto (x + 0.002)^{-0.74}$, declined rapidly in the vicinity of birth by approximately $(1 - 2^{-0.74}) \times 100 = 40$ percent for every doubling of age whereas the probability of a shock leading to death, $p(x) \propto e^{-bx}$, declined by about 0.9 percent per additional day of age.

Why use the power law for the rate of shocks and the exponential term for the shock lethality instead of the other way around – after all, both options lead to the same expression for $h(x)$? I find it likely that the rapid neonatal mortality decline is predominantly a result of the waning stresses of birth – a sudden transition which may inflict a series of "shocks" to the infant – and not the result of a fast decline in the mortality risk associated with each shock. Furthermore, as $\lim_{x \rightarrow \infty} \frac{h'_{EP}(x)}{h_{EP}(x)} = 0$, the power-law approaches a constant hazard as age increases, allowing it to capture the age-independent rate of accidents which may dominate the rate of shocks later in infancy.

A particular shock-recovery process is described by the Strehler-Mildvan model of senescent mortality. Strehler and Mildvan (1960) propose a model where individuals experience

shocks to their health at a constant rate α . The magnitude of each shock, ranging from mild to severe, is a value drawn from an exponential random variable with rate β . The shocks are counteracted by the vitality of an individual, which is a positive and declining function of age. When the magnitude of a shock at age x exceeds the individual's vitality at that age, death occurs. Strehler and Mildvan (1960) show that this process leads to a Gompertz distribution of life-times with corresponding hazard function $h(x) = \alpha e^{\beta x}$.

The power-exponential hazard of infant mortality can be derived from such a Strehler-Mildvan process by changing two assumptions: 1) Where Strehler and Mildvan (1960) assume a decrease of vitality with time due to aging, one assumes an increase due to growth, and 2) instead of that shocks arrive with a constant rate α , one assumes that the risk of experiencing complications is highest at birth and falls over time (according to a shifted Weibull distribution).

7.2 A mortality selection process

In the multiplicative frailty model (Vaupel et al. 1979), it is assumed that all individuals in a population share the same age-specific “baseline hazard” of death $h_0(x)$ but on different “frailty” levels z which act multiplicatively on the baseline. Consequently, the age-specific hazard conditioned on frailty is given by

$$h(x|z) = z h_0(x).$$

Frailty is treated as a random variable Z with density $f(z|x)$ at age x . Integrating out the frailty yields the expression for the hazard observed at the population level, which is a mixture of the individual level hazards weighted by the age-specific distribution of frailties

$$\bar{h}(x) = \int_0^\infty h(x|z) f(z|x) dz,$$

which may be re-expressed as

$$\bar{h}(x) = h_0(x) \int_0^\infty z f(z|x) dz = h_0(x) E[Z|x],$$

showing that the population hazard is a product of the baseline hazard and the average frailty among the population at age x . By choosing $h_0(x) = ae^{-bx}$ and $E[Z|x] = (x+c)^{-p}$ we express the power-exponential hazard h_{PE} as a multiplicative frailty model.

Frailty models can be interpreted in terms of *mortality selection*: Because individuals with high frailty on average die earlier than those with lower values for z , the average frailty among a cohort of individuals declines over time. Above, we modeled this decline as a shifted-power function of age, and consequently, p can be interpreted as the approximate elasticity of average frailty w.r.t. age, 0.69 for the U.S. birth cohort 2005-1999, corresponding to an approximate drop in average frailty by 38 percent for every doubling of age – a substantial mortality selection shortly after birth.

While differing in frailty, all individuals of a cohort are assumed to share the same baseline hazard. By modeling this *individual level* risk as an exponential function of age, we assume that each additional unit of age decreases an infants risk of death by a factor $\exp(-b)$, around 0.4 percent per additional day of age for the 2005-1999 U.S. birth cohort (Figure 3F). This relatively slow rate of decline may be attributed to *acquired robustness* (Levitis 2011) due to the infant's continued growth and development.

Hougaard (1986) describes a class of multiplicative frailty models that exhibit a shifted-power law decline in average frailty over age. Frailty is assumed to be distributed according to a three-parameter extension of the stable distributions $f_Z(z; \alpha, \delta, \theta)$, a density without closed-form representation, but with closed-form Laplace transform

$$\mathcal{L}\{f_Z\}(s) = E[e^{-sZ}] = \exp\left[-\frac{\delta}{\alpha} [(\theta + s)^\alpha - \theta^\alpha]\right].$$

Substituting the cumulative baseline hazard $H_0(x) = \int_0^x h_0(s) ds$ for argument s one recovers the population survival function

$$\bar{S}(x) = E[e^{-H_0(x)Z}] = \exp\left[-\frac{\delta}{\alpha} [(\theta + H_0(x))^\alpha - \theta^\alpha]\right]$$

and corresponding population hazard

$$\begin{aligned} -\frac{d}{dx} \log \bar{S}(x) &= \bar{h}(x) \\ &= E[Z|x]h_0(x) \\ &= \delta(\theta + H_0(x))^{\alpha-1}h_0(x). \end{aligned}$$

Assuming a negative-Gompertz baseline hazard $h_0 = \exp(-bx)$ and substituting $a = \delta$, $c = \theta$ and $p = -\alpha + 1$ into $\bar{h}(x)$ yields the Hougaard-Negative-Gompertz hazard

$$h_{HG}(x) = a \left(\frac{1 - e^{-bx}}{b} + c \right)^{-p} e^{-bx}.$$

This hazard has the same qualitative behavior as the power-exponential expression, namely a power-law decline shortly after birth and a gradual transition into an exponential tail. Both models achieve a virtually identical fit to the U.S. data. Under a frailty interpretation, both hazards lead to the same inference: mortality selection explains most of the mortality decline over the first month of life. The estimated $c = \theta$ parameter in the neighborhood of 0 approaches a positive-stable distribution of frailties, which has extreme positive skewness and exhibits infinite mean and variance.

Of course one could, to the same effect, also choose $h_0(x) = a(x+c)^{-p}$ and $E[Z|x] = e^{-bx}$. This model implies that the power-law behavior of the population hazard (mostly seen during the first month of life) arises from individual-level processes, while above, we have assumed that the rapid mortality decline after birth is mostly due to changing average frailty, i.e., mortality selection.

Mortality selection can also be modeled via finite mixtures (discrete frailty models) of the form $F_{\text{FM}}(x) = p_1 F_1(x) + p_2 F_2(x)$, where $F_{\text{FM}}(x)$ is the probability of death until age x , p_1 and $p_2 = 1 - p_1$ are the relative proportions of population sub-groups 1 and 2 at birth and F_1, F_2 denote the corresponding stratum-specific cumulated probabilities of death. Choosing the form of a negative-Gompertz distribution for F_1 and F_2 , yet allowing the parameters to differ between both populations, can produce hazards that smoothly transition into an exponential tail similar to the power-exponential expression (e.g., Marshall and Olkin 2007, cp. 3)⁹. Different choices for the baseline hazard and the distribution of frailties can result in qualitatively or mathematically equivalent expression for the population hazard – an identifiability problem well-known in the frailty-model literature (e.g., Hougaard 1995).

8. Discussion

Using highly detailed individual-level data on the timing of death over the first year of life, I found strong evidence for an exponentially modulated power-law behavior of the hazard of infant death in two recent U.S. birth cohorts. The shift from a power-law regime to an exponential decline has not previously been noted in the literature and invites speculation regarding the mechanisms giving rise to such a pattern. Observed hazards may be the result of mechanisms that have been discussed at length in the context of senescent risk of death: mortality selection due to heterogeneous frailties and a shock-recovery process. The frailty hypothesis may be tested via a decomposition analysis. Vaupel and Zhang (2010) prove that, if the population hazard $\bar{h}(x)$ and the stratum specific hazards $h(x|z)$ are known for a cohort, then the rate of change over age of $\bar{h}(x)$ can be decomposed into a “direct change” component and change due to the process of mortality selection. Using this decomposition one could, for example, calculate how much of the decline in the risk of death over the first week of life as shown in Figure 2 is due to the changing population composition by prematurity status resulting from the early death of extremely premature infants, i.e., mortality selection.

A test of the shock-recovery model is less straightforward. It requires both a clear definition of what constitutes a shock and data on the timing of such shocks to see if their rate of occurrence corresponds to either the exponential or the power-law component of the power-exponential hazard.

Note that the power-exponential hazard discussed in this paper does not permit an interpretation as a competing-risks model. Such a model was implied by Bourgeois-Pichat (1951) for the age trajectory of infant mortality, which he partitioned into deaths due to “intrinsic” and “extrinsic” causes. An alternative competing-risks model featuring a power-law and an exponential term could take the form $h_{\text{CR}}(x) = a_1(x + c)^{-p} + a_2 \exp(-bx)$, which may be re-written as $h_{\text{CR}}(x) = \exp[\log a_1 - p \log(x + c)] + \exp[\log a_2 - bx]$. Sums-of-exponentials can be fit in the GLM framework by using a composite-link-function

⁹ Adopting this strategy and increasing the number of subpopulations one can approximate the hazard trajectory of human mortality over the entire lifespan, as demonstrated by Avraam et al. (2013), Avraam et al. (2014).

(Thompson and Baker 1981; Camarda et al. 2016). Assuming that deaths due to intrinsic causes follow a power-law behavior, whereas extrinsic deaths feature the hazard of a negative-Gompertz distribution, this competing-risks formulation of the age-specific hazard of infant death over time permits a shape-based cause-of-death decomposition.

The results of this paper indicate that the proportional hazards assumption does not hold across Apgar score and prematurity strata. The association of those variables with the baseline hazard of death over the first year of life is highly non-proportional with much of the “effect” focused on the first weeks of life. Indeed differences in the rate of post-neonatal mortality decline imply that the relative difference in mortality between very frail and less frail infants diminishes over age to some degree.

It must be noted that without further study, the results of this paper can not be generalized to populations other than present-day U.S. infants. While similar results for countries with similar overall levels of infant mortality (implying a similar level of development) are to be expected, it would be foolish to assume the same age pattern of infant mortality in pre-20th century populations or present populations suffering under a crisis: Historically the age-pattern of infant mortality was very much shaped by the interaction of seasonality effects, improper substitutes for breastfeeding, and deadly infectious diseases (Knodel and Kintner 1977; Huck 1995), factors which have lost relevance in the U.S. over the course of the 20th century. Likewise, an analysis of 21st century U.S. infant mortality yields little insight into the characteristics of infant death in parts of the world suffering from humanitarian crises and violent conflicts.

Insofar as the power-exponential hazard *does* generalize to populations other than the present-day U.S., it can become a valuable tool for working with low-quality data on the timing of infant deaths. Based on h_{PE} , one can calculate life table a_0 from coarse data; design model infant-life tables; smooth over data artifacts such as age-heaping; estimate seasonal effects on mortality separately from age effects, or include realistic infant mortality schedules into a simulation model.

A. Parameter estimates and confidence intervals for the power-exponential hazard

Table 3: The factor of mortality reduction over the first 7 days of life. Parameter estimates and 95% CIs calculated from the power-exponential hazard GLM fits for various U.S. infant cohorts.

		Female	Male
1995-1999			
APGAR	Very low [0,5)	1011 (826, 1242)	962 (810, 1157)
	Low [5,9)	8 (6, 10)	8 (6, 10)
	Regular 9+	10 (7, 14)	8 (5, 10)
Origin	Non-Hispanic Black	328 (282, 385)	315 (277, 357)
	Non-Hispanic White	303 (272, 340)	275 (249, 304)
	Hispanic	320 (262, 391)	277 (229, 331)
	Other	329 (228, 498)	303 (219, 444)
Prematurity	Extremely preterm <28w	524 (449, 604)	448 (399, 508)
	Very preterm [28,32)w	181 (135, 246)	145 (113, 188)
	Moderate to late preterm [32,37)w	147 (116, 185)	127 (103, 158)
	Term 37w+	58 (49, 67)	49 (43, 57)
Education	Elementary or less	281 (203, 385)	236 (178, 316)
	High school	280 (254, 312)	256 (232, 281)
	College or university	330 (286, 377)	303 (268, 345)
2000-2005			
APGAR	Very low [0,5)	1039 (866, 1241)	1008 (869, 1193)
	Low [5,9)	6 (5, 8)	7 (5, 8)
	Regular 9+	14 (11, 18)	13 (10, 16)
Origin	Non-Hispanic Black	318 (272, 373)	340 (299, 391)
	Non-Hispanic White	301 (268, 338)	277 (250, 304)
	Hispanic	326 (278, 389)	310 (268, 359)
	Other	348 (243, 508)	347 (258, 472)
Prematurity	Extremely preterm <28w	538 (471, 613)	477 (427, 531)
	Very preterm [28,32)w	194 (152, 249)	178 (141, 225)
	Moderate to late preterm [32,37)w	142 (115, 175)	119 (98, 144)
	Term 37w+	60 (51, 69)	58 (50, 66)
Education	Elementary or less	310 (221, 436)	290 (218, 397)
	High school	280 (248, 312)	272 (248, 300)
	College or university	320 (285, 366)	315 (282, 351)

Table 4: Estimated α parameters of power-exponential hazard GLM fits for various U.S. infant cohorts. Mean estimates and 95% confidence intervals are based on 1000 parametric bootstrap replications.

		Female	Male
1995-1999			
APGAR	Very low [0,5)	2.5e-2 (2.5e-2, 2.6e-2)	2.6e-2 (2.5e-2, 2.6e-2)
	Low [5,9)	2.9e-3 (2.7e-3, 3.2e-3)	3.3e-3 (3.1e-3, 3.6e-3)
	Regular 9+	3.0e-5 (2.9e-5, 3.2e-5)	3.8e-5 (3.6e-5, 3.9e-5)
Origin	Non-Hispanic Black	4.8e-4 (4.7e-4, 4.9e-4)	5.8e-4 (5.7e-4, 5.9e-4)
	Non-Hispanic White	2.0e-4 (1.9e-4, 2.0e-4)	2.5e-4 (2.4e-4, 2.5e-4)
	Hispanic	2.0e-4 (1.9e-4, 2.0e-4)	2.4e-4 (2.3e-4, 2.4e-4)
	Other	1.8e-4 (1.8e-4, 1.9e-4)	2.1e-4 (2.1e-4, 2.2e-4)
Prematurity	Extremely preterm <28w	2.4e-2 (2.3e-2, 2.4e-2)	2.8e-2 (2.7e-2, 2.8e-2)
	Very preterm [28,32)w	2.2e-3 (2.1e-3, 2.3e-3)	2.7e-3 (2.6e-3, 2.8e-3)
	Moderate to late preterm [32,37)w	4.3e-4 (4.1e-4, 4.4e-4)	4.9e-4 (4.8e-4, 5.0e-4)
	Term 37w+	6.3e-5 (6.2e-5, 6.5e-5)	7.5e-5 (7.3e-5, 7.6e-5)
Education	Elementary or less	2.5e-4 (2.4e-4, 2.6e-4)	2.9e-4 (2.8e-4, 3.1e-4)
	High school	2.7e-4 (2.7e-4, 2.8e-4)	3.4e-4 (3.4e-4, 3.4e-4)
	College or university	1.9e-4 (1.8e-4, 1.9e-4)	2.2e-4 (2.2e-4, 2.3e-4)
2000-2005			
APGAR	Very low [0,5)	1.8e-2 (1.8e-2, 1.8e-2)	1.8e-2 (1.7e-2, 1.8e-2)
	Low [5,9)	1.6e-3 (1.4e-3, 1.7e-3)	1.8e-3 (1.7e-3, 2.0e-3)
	Regular 9+	2.7e-5 (2.6e-5, 2.8e-5)	3.1e-5 (3.0e-5, 3.2e-5)
Origin	Non-Hispanic Black	4.5e-4 (4.4e-4, 4.6e-4)	5.4e-4 (5.3e-4, 5.5e-4)
	Non-Hispanic White	1.9e-4 (1.8e-4, 1.9e-4)	2.3e-4 (2.3e-4, 2.3e-4)
	Hispanic	1.8e-4 (1.8e-4, 1.9e-4)	2.2e-4 (2.2e-4, 2.3e-4)
	Other	1.7e-4 (1.6e-4, 1.8e-4)	2.0e-4 (1.9e-4, 2.1e-4)
Prematurity	Extremely preterm <28w	2.0e-2 (1.9e-2, 2.0e-2)	2.3e-2 (2.3e-2, 2.3e-2)
	Very preterm [28,32)w	1.7e-3 (1.6e-3, 1.8e-3)	2.0e-3 (1.9e-3, 2.1e-3)
	Moderate to late preterm [32,37)w	3.0e-4 (2.9e-4, 3.0e-4)	3.2e-4 (3.2e-4, 3.3e-4)
	Term 37w+	5.3e-5 (5.2e-5, 5.5e-5)	6.1e-5 (6.0e-5, 6.3e-5)
Education	Elementary or less	2.2e-4 (2.1e-4, 2.3e-4)	2.6e-4 (2.4e-4, 2.7e-4)
	High school	2.6e-4 (2.6e-4, 2.7e-4)	3.3e-4 (3.2e-4, 3.3e-4)
	College or university	1.8e-4 (1.7e-4, 1.8e-4)	2.1e-4 (2.1e-4, 2.1e-4)

Table 5: Estimated b parameters of power-exponential hazard GLM fits for various U.S. infant cohorts. Mean estimates and 95% confidence intervals are based on 1000 parametric bootstrap replications.

		Female	Male
1995-1999			
APGAR	Very low [0,5)	8.0e-3 (7.1e-3, 8.8e-3)	7.3e-3 (6.7e-3, 8.1e-3)
	Low [5,9)	2.2e-3 (1.7e-3, 2.7e-3)	2.5e-3 (2.1e-3, 3.0e-3)
	Regular 9+	7.0e-3 (6.7e-3, 7.2e-3)	7.2e-3 (6.9e-3, 7.4e-3)
Origin	Non-Hispanic Black	3.1e-3 (2.8e-3, 3.4e-3)	3.6e-3 (3.3e-3, 3.8e-3)
	Non-Hispanic White	4.5e-3 (4.3e-3, 4.8e-3)	4.5e-3 (4.3e-3, 4.7e-3)
	Hispanic	3.9e-3 (3.5e-3, 4.3e-3)	4.1e-3 (3.8e-3, 4.4e-3)
	Other	3.0e-3 (2.3e-3, 3.7e-3)	3.7e-3 (3.1e-3, 4.3e-3)
Prematurity	Extremely preterm <28w	9.4e-3 (8.9e-3, 9.9e-3)	9.2e-3 (8.8e-3, 9.6e-3)
	Very preterm [28,32]w	7.2e-3 (6.5e-3, 7.8e-3)	7.0e-3 (6.5e-3, 7.6e-3)
	Moderate to late preterm [32,37]w	5.0e-3 (4.6e-3, 5.4e-3)	5.1e-3 (4.8e-3, 5.6e-3)
	Term 37w+	5.1e-3 (4.9e-3, 5.3e-3)	5.3e-3 (5.1e-3, 5.5e-3)
Education	Elementary or less	3.8e-3 (3.2e-3, 4.3e-3)	3.8e-3 (3.3e-3, 4.3e-3)
	High school	3.7e-3 (3.5e-3, 3.9e-3)	4.0e-3 (3.8e-3, 4.2e-3)
	College or university	4.7e-3 (4.4e-3, 4.9e-3)	4.7e-3 (4.4e-3, 5.0e-3)
2000-2005			
APGAR	Very low [0,5)	7.7e-3 (7.0e-3, 8.4e-3)	7.6e-3 (7.1e-3, 8.1e-3)
	Low [5,9)	3.9e-3 (3.4e-3, 4.4e-3)	3.5e-3 (3.1e-3, 3.9e-3)
	Regular 9+	7.1e-3 (6.8e-3, 7.3e-3)	7.7e-3 (7.5e-3, 7.9e-3)
Origin	Non-Hispanic Black	4.1e-3 (3.8e-3, 4.3e-3)	3.8e-3 (3.5e-3, 4.0e-3)
	Non-Hispanic White	4.5e-3 (4.3e-3, 4.7e-3)	4.7e-3 (4.5e-3, 4.9e-3)
	Hispanic	4.0e-3 (3.6e-3, 4.3e-3)	4.4e-3 (4.1e-3, 4.7e-3)
	Other	3.4e-3 (2.7e-3, 4.1e-3)	3.7e-3 (3.1e-3, 4.3e-3)
Prematurity	Extremely preterm <28w	8.8e-3 (8.3e-3, 9.3e-3)	8.6e-3 (8.3e-3, 9.0e-3)
	Very preterm [28,32]w	7.7e-3 (7.1e-3, 8.3e-3)	7.2e-3 (6.7e-3, 7.8e-3)
	Moderate to late preterm [32,37]w	5.3e-3 (4.9e-3, 5.7e-3)	5.4e-3 (5.1e-3, 5.7e-3)
	Term 37w+	5.2e-3 (5.0e-3, 5.4e-3)	5.3e-3 (5.1e-3, 5.5e-3)
Education	Elementary or less	3.7e-3 (3.1e-3, 4.3e-3)	4.7e-3 (4.1e-3, 5.3e-3)
	High school	4.1e-3 (3.9e-3, 4.3e-3)	4.2e-3 (4.0e-3, 4.3e-3)
	College or university	4.8e-3 (4.5e-3, 5.0e-3)	4.8e-3 (4.6e-3, 5.0e-3)

Table 6: Estimated c parameters of power-exponential hazard GLM fits for various U.S. infant cohorts. Mean estimates and 95% confidence intervals are based on 1000 parametric bootstrap replications.

		Female	Male
1995-1999			
APGAR	Very low [0,5)	2.7e-3 (2.6e-3, 2.9e-3)	2.7e-3 (2.6e-3, 2.8e-3)
	Low [5,9)	8.1e-1 (7.1e-1, 9.2e-1)	7.9e-1 (7.1e-1, 8.8e-1)
	Regular 9+	5.7e-6 (4.2e-7, 2.6e-5)	1.6e-5 (1.2e-6, 7.2e-5)
Origin	Non-Hispanic Black	1.1e-3 (1.0e-3, 1.2e-3)	1.0e-3 (9.1e-4, 1.1e-3)
	Non-Hispanic White	5.6e-4 (5.2e-4, 6.1e-4)	5.9e-4 (5.5e-4, 6.4e-4)
	Hispanic	6.1e-4 (5.2e-4, 7.1e-4)	6.9e-4 (6.0e-4, 8.0e-4)
	Other	5.4e-4 (3.9e-4, 7.2e-4)	4.3e-4 (3.1e-4, 5.8e-4)
Prematurity	Extremely preterm <28w	1.7e-3 (1.6e-3, 1.8e-3)	1.5e-3 (1.4e-3, 1.6e-3)
	Very preterm [28,32)w	7.8e-4 (5.8e-4, 1.0e-3)	1.0e-3 (7.8e-4, 1.3e-3)
	Moderate to late preterm [32,37)w	5.7e-4 (4.5e-4, 7.2e-4)	8.2e-4 (6.5e-4, 1.0e-3)
	Term 37w+	1.3e-4 (9.2e-5, 1.8e-4)	1.3e-4 (9.2e-5, 1.8e-4)
Education	Elementary or less	5.3e-4 (3.9e-4, 6.7e-4)	6.5e-4 (5.1e-4, 8.3e-4)
	High school	6.3e-4 (5.8e-4, 6.8e-4)	6.4e-4 (6.0e-4, 6.9e-4)
	College or university	7.9e-4 (7.2e-4, 8.6e-4)	7.8e-4 (7.0e-4, 8.5e-4)
2000-2005			
APGAR	Very low [0,5)	2.6e-3 (2.4e-3, 2.7e-3)	2.3e-3 (2.2e-3, 2.4e-3)
	Low [5,9)	8.0e-1 (6.9e-1, 9.3e-1)	7.4e-1 (6.4e-1, 8.3e-1)
	Regular 9+	6.6e-7 (4.6e-8, 2.9e-6)	6.3e-9 (1.0e-10, 3.5e-8)
Origin	Non-Hispanic Black	8.2e-4 (7.3e-4, 9.1e-4)	7.4e-4 (6.7e-4, 8.1e-4)
	Non-Hispanic White	5.5e-4 (5.1e-4, 6.1e-4)	5.1e-4 (4.7e-4, 5.5e-4)
	Hispanic	7.0e-4 (6.2e-4, 7.9e-4)	7.0e-4 (6.2e-4, 7.9e-4)
	Other	6.3e-4 (4.8e-4, 8.0e-4)	4.2e-4 (3.2e-4, 5.3e-4)
Prematurity	Extremely preterm <28w	1.5e-3 (1.4e-3, 1.6e-3)	1.3e-3 (1.2e-3, 1.4e-3)
	Very preterm [28,32)w	5.6e-4 (4.3e-4, 7.2e-4)	7.1e-4 (5.8e-4, 8.7e-4)
	Moderate to late preterm [32,37)w	5.2e-4 (4.1e-4, 6.4e-4)	6.2e-4 (5.0e-4, 7.6e-4)
	Term 37w+	9.5e-5 (6.5e-5, 1.4e-4)	6.1e-5 (4.3e-5, 8.4e-5)
Education	Elementary or less	6.6e-4 (5.1e-4, 8.4e-4)	4.9e-4 (3.8e-4, 6.3e-4)
	High school	5.5e-4 (5.0e-4, 6.0e-4)	5.0e-4 (4.6e-4, 5.4e-4)
	College or university	7.7e-4 (7.0e-4, 8.5e-4)	7.1e-4 (6.6e-4, 7.8e-4)

Table 7: Estimated p parameters of power-exponential hazard GLM fits for various U.S. infant cohorts. Mean estimates and 95% confidence intervals are based on 1000 parametric bootstrap replications.

		Female	Male
1995-1999			
APGAR	Very low [0,5)	8.7e-1 (8.6e-1, 8.8e-1)	8.7e-1 (8.6e-1, 8.8e-1)
	Low [5,9)	9.3e-1 (9.0e-1, 9.7e-1)	9.3e-1 (9.1e-1, 9.6e-1)
	Regular 9+	1.6e-1 (1.5e-1, 1.7e-1)	1.5e-1 (1.4e-1, 1.6e-1)
Origin	Non-Hispanic Black	6.6e-1 (6.5e-1, 6.6e-1)	6.5e-1 (6.4e-1, 6.5e-1)
	Non-Hispanic White	6.0e-1 (6.0e-1, 6.1e-1)	6.0e-1 (5.9e-1, 6.0e-1)
	Hispanic	6.1e-1 (6.0e-1, 6.2e-1)	6.1e-1 (6.0e-1, 6.1e-1)
	Other	6.1e-1 (5.9e-1, 6.3e-1)	5.8e-1 (5.7e-1, 6.0e-1)
Prematurity	Extremely preterm <28w	7.4e-1 (7.4e-1, 7.5e-1)	7.2e-1 (7.1e-1, 7.2e-1)
	Very preterm [28,32)w	5.6e-1 (5.5e-1, 5.8e-1)	5.5e-1 (5.4e-1, 5.7e-1)
	Moderate to late preterm [32,37)w	5.3e-1 (5.1e-1, 5.4e-1)	5.3e-1 (5.2e-1, 5.4e-1)
	Term 37w+	3.7e-1 (3.6e-1, 3.8e-1)	3.5e-1 (3.5e-1, 3.6e-1)
Education	Elementary or less	5.9e-1 (5.7e-1, 6.0e-1)	5.8e-1 (5.7e-1, 6.0e-1)
	High school	6.0e-1 (6.0e-1, 6.1e-1)	5.9e-1 (5.9e-1, 6.0e-1)
	College or university	6.3e-1 (6.3e-1, 6.4e-1)	6.2e-1 (6.2e-1, 6.3e-1)
2000-2005			
APGAR	Very low [0,5)	8.7e-1 (8.6e-1, 8.8e-1)	8.6e-1 (8.5e-1, 8.6e-1)
	Low [5,9)	8.1e-1 (7.8e-1, 8.4e-1)	8.2e-1 (8.0e-1, 8.5e-1)
	Regular 9+	1.6e-1 (1.4e-1, 1.7e-1)	1.2e-1 (1.0e-1, 1.3e-1)
Origin	Non-Hispanic Black	6.3e-1 (6.3e-1, 6.4e-1)	6.3e-1 (6.3e-1, 6.4e-1)
	Non-Hispanic White	6.0e-1 (6.0e-1, 6.1e-1)	5.9e-1 (5.8e-1, 5.9e-1)
	Hispanic	6.2e-1 (6.2e-1, 6.3e-1)	6.2e-1 (6.1e-1, 6.3e-1)
	Other	6.2e-1 (6.0e-1, 6.4e-1)	6.0e-1 (5.8e-1, 6.1e-1)
Prematurity	Extremely preterm <28w	7.3e-1 (7.3e-1, 7.4e-1)	7.1e-1 (7.0e-1, 7.1e-1)
	Very preterm [28,32)w	5.5e-1 (5.4e-1, 5.6e-1)	5.6e-1 (5.5e-1, 5.7e-1)
	Moderate to late preterm [32,37)w	5.2e-1 (5.1e-1, 5.3e-1)	5.1e-1 (5.0e-1, 5.2e-1)
	Term 37w+	3.6e-1 (3.5e-1, 3.7e-1)	3.4e-1 (3.4e-1, 3.5e-1)
Education	Elementary or less	6.1e-1 (6.0e-1, 6.3e-1)	5.9e-1 (5.7e-1, 6.0e-1)
	High school	5.9e-1 (5.9e-1, 6.0e-1)	5.8e-1 (5.8e-1, 5.9e-1)
	College or university	6.3e-1 (6.2e-1, 6.4e-1)	6.2e-1 (6.2e-1, 6.3e-1)

References

- M. Abramowitz and I. A. Stegun. *Handbook of Mathematical Functions with Formulas, Graphs and Mathematical Tables*. National Bureau of Standards, Washington, D. C., 10th edition, 1964. doi:10.2307/2004284.
- M. Aitkin and D. Clayton. The fitting of exponential, Weibull and extreme value distributions to complex censored survival data using GLIM. *Journal of the Royal Statistical Society C*, 29(2):156–163, 1980. doi:10.2307/2986301.
- V. Apgar. A proposal for a new method of evaluation of the newborn infant. *Current Researches in Anesthesia and Analgesia*, 32(4):260–267, 1953. doi:10.1213/ANE.0b013e31829bdc5c.
- D. Avraam, J. P. de Magalhaes, and B. Vasiev. A mathematical model of mortality dynamics across the lifespan combining heterogeneity and stochastic effects. *Experimental Gerontology*, 48(8):801–811, 2013. doi:10.1016/j.exger.2013.05.054 .
- D. Avraam, S. Arnold, D. Jones, and B. Vasiev. Time-evolution of age-dependent mortality patterns in mathematical model of heterogeneous human population. *Experimental Gerontology*, 60:18–30, 2014. doi:10.1016/j.exger.2014.09.006.
- S. Berrut, V. Pouillard, P. Richmond, and B. M. Roehner. Deciphering infant mortality. *Physica A: Statistical Mechanics and its Applications*, 463:400–426, 2016. doi:10.1016/j.physa.2016.07.031.
- J. Bourgeois-Pichat. La mesure de la mortalité infantile. II. les causes de décès. *Population*, 6(3):459–480, 1951. doi:10.2307/1523958.
- D. R. Brillinger. A justification of some common laws of mortality. In *Transactions of the Society of Actuaries*, volume XIII, pages 115–119, 1961.
- C. G. Camarda, P. H. Eilers, and J. Gampe. Sums of smooth exponentials to decompose complex series of counts. *Statistical Modelling*, 16(4):279–296, 2016. doi:10.1177/1471082X16641796.
- J. H. Cha and M. Finkelstein. Justifying the Gompertz curve of mortality via the generalized Polya process of shocks. *Theoretical Population Biology*, 109:54–62, 2016. doi:10.1016/j.tpb.2016.03.001.
- M. K. Choe. Fitting the age pattern of infant and child mortality with the Weibull survival distribution. In *Asian and Pacific census forum*, volume 7, pages 10–13, 1981.
- D. Clayton and J. Cuzick. Multivariate generalizations of the proportional hazards model. *Journal of the Royal Statistical Society A*, 148(2):82–108, 1985. doi:10.2307/2981943.
- D. G. Clayton. Fitting a general family of failure-time distributions using GLIM. *Applied Statistics*, 32(2):102–109, 1983. doi:10.2307/2347288.
- D. R. Cox. Regression models and life-tables. *Journal of the Royal Statistical Society B*, 34(2):187–220, 1972. doi:10.1007/978-1-4612-4380-9_37.

- I. D. Currie. On fitting generalized linear and non-linear models of mortality. *Scandinavian Actuarial Journal*, 2016(4):356–383, 2016. doi:10.1080/03461238.2014.928230.
- J. de Beer and F. Janssen. A new parametric model to assess delay and compression of mortality. *Population Health Metrics*, 14(1):46, 2016. doi:10.1186/s12963-016-0113-1.
- P. H. C. Eilers and B. D. Marx. Flexible smoothing with B-splines and penalties. *Statistical Science*, 11(2):89–102, 1996. doi:10.1214/ss/1038425655.
- M. S. Finkelstein. Lifesaving explains mortality decline with time. *Mathematical Biosciences*, 196(2):187–197, 2005. doi:10.1016/j.mbs.2005.04.004.
- T. B. Gage and B. Dyke. Parameterizing abridged mortality tables: The Siler three-component hazard model. *Human Biology*, 58(2):275–291, 1986.
- L. Heligman and J. H. Pollard. The age pattern of mortality. *Journal of the Institute of Actuaries*, 107(1):49–80, 1980. doi:10.1017/s0020268100040257.
- P. Hougaard. Life table methods for heterogeneous populations: Distributions describing the heterogeneity. *Biometrika*, 71(1):75–83, 1984. doi:10.1093/biomet/71.1.75.
- P. Hougaard. Survival models for heterogeneous populations derived from stable distributions. *Biometrika*, 73(2):387–396, 1986. doi:10.1093/biomet/73.2.387.
- P. Hougaard. Frailty models for survival data. *Lifetime Data Analysis*, 1(3):255–273, 1995. doi:10.1007/bf00985760.
- P. Huck. Infant mortality and living standards of English workers during the industrial revolution. *The Journal of Economic History*, 55(3):528–550, 1995. doi:10.1017/s0022050700041620.
- H. C. Kinney and B. T. Thach. The sudden infant death syndrome. *New England Journal of Medicine*, 361(8):795–805, 2009. doi:10.1056/nejmra0803836.
- J. Knodel and H. Kintner. The impact of breast feeding patterns on the biometric analysis of infant mortality. *Demography*, 14(4):391–409, 1977. doi:10.2307/2060586.
- E. H. Lehman. Shapes, moments and estimators of the Weibull distribution. *IEEE Transactions on Reliability*, 12(3):32–38, 1963. doi:10.1109/tr.1963.5218214.
- D. A. Levitis. Before senescence: the evolutionary demography of ontogenesis. *Proceedings of the Royal Society B*, 278(1707):801–809, 2011. doi:10.1098/rspb.2010.2190.
- K. S. Lomax. Business failures: Another example of the analysis of failure data. *Journal of the American Statistical Association*, 49(268):847–852, 1954. doi:10.1080/01621459.1954.10501239.
- A. W. Marshall and I. Olkin. *Life Distributions*. Springer, New York, 2007. ISBN 9780387203331. doi:10.1007/978-0-387-68477-2.
- P. McCullagh and J. A. Nelder. *Generalized Linear Models*. Monographs on Statistics and Applied Probability. CRC Press, New York, 2nd edition, 1989. ISBN 9780412317606.

- D. McFadden. Conditional logit analysis of qualitative choice behavior. In P. Zarembka, editor, *Frontiers in econometrics*, pages 105–142. Academic Press, New York, 1974.
- C. J. Mode and R. C. Busby. An eight-parameter model of human mortality—the single decrement case. *Bulletin of Mathematical Biology*, 44(5):647–659, 1982. doi:10.1007/bf02462273.
- National Center for Health Statistics. Birth cohort linked birth-infant death data files (U.S. data), 2016. URL ftp://ftp.cdc.gov/pub/Health_Statistics/NCHS/Datasets/DVS/cohortlinkedus/.
- Oppermann. On the graduation of life tables, with special application to the rate of mortality in infancy and childhood. *Insurance Record*, page 42, Feb. 1870. Minutes from a meeting in the Institute of Actuaries.
- A. Prékopa. On secondary processes generated by a random point distribution of Poisson type. *Annales Univ. Sci. Budapest de Eötvös Nom. Sectio Math*, 1:153–170, 1958.
- R Core Team. *R: A Language and Environment for Statistical Computing*. R Foundation for Statistical Computing, Vienna, Austria, 2020. URL <https://www.R-project.org/>.
- H. Rinne. *The Weibull Distribution*. CRC Press, New York, 1st edition, 2009. ISBN 978-1-4200-8743-7. doi:10.1201/9781420087444.
- A. Rogers and J. S. Little. Parameterizing age patterns of demographic rates with the multiexponential model schedule. *Mathematical Population Studies*, 4(3):175–195, 1994. doi:10.1080/08898489409525372.
- W. Siler. A competing-risk model for animal mortality. *Ecology*, 60(4):750–757, 1979. doi:10.2307/1936612.
- J. F. Steffensen. Infantile mortality from an actuarial point of view. *Scandinavian Actuarial Journal*, 1930(2):272–286, 1930. doi:10.1080/03461238.1930.10416902.
- B. L. Strehler and A. S. Mildvan. General theory of mortality and aging. *Science*, 132 (3418):14–21, 1960. ISSN 0036-8075. doi:10.1126/science.132.3418.14.
- T. N. Thiele. On a mathematical formula to express the rate of mortality throughout the whole of life, tested by a series of observations made use of by the Danish Life Insurance Company of 1871. *Journal of the Institute of Actuaries*, 16(5):313–329, 1871. doi:10.1017/s2046167400043688.
- R. Thompson and R. J. Baker. Composite link functions in Generalized Linear Models. *Journal of the Royal Statistical Society C*, 30(2):125–131, 1981. doi:10.2307/2346381.
- J. W. Vaupel and A. I. Yashin. The deviant dynamics of death in heterogeneous populations. Technical report, Laxenburg, Austria, 1983. URL <http://user.demogr.mpg.de/jwv/pdf/IIASA-83-001.pdf>.
- J. W. Vaupel and A. I. Yashin. Heterogeneity's ruses: Some surprising effects of selection on population dynamics. *The American Statistician*, 39(3):176–185, 1985. doi:10.2307/2683925.

- J. W. Vaupel and Z. Zhang. Attrition in heterogeneous cohorts. *Demographic Research*, 23(26):737–748, 2010. doi:10.4054/DemRes.2010.23.26.
- J. W. Vaupel, K. G. Manton, and E. Stallard. The impact of heterogeneity in individual frailty on the dynamics of mortality. *Demography*, 16(3):439–54, 1979. doi:10.2307/2061224.
- A. Wienke. *Frailty Models in Survival Analysis*. Biostatistics Series. Chapman and Hall, Boca Raton, 2011. ISBN 978-1-4200-7388-1. doi:10.1111/j.1541-0420.2012.01769.x.
- T. Wittstein and D. A. Bumsted. The mathematical law of mortality. *Journal of the Institute of Actuaries and Assurance Magazine*, 24(3):153–173, 1883. doi:10.1017/s0020268100006260.
- World Health Organization. *Neonatal and Perinatal Mortality: Country, Regional and Global Estimates*. World Health Organization, 2006. ISBN 9241563206.
- World Health Organization. *Health in 2015. From Millennium Development Goals to Sustainable Development Goals*. World Health Organization, 2015. ISBN 9789241565110. doi:10.1111/padr.12006.

Chapter III

The impact of population heterogeneity on the age trajectory of neonatal mortality

The impact of population heterogeneity on the age trajectory of neonatal mortality

Jonas Schöley*

Abstract

Background The risk of death declines rapidly over the first month of life. It has been theorized that the fast pace of the decline is explained by hidden population heterogeneity resulting in a mortality selection process whereby the frailest infants leave the population at the fastest rate. A competing explanation situates the rapid mortality decline on the individual level, pointing towards the risky transition of birth and the subsequent adaptation of the newborn to the unfamiliar surroundings.

Objective To estimate heterogeneity in the level and shape of age-specific mortality within a cohort of newborns and to quantify the degree to which mortality selection explains the shape of the average neonatal mortality trajectory.

Methods Given individual-level data on 20,322,147 births and 82,562 neonatal deaths from the 2008-2012 U.S. birth cohort, I calculate life-tables for 252 mutually exclusive strata each defined by a unique combination of observed birth characteristics. Using this information, I characterize the distribution of mortality risk and its evolution over the first 28 days of life and decompose changes in key characteristics of this distribution – the mean, the variance, and the mean-mode ratio – into a mortality selection and a direct component.

Results The average age trajectory of neonatal mortality is highly influenced by a small group of frail newborns and does not reflect the rather flat age effect estimated for the healthy majority of the birth cohort. While the risk decline over the first day of life is substantially influenced by mortality selection, the overall age trajectory is better explained by the convergence of high-risk towards low-risk population strata.

*Interdisciplinary Centre on Population Dynamics, University of Southern Denmark. Correspondence: jschooley@health.sdu.dk. During the writing of this article the author was a guest at the Max-Planck Institute for Demographic Research and funded by a grant from AXA Insurance.

1. Introduction

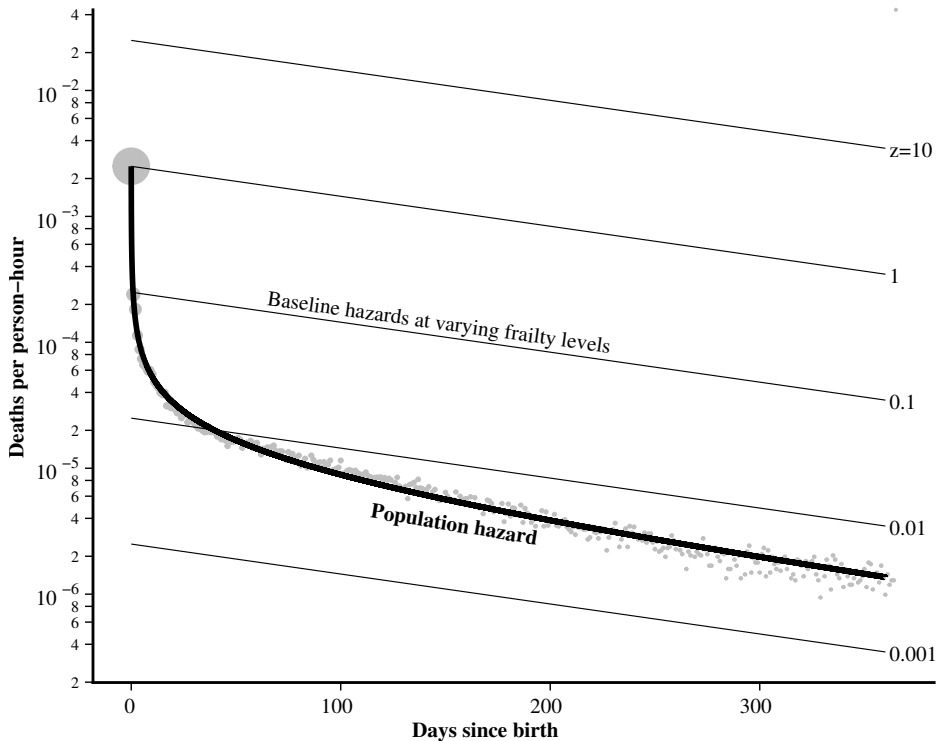
Never again throughout the existence of a cohort will the hazard of death change as rapidly as it does during the first few weeks following birth. For the 2009–2012 U.S. birth cohort, the risk of death falls tenfold over the first day of life, and again by a factor of ten over the next four weeks. But how reflective is this population-level phenomenon of a single newborn’s risk trajectory? Is the period of exceptional risk right after birth part of every human’s experience, or have we been led astray by one more of “Heterogeneity’s Ruses” (Vaupel and Yashin 1985)? In this paper, I seek to quantify the impact of population heterogeneity on the age trajectory of neonatal mortality based on *observed* mortality differences in a cohort of U.S. born infants.

Populations in which members are heterogeneous concerning their risk of death are subjected to mortality selection, which may be defined as the changing composition of a cohort over age due to heterogeneous mortality. As mortality is nothing but the rate of leaving a population due to death, with time, the proportion of low-mortality strata will increase, whereas strata with high mortality will become less prevalent. In consequence, any observed change of a cohorts trait over age (such as income, health, risk of death) may either be the result of within-stratum trait changes or result from a change in the cohort’s composition along those strata over age due to mortality selection.

A rich (bio)demographic literature exists for the special case of mortality selection driving the shape of the population level hazard of death over age thus explaining phenomena such as late-life mortality plateaus (e.g., Beard 1959; Vaupel et al. 1979; Vaupel and Carey 1993; Steinsaltz and Wachter 2006; Missov and Vaupel 2015; Colchero and Kiyakoglu 2019), the adolescent “accident hump” (Remund 2015), declining mortality following surgery (Hougaard 1986) or the age pattern of early life mortality (Vaupel and Yashin 1983; Hsieh 1985; Trussell and Richards 1985; Avraam et al. 2014). All of the aforementioned literature features frailty models as a means to formalize, understand, and estimate the impact of population heterogeneity on the age trajectory of mortality. In these models, an individual’s risk of death depends on a random quantity coined *frailty* (Vaupel et al. 1979) that, on account of being unobserved, may be thought of as hidden heterogeneity between members of a cohort. Frailty is most commonly expressed in a proportional hazards framework where the hazard of death at age x of an individual with frailty z is given by $h(x|z) = zh_0(x)$ and $h_0(x)$ is a *baseline hazard* shared by all members of the population. An expression for the population/marginal/unconditional hazard $\bar{h}(x)$ can be derived¹ by assuming a distribution of survival times for the case where $z = 1$ with corresponding hazard h_0 and a distribution for the frailties at age $x = 0$. It is then possible to fit $\bar{h}(x)$ to observed survival times or a life table and – given the parameters of the fit and an array of formal relationships (Vaupel and Yashin 1983; Vaupel and Missov 2014) – to determine how hidden heterogeneity acts in the population under investigation. Herein lies one central attraction of frailty models: they allow inference about population heterogeneity even if none has been observed. The quality of the inference then, of course, crucially depends on the adequacy of the assumptions going into the model.

¹ An excellent introduction to this technique can be found in Wienke (2011).

Figure 1: Predicted hazard (black) vs. life table mortality rates (gray) for the 2008–2012 U.S. birth cohort. Daily mortality rates over the first 365 days of life are well described by a Gompertz baseline distribution with Hougaard distributed frailties. Via the process of mortality selection, a mixture of log-linear individual level hazards, here drawn for various levels of frailty z , gives rise to a population level hazard with extreme curvature on the log scale. The area of the circles is in rough proportion to the number of deaths each day.



A frailty explanation for the age trajectory of mortality following birth has been put forward multiple times in the literature but never seriously followed up upon. Vaupel and Yashin (1983) modeled the hazard of infant death, assuming a constant baseline hazard and multiplicative Gamma distributed frailty with unity mean and a variance of 500. Such a model implies that the majority of infants at birth are at virtually no risk of death with a small minority of critical cases². Trussell and Richards (1985) demonstrated how sensitive the choice of baseline hazard is when modeling infant mortality via a frailty model, with the Gompertz leading to decreasing and the Weibull to increasing individual-level risk trajectories. Hougaard (1984) hypothesized that the high mortality during the first year of life and the subsequent rapid decline might be the result of an “extreme frailty distribution” upon birth, meaning a distribution with a long right tail, and he proposed the inverse-Gamma distribution as a suitable candidate. Hougaard (1986) introduced a

² A Gamma distribution with unity mean and variance 500 has more than 98.8 percent of its probability mass below the mean and 0.24 percent at least 100 times above.

particularly flexible family of frailty distributions, including the Gamma, the inverse-Gaussian, and distributions derived from the positive-stable. He fitted a corresponding frailty model to data on time until death after myocardial infarct, a survival scenario not unlike the neonatal case as there is a stressor at time zero with mortality declining quickly and monotonically thereafter.

Indeed the Hougaard frailty model with a Gompertz baseline hazard (see Appendix A for the model specification) gives an excellent fit not only to neonatal mortality but to the entire day-to-day infant life table of the 2009–2012 U.S. birth cohort, capturing the extremely steep decrease in hazard following birth and the subsequent log-linear decline during the post-neonatal period (Figure 1). While by no means a proof of the frailty hypothesis, this simple model shows that a mortality selection explanation is consistent with the dynamics of daily mortality rates observed on the population level.

More recently, the heterogeneous frailty hypothesis was discussed by Levitis (2011) and Levitis and Martínez (2013) as an alternative to evolutionary explanations for “ontogenescence,” i.e., the declining hazard of death following birth observed in many species. Via simulation Levitis demonstrated how age-independent individual-level risk leads to age-dependent population mortality rates. In a further variation on the theme, Avraam et al. (2014) captured the decline in mortality from birth to adolescence by employing a discrete frailty model with subgroups featuring either exponentially increasing or constant hazards.

Without data on heterogeneous risks, the hypothesis of mortality selection can only be tested indirectly. While frailty models do provide heterogeneity estimates from population-level data alone, this can only be taken as suggestive evidence for a selection explanation. The estimated amount of heterogeneity depends crucially on the choice of baseline hazard, the choice of frailty distribution, the assumption of fixed versus changing frailty, and the specific way that frailty modulates the baseline hazards (proportional hazards vs. accelerated failure time). These assumptions can not be validated on population-level data as different model specifications yield the same parametric form for the marginal hazard (Trussell and Richards 1985; Hoem 1990; Yashin et al. 2000). I argue that a more convincing case for the impact of population heterogeneity on the age trajectory of mortality can be made by analyzing the distribution of risk in a cohort stratified by *observed* characteristics. For infants, such data is available on birth certificates.

A birth certificate contains a wealth of information that identifies potentially frail newborns. Routinely collected are birth weight, the length of pregnancy, and the Apgar score, an index of the vitality of the child shortly after delivery. The combination of these characteristics delineates hundreds of highly specific subpopulations within a single birth cohort and, based on the distribution of deaths and exposure times across these strata, I analyze the impact of population heterogeneity on the age trajectory of neonatal mortality using both discrete-time life table decomposition methodology and continuous-time hazard modeling in connection with results from formal demography. This approach of describing mortality selection along observed mortality differentials has little precedence as far as human mortality is concerned, an exception being Remund (2015) who, based

on an analysis of French individual level survival data with covariates, found that selection effects contribute to the “accident hump” observed in the hazard trajectory of young adults.

Following the description of the U.S. 2008–2012 birth cohort, I outline a discrete life table approach and a complementary continuous time hazard method to quantify population heterogeneity and mortality selection and its impact on the age trajectory of neonatal mortality. This is followed by results on the distribution of neonatal mortality risks as it changes over age, the heterogeneity of hazard trajectories, and various decompositions of population-level statistics along the age dimension. A discussion of the results concludes the paper.

2. Data

As population heterogeneity drives mortality selection, one can learn about selection effects by estimating the hazard of death across a diverse collection of population strata. Such estimation is possible given the publicly available “NCHS Cohort Linked Birth – Infant Death Data Files” (National Center for Health Statistics 2016) which contain a complete census of births and infant deaths on the territory of the United States (excluding overseas territories) and feature most fields present on the birth and death certificates. The size and detail of the data allow the calculation of neonatal life tables over hundreds of subpopulations, capturing observed heterogeneity in mortality following birth.

To increase the sample size and thus the reliability of the stratum specific mortality estimates, I pool births and deaths across cohorts 2008 to 2012. This leaves a sample size of 20,322,147 births contributing 567,031,738 person-days of exposure to risk over the first 28 days of life, during which 82,562 neonatal deaths were registered.

Following the practice of statistical offices, I compute mortality rates based on *all* registered births and deaths, including cases with missing data on key birth characteristics and unreasonable covariate combinations (e.g., extremely preterm delivery with average birth weight). While this approach challenges any causal interpretation of the determinants of neonatal death, it allows one to capture, in great detail, the observed heterogeneity giving rise to the usual population-level estimates. For this paper, it is of no concern whether the relationship between observed characteristics at birth and risk of death is causal or not as the phenomenon of interest – mortality selection – is induced by any mortality differential between population strata, no matter the cause.

For stratification, I use the information on birth weight, age of gestation at delivery, and 5 minute Apgar score. These variables are routinely recorded upon birth and highly predictive of neonatal death (Pollack et al. 2000; Casey et al. 2001; Park et al. 2018). As the inclusion of further strata only contributes minimal additional heterogeneity compared to what is already captured by the Apgar-birth weight-prematurity trias but considerably increases the computational demands of the model fitting procedure, I opted against it.

The variables are defined and discretized as follows:

Gestation at delivery alias prematurity The number of weeks from conception to delivery commonly estimated by the time since the first day of the mother's last menstrual cycle plus 14 days. Discretized into five groups *Extremely preterm* (earlier than 28 weeks), *Very preterm* (28 to 32 weeks), *Moderate to late preterm* (32 to 37 weeks), *Term or post-term* (37 weeks or later), and *Missing*.

Birth weight The weight of the newborn child measured in the minutes following birth discretized into the five categories *Extremely low* (<1000g), *Very low* (1000–1500g), *Low* (1500–2500g), *Regular or high* (2500g and above) and *Missing*.

5 minute Apgar score A measure of the infant's physical condition five minutes following birth, based on muscle activity, pulse, response to stimulation, skin color, and respiration of the newborn (Apgar 1953). Vitality increases over integers zero to ten, with missings being treated explicitly as a twelfth category.

Table 1 shows births, death counts, and empirical 28-day survival for the complete 2008 to 2012 birth cohort by level of gestation, birth weight, and Apgar score, respectively.

Table 1: Summary statistics of the U.S. 2008–2012 birth cohort.

	Births	(%)	Deaths	(%)	% 28 day survival
Total	20,322,147	(100.0)	82,562	(100.0)	99.5
5 minute Apgar score					
0	9,981	(0.1)	5,154	(6.3)	48.3
1	45,091	(0.3)	28,430	(34.5)	36.9
2	30,569	(0.2)	9,839	(12.0)	67.8
3	31,941	(0.2)	4,987	(6.1)	84.3
4	43,408	(0.3)	3,705	(4.5)	91.4
5	72,970	(0.4)	3,781	(4.6)	94.8
6	135,842	(0.7)	4,456	(5.4)	96.7
7	364,256	(1.8)	5,119	(6.3)	98.5
8	2,017,526	(10.0)	5,577	(6.8)	99.7
9	16,746,692	(82.5)	7,869	(9.6)	99.9
10	715,842	(3.6)	242	(0.3)	99.9
(Missing)	108,029	(0.6)	3,403	(4.2)	96.8
Gestation at delivery					
Extremely preterm	149,760	(0.8)	50,606	(61.3)	66.2
Very preterm	246,770	(1.3)	6,990	(8.5)	97.1
Moderate to late preterm	2,029,693	(10.0)	9,484	(11.5)	99.5
Term or post-term	17,870,545	(88.0)	14,493	(17.6)	99.9
(Missing)	25,379	(0.2)	989	(1.2)	96.1
Birth weight					
Extremely low	146,303	(0.8)	52,350	(63.5)	64.2
Very low	151,709	(0.8)	5,692	(6.9)	96.2
Low	1,355,547	(6.7)	10,573	(12.9)	99.2
Regular or high	18,663,662	(91.9)	13,363	(16.2)	99.9
(Missing)	4,926	(0.1)	584	(0.8)	88.1

3. Methods

From neonatal life tables stratified by birth characteristics, I derive the empirical distribution of mortality rates conditioned on time since birth for a cohort of newborns. Age differences in three key characteristics of this distribution – the mean, the variance, and the mean to mode ratio – are then decomposed into components due to mortality selection and due to “direct” effects. Adopting a continuous-time perspective, I estimate hazard trajectories and survival curves for every subpopulation and a corresponding population hazard. By employing the Vaupel-Zhang equality, I calculate the degree to which the between-stratum variance in hazard rates compounds the slope of the population hazard at selected exact ages.

3.1 Stratified infant life-tables

Consider a cohort of $i = 1, \dots, N$ newborns stratified into subpopulations $k = 1, \dots, K$ according to the combined discrete characteristics birth weight, age of gestation at birth and five minute Apgar score. Observed for every newborn are a survival time t_{ik} in days since birth censored at day 28 and a binary death indicator δ_{ik} . I partition the survival time into $j = 1, \dots, J$ non-overlapping daily age intervals $[x_j, x_j + 1)$, where x_j is the start of the j th age interval, and for each interval calculate stratum specific death counts $D_{jk} = \sum_i \delta_{ijk}$, population alive at the beginning of the age interval

$$N_{jk} = \begin{cases} \text{Births}_k & \text{for } j = 1 \\ \text{Births}_k - \sum_{s=1}^{s=j} D_{j=s,k} & \text{for } j > 1 \end{cases},$$

and person-days of exposure $E_{jk} = N_{j+1,k} + a_{jk} D_{jk}$, with a_{jk} as the average time of death of those dying in age interval j . For the first day of life I calculate a_j using information on the proportion of deaths during the first hour of life while for the other days the usual mid-point assumption $a_{jk} = 0.5$ is employed. I then calculate stratum specific life table death rates $m_{jk} = \frac{D_{jk}}{E_{jk}}$ for each age interval and corresponding population level death rates $\bar{m}_j = \frac{\sum_k D_{jk}}{\sum_k E_{jk}}$ and relative exposures $p_{jk} = \frac{E_{jk}}{\sum_k E_{jk}}$. These tabulated counts, exposures, rates and proportions form the basis of all subsequent analyses.

3.2 Discrete-time life table analysis

Decomposing change in mean mortality over age

Using the shorthand $\Delta f_x = f_{x+1} - f_x$ let $\Delta \bar{m}_j$ denote the change in population-level mortality from age interval j to $j+1$. How much of this difference is explained by a change of the subpopulation hazards and how much due to a change in the population composition induced by mortality selection? A straightforward solution to this decomposition problem can be derived by writing $\bar{m}_j = \sum_k p_{jk} m_{jk}$ and applying the product rule for finite

differences (Boole 1880) to the equivalent products $m_{jk}p_{jk} = p_{jk}m_{jk}$ yielding the two expressions

$$\begin{aligned}\Delta\bar{m}_j &= \sum_k p_{jk}\Delta m_{jk} + \sum_k m_{j+1,k}\Delta p_{jk} \\ &= \sum_k m_{jk}\Delta p_{jk} + \sum_k p_{j+1,k}\Delta m_{jk},\end{aligned}$$

which when averaged give the well known Kitagawa decomposition (Kitagawa 1955),

$$\Delta\bar{m}_j = \underbrace{\sum_k \frac{p_{jk} + p_{j+1,k}}{2}\Delta m_{jk}}_{\text{Direct change } \Delta\bar{m}_j^D} + \underbrace{\sum_k \frac{m_{jk} + m_{j+1,k}}{2}\Delta p_{jk}}_{\text{Compositional change } \Delta\bar{m}_j^C}. \quad (1)$$

The two terms represent the change in the population mortality rate due to changes in the group-specific mortality rates and due to changing group composition. Of particular interest is the ratio $\frac{\Delta\bar{m}_j^C}{\Delta\bar{m}_j}$, which for $\Delta\bar{m}_j^C < 0$ and $\Delta\bar{m}_j < 0$ is the share of the decline in population mortality explained by a compositional shift of the population. If mortality selection is indeed the main driver of the age decline in mortality over the neonatal period, then the aforementioned ratio has to be greater than 0.5.

Decomposing change in mortality rate variance over age

In addition to compounding the effect of age on the average risk of death, mortality selection can lower the variance of mortality rates across population strata as the survivors concentrate in more resilient subgroups. Alternatively, any change in population variance may result from stratum specific mortality rates converging over age. Because the variance of mortality rates across strata k among the survivors in age group j is the weighted average $v_j(x) = \sum_k p_{jk}s_{jk}$, with $s_{jk} = (m_{jk} - \bar{m}_j)^2$, one can follow the same strategy as before to yield the Kitagawa-style decomposition

$$\Delta v_j = \underbrace{\sum_k \frac{p_{jk} + p_{j+1,k}}{2}\Delta s_{jk}}_{\text{Direct change } \Delta v_j^D} + \underbrace{\sum_k \frac{s_{jk} + s_{j+1,k}}{2}\Delta p_{jk}}, \quad (2)$$

with v_j^D denoting the change in variance due to convergence or divergence of stratum specific mortality rates over age towards the population mean and v_j^C the age-decline in variance due to changing population composition, i.e., mortality selection.

Decomposing change in the ratio of mean to modal mortality over age

If the distribution of death rates in a cohort of infants exhibits positive skewness, mortality selection can reduce the mean-mode ratio of this distribution by “thinning the tail,” i.e., by

reducing the relative proportion of very frail subpopulations. However, any such decline may also result from genuine convergence of stratum specific death rates towards the death rates of the most prevalent stratum, the modal mortality rate, formally $\mathcal{M}_j = m_{j,k=r}$ with r such that $p_{j,k=r} = \max(p_{j1}, \dots, p_{jK})$.

A Kitagawa-style decomposition of the mean-mode ratio $\frac{\bar{m}_j}{\mathcal{M}_j} = \sum_k p_{jk} \frac{m_{jk}}{\mathcal{M}_j}$, shortened to r_j , gives the two components

$$\Delta r_j = \underbrace{\sum_k \frac{p_{jk} + p_{j+1,k}}{2} \Delta \frac{m_{jk}}{\mathcal{M}_j}}_{\text{Direct change } \Delta r_j^D} + \underbrace{\sum_k \frac{\frac{m_{jk}}{\mathcal{M}_j} + \frac{m_{j+1,k}}{\mathcal{M}_{j+1}}}{2} \Delta p_{jk}}_{\text{Compositional change } \Delta r_j^C}, \quad (3)$$

where Δr_j^D captures the changing ratios of stratum specific mortality rates to modal mortality and Δr_j^C referring to changes in the population composition.

3.3 Continuous-time hazard analysis

In the following, I outline a methodology to decompose the age derivative of the population hazard of death into a “direct” component reflecting actual age-effect within the population strata, and a “compositional component” capturing the confounding effect of population heterogeneity.

Estimating stratum specific hazard and survival

Stratum specific hazards during the neonatal period are well captured by the expression

$$h_k(x) = e^{\beta_{0k} + \beta_{1k} \log(x+1) + \beta_{2k} \log^2(x+1)}, \quad (4)$$

which can be interpreted as a Weibull hazard extended by a log-quadratic term over day of life (Appendix B). The curve has the advantage of being linear on the log scale, thus allowing it to be fit as a generalized linear mixed/multilevel model, which greatly facilitates a stable estimation of stratum specific hazards. There are in total 252 strata in the population of newborns with each stratum k marking a unique combination of “Prematurity,” “Birth weight,” and “Apgar score” levels. Fitting the hazard separately to each stratum will result in erratic estimates as some strata do not contain enough observations to inform the model. A solution to this problem is to fit a multilevel model where instead of estimating $\beta_{0k}, \beta_{1k}, \beta_{2k}$ directly one models the coefficient’s distribution at different grouping levels.

Given the observed death counts D_{jk} in age group j and stratum k and associated person-days of exposure to risk E_{jk} I fit the model

$$\begin{aligned} D_{jk} &\sim \text{Pois}(\lambda_{jk} E_{jk}) \\ \lambda_{jk} &= e^{\beta_{0k} + \beta_{1k} \log(x_{jk}+1) + \beta_{2k} \log^2(x_{jk}+1)}, \end{aligned} \quad (5)$$

where λ_{jk} are mortality rates by age group and stratum. For each stratum, a smooth hazard is recovered by evaluating λ_{jk} over a continuous range of ages x as in equation (4).

The stratum specific coefficients $\beta_{0k}, \beta_{1k}, \beta_{2k}$ are sums of baseline coefficients β , prematurity effects β^{Pm} , prematurity-birth weight interactions $\beta^{Pm \times Bw}$, and prematurity-birth weight-Apgar interactions $\beta^{Pm \times Bw \times Ap}$ resulting in the multilevel structure

$$\begin{pmatrix} \beta_{0k} \\ \beta_{1k} \\ \beta_{2k} \end{pmatrix} = \underbrace{\begin{pmatrix} \beta_0 \\ \beta_1 \\ \beta_2 \end{pmatrix}}_{\text{lvl 0 baseline coef.}} + \underbrace{\begin{pmatrix} \beta_{0,p[k]}^{Pm} \\ \beta_{1,p[k]}^{Pm} \\ \beta_{2,p[k]}^{Pm} \end{pmatrix}}_{\text{lvl 1 deviations by prematurity}} + \underbrace{\begin{pmatrix} \beta_{0,p[k],b[k]}^{Pm \times Bw} \\ \beta_{1,p[k],b[k]}^{Pm \times Bw} \\ \beta_{2,p[k],b[k]}^{Pm \times Bw} \end{pmatrix}}_{\text{lvl 2 deviations by birth weight given prematurity}} + \underbrace{\begin{pmatrix} \beta_{0,p[k],b[k],a[k]}^{Pm \times Bw \times Ap} \\ \beta_{1,p[k],b[k],a[k]}^{Pm \times Bw \times Ap} \\ \beta_{2,p[k],b[k],a[k]}^{Pm \times Bw \times Ap} \end{pmatrix}}_{\text{lvl 3 deviations by Apgar given prematurity and birth weight}}$$

where $p[k], b[k]$ and $a[k]$ denote the prematurity, birth weight and Apgar level associated with stratum k . Except for the baseline β 's each set of coefficients is assumed to be drawn from a multivariate-Normal distribution with zero mean and covariance matrix

$$\Sigma = \begin{pmatrix} \sigma_{\beta_0}^2 & \sigma_{\beta_0\beta_1} & \sigma_{\beta_0\beta_2} \\ \sigma_{\beta_0\beta_1} & \sigma_{\beta_1}^2 & \sigma_{\beta_1\beta_2} \\ \sigma_{\beta_0\beta_2} & \sigma_{\beta_1\beta_2} & \sigma_{\beta_2}^2 \end{pmatrix},$$

with separate estimates for levels one to three.

Treating the coefficients as realizations from a multivariate-Normal distribution with zero mean acts as a regularizer on the estimated hazard trajectories. In cases where zero or very few deaths are observed, the stratum specific deviations will be “pulled” towards zero with the effect that the estimated hazard resembles the hazard of the next higher hierarchy level (Gelman and Hill 2007). Take as an example the 303 infants delivered “Very preterm” with “Very low” birth weight and given an Apgar score of 10. Because all newborns survived the neonatal period, there is no information available to learn the shape of the underlying hazard. In the multilevel model, the larger population of infants delivered “Very preterm” with “Very low” birth weight will inform the hazard of the Apgar 10 subgroup. If plenty of data is available, then the hazard estimate will follow that data closely.

I fit model (5) as a Generalized Linear Mixed Model using the `lme4` library in R (Bates et al. 2015) and use the fitted coefficients to compute stratum specific hazard trajectories and

survival curves – the basis for the Vaupel-Zhang decomposition – using the expressions given in Appendix C.

Vaupel-Zhang decomposition

The Vaupel-Zhang equality (Vaupel and Zhang 2010) states that in any cohort stratified by some random characteristic K with initial distribution $\pi_k = P(K = k)$ the age derivative of the average hazard of death amongst the survivors at age x can be written as

$$\dot{\bar{h}}(x) = \bar{h}(x) - \sigma_h^2(x),$$

where $\bar{h}(x)$ denotes average slope and $\sigma_h^2(x)$ the average variance of hazards for the survivors at x . This result can be interpreted as a decomposition of the slope in the population hazard at x into a direct and a compositional component: The first component is based upon the actual slopes of hazards within each stratum k . Only if the population is completely homogeneous with respect to the levels of their hazards is the slope in the population hazard equal to the average slope in the stratum specific hazards. When, however, the variance of hazards is not zero, i.e., the population differs in their risk of death, mortality selection biases the slope in the population level hazard downwards. In other words, the trajectory of the population hazard over age is explained by the average hazard trajectory across population strata compounded by heterogeneity in the level of hazard.

The quantity of interest is the ratio $v(x) = \frac{-\sigma_h^2(x)}{\bar{h}(x)}$ which, given that $\dot{\bar{h}}(x) < 0$, is the share of decline in the population hazard at x explained by population heterogeneity in the level of mortality. From the observed distribution of birth characteristics $\pi_k = \frac{\text{Births}_k}{\sum_k \text{Births}_k}$ and the estimated stratum specific hazards $h_k(x)$ and survival $S_k(x)$ I calculate the population survival curve $S(x) = \sum_k \pi_k S_k(x)$ and the stratum distribution conditioned on survival to a given age $\pi_k(x) = \frac{S_k(x)\pi_k}{S(x)}$ which in turn gives rise to the population hazard curve $\bar{h}(x) = \sum_k \pi_k(x)h_k(x)$, and the variance of hazards over population strata $\sigma_h^2(x) = \sum_k \pi_k(x)(h_k(x) - \bar{h}(x))^2$. See Appendix C for a derivation of the stated equalities.

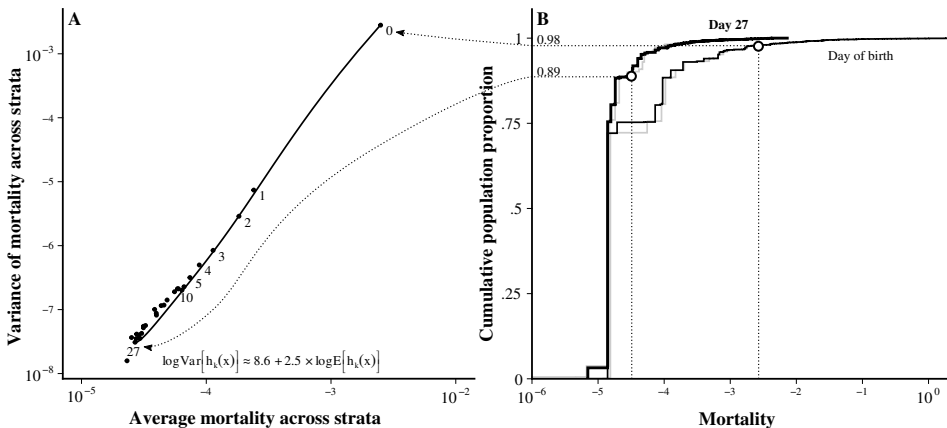
4. Results

4.1 Extreme skewness and Taylor's law in the distribution of mortality

The distribution of mortality rates over population strata conditioned on neonatal age is characterized by the high proportion of lowest-low mortality infants, an extremely long right tail of high-risk subpopulations, and a power-law relationship between expectation and variance (Taylor's law). With more than 72 percent share on the total population, the group of infants who are born on term or post-term with regular or high birth weight and a five minute Apgar score of nine, are the most prevalent stratum throughout the entire neonatal period. Their mortality (the mode of the distribution of mortality risk)

is among the lowest observed and remains relatively constant throughout the first four weeks of life. The quantile of average mortality well demonstrates the extremely long right tail of the mortality risk distribution: On the day of birth, 98 percent of newborns are part of a stratum with a risk of death lower than the population average. Over the next four weeks, the skewness decreases, but the expected value remains a bad measure of centrality (Figure 2B). On a log-log plot, the relationship between mean and variance of the distribution of mortality risk over the first 28 days of life is almost perfectly linear with a slope of 2.5. The fitted regression model reproduces this linearity (Figure 2A).

Figure 2: Mean-variance relationship over day of age (A) and age-specific distribution function (B) of the mortality/hazard rates in a cohort of newborns across birth weight, gestational age, and Apgar score strata. The points in (A) mark mean and variance of the life table mortality rates, whereas the smooth line is the prediction from the Poisson regression. In plot (B), the gray lines refer to the life table estimates and the black lines to the model predictions.



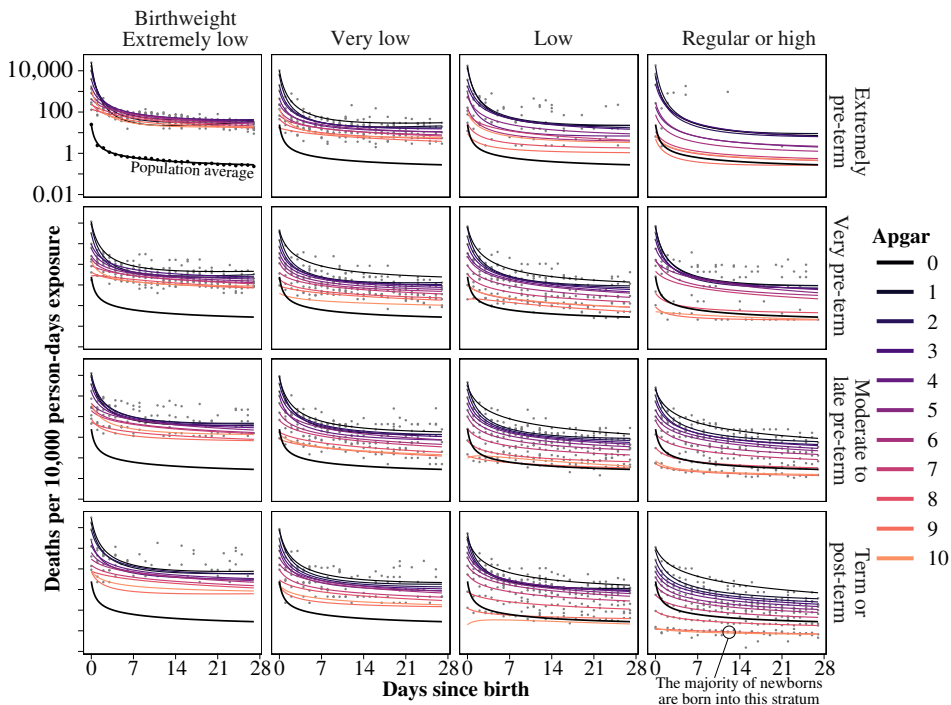
4.2 Shape and level of hazards are heterogeneous

The hazard trajectories predicted by the multilevel Poisson regression model (5) closely match the mortality rate estimates from the life table. They reflect a high degree of heterogeneity among the 252 birth weight×prematurity×Apgar score strata of the U.S. 2009–2012 birth cohort (Figure 3), varying both in level and shape. The heterogeneity is well illustrated by contrasting the lowest-low mortality subgroup (term-born infants with regular birth weight and an Apgar score of ten) with the highest-high mortality stratum (extremely premature infants with extremely low birth weight and an Apgar score of zero). At birth, the force of mortality ranges across five orders of magnitude with a hazard ratio of roughly 244-thousand (!) between the extremes but over time hazards converge as there is a strong positive correlation between the level of the hazard at birth and the rate of mortality decline over the neonatal period. While the lowest-low mortality group features a comparatively flat hazard over age, declining by 39 percent over days 0 to 28, the hazard of the highest-high stratum drops by 99.8 percent over the same

period. Hazard trajectories by Apgar score are stratified as expected on a low-high mortality continuum from ten to zero stretching multiple orders of magnitude within all birth weight \times prematurity combinations. However, hazards by Apgar score are clustered more closely among extremely preterm infants with extremely low birth-weight compared to term-born infants of regular or high birth weight.

While the hazards are heterogeneous when compared directly, the majority of newborns are born on full-term, with regular birth weight and an Apgar score of nine. Thus the majority of the birth cohort is homogeneous with respect to their hazard trajectory.

Figure 3: Estimated hazard rates versus life table mortality rates over age by prematurity, birth weight, and Apgar score. There is substantial heterogeneity in the level and the shape of the neonatal hazard trajectories ruling out the hypothesis of proportional frailties. The black line in each panel shows the estimated hazard trajectory for the entire birth cohort.



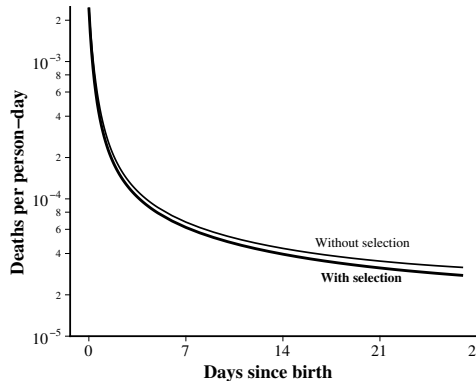
4.3 Mortality selection mainly acts shortly after birth

Population-level mortality during the first day of life is ten times higher than mortality over the following day. This 90 percent mortality decline over 24 hours is mostly the result of a corresponding drop in the stratum specific mortality rates, which, on average, declined by 71 percent between both time points. The remaining 19 percent decline is

explained by a change in population composition due to mortality selection on the day of birth. Over the following time intervals, mortality continues to decline at a fast pace with compositional effects ceasing to contribute substantially to this decline. At no point is the ratio of compositional mortality decline to total mortality decline $\frac{\Delta\bar{m}_j^C}{\Delta\bar{m}_j}$ higher, or even near 0.5 (Table 2).

The results from the discrete-time life table analysis are mirrored by the Vaupel-Zhang decomposition of the hazard's rate of change at different ages. The contribution of mortality rate variance across strata to the slope in the hazard is around 23 percent at birth but merely 4.6 percent 24 hours later staying in the single digits over the remainder of the first month of life (Table 3).

Figure 4: Keeping the population composition fixed at the distribution observed at birth only results in a minor change of the population hazard trajectory.



In order to understand the impact of mortality selection on the overall shape of the hazard trajectory I compare the estimated population average hazard over age with a counterfactual population hazard based on the stratum specific hazard estimates of model (5) but assuming the stratum specific population proportions to be fixed, thereby negating the effect of mortality selection on the population hazard. Figure 4 clearly shows that the steep decline in the risk of death following birth is not explained by selection due to differential mortality along the birth weight, Apgar score, and prematurity strata. However, mortality selection has some noticeable effect on the level of risk: Without selection, the hazard of death at day 28 would be an estimated 14 percent higher.

4.4 Stratum specific mortality converges

Following birth, the stratum specific mortality rates rapidly converge, explaining both the sudden decline in variance and mean-mode ratio of the mortality rate distribution (Figures 2, 5).

Table 2: Direct and compositional components of mortality rate decline over the neonatal period.

Age refers to single day age groups.

Table 3: Vaupel-Zhang decomposition of the slope in the hazard of death into direct and compositional components at selected ages.

Age x	$h(x)$	$\dot{h}(x)$	$\bar{h}(x)$	$\sigma_h^2(x)$	$v(x)\%$
0	2.5e-3	-1.2e-2	-9.0e-3	2.8e-3	23.5
1	3.1e-4	-3.0e-4	-2.8e-4	1.4e-5	4.6
7	6.2e-5	-6.1e-6	-5.9e-6	1.8e-7	2.9
14	4.0e-5	-1.7e-6	-1.6e-6	6.1e-8	3.6
21	3.1e-5	-7.9e-7	-7.6e-7	3.7e-8	4.7
27	2.8e-5	-4.7e-7	-4.4e-7	3.1e-8	6.5

Figure 5: The ratio of the population average and the modal mortality rates over the first four weeks of life. Following birth population mortality converges towards the low mortality of the most prevalent stratum (Apgar 9, Regular or high birth weight, born term or post-term) which is due to the convergence of high-risk strata.

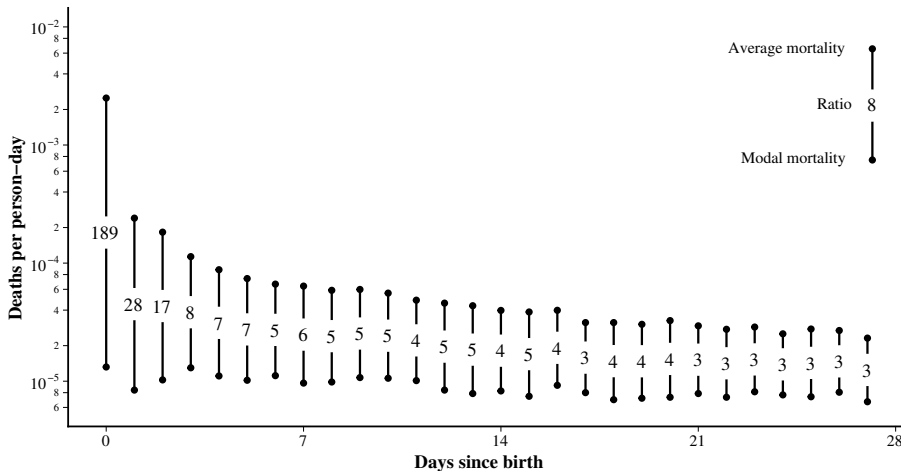


Table 4: Direct and compositional components of mortality rate variance decline over the neonatal period.

Age	v_j	Δv_j	(%)	Δv_j^D	(%)	Δv_j^C	(%)	$\frac{\Delta v_j^C}{\Delta v_j^D} \%$
0	2.5e-3	↑	-2.3e-3	-90.4	-1.8e-3	-71.1	-4.8e-4	-19.2
1	2.4e-4	↑	-1.8e-4	-73.4	-1.7e-4	-70.1	-7.9e-6	-3.3
7	6.4e-5	↑	-2.4e-5	-37.8	-2.3e-5	-36.4	-8.9e-7	-1.4
14	4.0e-5	↑	-1.0e-5	-25.9	-1.0e-5	-25.1	-3.4e-7	-0.9
21	2.9e-5	↑	-6.3e-6	-21.3	-6.1e-6	-20.9	-1.3e-7	-0.4
27	2.3e-5							2.1

Age refers to single day age groups.

Table 5: Direct and compositional components of mean-mode ratio decline over the neonatal period.

Age	r_j	Δr_j	(%)	Δr_j^D	(%)	Δr_j^C	(%)	$\frac{\Delta r_j^C}{\Delta r_j^D} \%$
0	189	↑	-160	-84.9	-123	-65.0	-37	-19.9
1	28	↑	-21	-76.8	-21	-73.6	0	-3.2
7	6	↑	-1	-27.5	-1	-26.0	0	-1.5
14	4	↑	-1	-22.1	-1	-21.2	0	-0.9
21	3	↑	0	-7.6	0	-7.2	0	-0.5
27	3							6.2

Age refers to single day age groups.

The variance of death rates over strata is highest at birth and falls by more than 90 percent from day 0 to day 1 of age. The decline in variance is mainly the result of stratum specific death rates converging towards the population average, with only 19 percentage points decline explained by mortality selection. The mortality variance continues to decline substantially over the remainder of the first month of life, with mortality selection never contributing more than 4.5 percent to the total decline (Table 4).

During the first day of life, population mortality is 189 times higher than the mortality of the most prevalent stratum. This ratio declines by 85 percent over the next day of life, with only 20 percentage points of this decline explained by a shifting population composition. During the remainder of the neonatal period, mortality selection only minimally influences the continuing changes in the mean-mode mortality ratio, which eventually arrives at a value of around 3, a drop by 98 percent compared to the value at birth.

5. Discussion

Frailty theory cautions us against taking the population level hazard shape as representative for the risk trajectory of the population members. The analysis of neonatal mortality indeed clearly demonstrates the potential severity of this ecological fallacy, with the majority of newborns experiencing a hazard trajectory radically different from what is observed on the aggregate level. Yet, this difference does not arise from mortality selection but from the non-proportionality of stratum specific hazards. Neonatologists know that the first 24 hours of life are the most critical in determining the further survival of the preterm infant. Once the one-day threshold is passed, the survival chances not only drastically improve but, as shown in this paper, converge towards the survival chances of healthy term-born infants. The popular proportional frailty model is severely misspecified for situations where an individual may be saved due to medical intervention, i.e., where the physiological state of an individual and thus the associated frailty changes abruptly. In consequence, even if the model fits the aggregate age pattern well, as it does in case of the Hougaard-Gompertz fit to the age trajectory of infant mortality (Figure 1), inferences drawn from it are biased.

To escape the strong assumptions of frailty models, I based the analysis in this paper on the *observed* heterogeneity in age-specific mortality across mutually exclusive population strata but, in turn, left open the possibility for *hidden* heterogeneity within a particular stratum. A further division of the population along the presence and severity of congenital malformations may uncover that the mortality decline following birth is primarily the effect of the vanishing subpopulation of newborns featuring congenital disabilities incompatible with life. While this particular hypothesis can be tested in a future publication, one can never exclude the possibility of further unobserved quantities influencing observed outcomes. All that can be confidently said based on the data analyzed above is that the heterogeneity in risk along birth weight, Apgar score, and prematurity has only a minimal impact on the shape of the population level age trajectory of neonatal mortality.

A peculiar finding is the near-perfect power-law relationship between the mean and the variance of the distribution of stratum-specific mortality rates over age – a further example of “Taylor’s law” in demography: Analyzing data on the spatial distribution of various species Taylor (1961) observed that the variance in population count per unit area is well predicted by a power of the average population count. Similar mean-variance relationships have been found for population densities in human populations (Cohen et al. 2013; Naccarato and Benassi 2018) and recently for time-series of age-specific mortality rates and rates of mortality improvement (Bohk et al. 2015; Cohen et al. 2018). Whereas the studies by Cohen, Bohk, and Rau are based on the concept of a “temporal mean/variance,” i.e., mean and variance are estimated from observations repeated over age or period, I contribute the first demonstration of Taylor’s law in human mortality based on the distribution of risk at any single point in time within a cohort of individuals followed over age.

6. Conclusion

The sudden drop in population mortality following birth is predominantly the result of stratum specific hazard rates quickly converging towards rather low levels. The compositional shift in the population resulting from mortality selection only has a minimal impact on the age trajectory of neonatal mortality.

It remains to be seen if the simple power-law expression that describes the time-evolution of mean and variance in mortality among a cohort of newborns replicates in other populations and at other ages. The prospect of having a 2-parameter expression for the mortality dynamics in a heterogeneous aging cohort may motivate future inquiries in that direction.

A. The Hougaard-Gompertz frailty model

Let the hazard of death at age x for a newborn with frailty z be $h_z(x|z) = zh_0(x)$ with z drawn from the three parameter frailty distribution proposed by Hougaard (1986) denoted with $Z \sim \text{Houg}(x; \alpha, \delta, \theta)$ and Gompertz baseline hazard $h_0(x) = ae^{bx}$ with corresponding cumulative hazard $H_0(x) = \int_0^x h_0(s) ds = a(e^{bx} - 1)/b$. The average frailty among the survivors at x then is $E[Z|X \geq x] = \delta(\theta + H_0(x))^{\alpha-1}$ (Hougaard 1986, p. 393). Substituting $\delta = \frac{1}{\theta^{\alpha-1}}$ eliminates one parameter from the model and fixes the average frailty at birth at one. The population hazard then is

$$h(x) = E[Z|X = x]h_0(x) = \left(\frac{\theta + a(e^{bx} - 1)/b}{\theta} \right)^{\alpha-1} ae^{bx},$$

with log-hazard

$$\log h(x) = (\alpha - 1) \log \left(\frac{\theta + a(e^{bx} - 1)/b}{\theta} \right) + \log a + bx$$

The above hazard is fitted to daily death counts D_j and exposure times E_j of the U.S. 2009–2012 infant life table via a Bayesian non-linear Poisson regression model

$$\begin{aligned} D_j &\sim \text{Pois}(\lambda_j E_j) \text{ for } j = 1, \dots, 365 \\ \lambda_j &= e^{\log h(x_j; a, b, \theta, \alpha)} \end{aligned}$$

with parameter transformations

$$\begin{aligned} a &= e^{\beta_0} \\ b &= \beta_1 \\ \theta &= e^{\beta_2} \\ \alpha &= \log \frac{\beta_3}{1 - \beta_3}, \end{aligned}$$

and priors

$$\begin{aligned} \beta_0 &\sim N(-8, 1) \\ \beta_1 &\sim N(-0.03, 1) \\ \beta_2 &\sim N(-6, 1) \\ \beta_3 &\sim N(0.5, 1). \end{aligned}$$

B. The quadratic hazard over log age

Quadratic relationships between log age and log mortality can be captured by the expression

$$h(x) = e^{\beta_0 + \beta_1 \log(x+1) + \beta_2 \log^2(x+1)},$$

with derivative wrt. x

$$h'(x) = (x+1)^{\beta_1 - 1} e^{\beta_0 + \beta_2 \log^2(x+1)} (\beta_1 + 2\beta_2 \log(x+1)),$$

and survival function

$$S(x) = \exp\left(\frac{\sqrt{\pi} \exp\left(b_0 - \frac{(b_1+1)^2}{4b_2}\right) \left(\operatorname{erfi}\left(\frac{b_1+1}{2\sqrt{b_2}}\right) - \operatorname{erfi}\left(\frac{b_1+2b_2 \log(x+1)+1}{2\sqrt{b_2}}\right)\right)}{2\sqrt{b_2}}\right).$$

An efficient algorithm for the evaluation of the imaginary error function $\operatorname{erfi}(x) = \frac{2}{\sqrt{\pi}} \int_0^x \exp(-t^2) dt$ exists (Poppe and Wijers 1990) and is implemented in the C++ library Faddeeva which can be called from within R via the package `RcppFaddeeva`.

C. The Vaupel-Zhang equality

I find it instructive to derive the Vaupel-Zhang equality from a simple finite mixture distribution of survival times as it gives justification to the weighted averages employed in this paper. Once the marginal hazard rate has been shown to be a weighted average of hazards among the survivors the proof is the same as Vaupel and Zhang (2010).

Let X be the positive real-valued random variable “age at death” and K be a random index denoting membership to the k th population stratum. The marginal density of ages at death is given by the discrete mixture distribution

$$f(x) = \sum_k f(x|k)P(k),$$

where $f(x|k)$ is the conditional density of deaths and $P(k)$ the probability of membership in stratum k . By definition the conditional and marginal survival functions are

$$\begin{aligned} S(x|k) &= P(X > x|k) = \int_x^\infty f(x|k) dx \\ S(x) &= P(X > x) = \int_x^\infty f(x) dx, \end{aligned}$$

which give rise to the conditional and marginal hazards via the relationships

$$\begin{aligned} h(x|k) &= -S'(x|k)/S(x|k) \\ h(x) &= -S'(x)/S(x), \end{aligned}$$

where the prime mark denotes the derivative with respect to age x .

The Vaupel-Zhang equality states that for the survivors at age x the age-derivative of their average hazard is equal to the average age derivative minus the variance of the hazards, in their notation

$$\dot{\bar{h}}(x) = \bar{h}'(x) - \sigma_h^2(x),$$

where

$$\begin{aligned} \dot{\bar{h}}(x) &= \left[\sum_k h(x|k)P(k|X > x) \right]' \\ \bar{h}(x) &= \sum_k h'(x|k)P(k|X > x) \\ \sigma_h^2(x) &= \sum_k h(x|k)^2 P(k|X > x) - \left[\sum_k h(x|k)P(k|X > x) \right]^2. \end{aligned}$$

Proof:

Bayes Theorem gives the probability of being in stratum k given survival to age x as

$$P(k|X > x) = \frac{P(X > x|k)P(k)}{P(X > x)} = \frac{S(x|k)P(k)}{S(x)}$$

The marginal survival $S(x)$ can be calculated from conditional survival $S(x|k)$ and stratum distribution $P(k)$ via the law of total probability as

$$\begin{aligned} S(x) &= P(X > x) \\ &= \sum_k P(X > x|k)P(k) \\ &= \sum_k S(x|k)P(k), \end{aligned}$$

with age derivative

$$\begin{aligned} S'(x) &= \sum_k S'(x|k)P(k) \\ &= \sum_k -h(x|k)S(x|k)P(k). \end{aligned}$$

By substituting $S'(x)$ into $h(x) = -\frac{S'(x)}{S(x)}$ one can express the marginal hazard as a weighted average of the hazards of the survivors:

$$\begin{aligned} h(x) &= -\frac{\sum_k -h(x|k)S(x|k)P(k)}{S(x)} \\ &= \sum_k \frac{h(x|k)S(x|k)P(k)}{S(x)} \\ &= \sum_k h(x|k)P(k|X > x). \end{aligned}$$

Taking the derivative of $h(x)$ gives

$$\begin{aligned} \dot{h}(x) &= \sum_k h'(x|k)P(k|X > x) + \sum_k h(x|k)P'(k|X > x) \\ &= \bar{h}(x) + \sum_k h(x|k)P'(k|X > x). \end{aligned}$$

The second term can be manipulated to yield

$$\begin{aligned}
 \sum_k h(x|k)P'(k|X > x) &= \sum_k h(x|k) \left[\frac{P(k)S'(x|k)}{S(x)} - \frac{P(k)S'(x)S(x|k)}{S(x)^2} \right]' \\
 &= \sum_k \frac{h(x|k)P(k)S'(x|k)}{S(x)} - \sum_k \frac{h(x|k)P(k)S'(x)S(x|k)}{S(x)^2} \\
 &= \sum_k \frac{h(x|k)P(k)S'(x|k)}{S(x)} - \frac{S'(x)}{S(x)} \sum_k h(x|k)P(k|X > x) \\
 &= \sum_k \frac{h(x|k)P(k)S'(x|k)}{S(x)} - h(x)^2 \\
 &= \sum_k \frac{-h(x|k)^2 P(k)S(x|k)}{S(x)} - h(x)^2 \\
 &= - \sum_k h(x|k)^2 P(k|X > x) - h(x)^2 \\
 &= -\sigma_h^2(x),
 \end{aligned}$$

completing the proof.

References

- V. Apgar. A proposal for a new method of evaluation of the newborn infant. *Current Researches in Anesthesia and Analgesia*, 32(4):260–267, 1953. doi:10.1213/ANE.0b013e31829bdc5c.
- D. Avraam, S. Arnold, D. Jones, and B. Vasiev. Time-evolution of age-dependent mortality patterns in mathematical model of heterogeneous human population. *Experimental Gerontology*, 60:18–30, 2014. doi:10.1016/j.exger.2014.09.006.
- D. Bates, M. Mächler, B. Bolker, and S. Walker. Fitting linear mixed-effects models using lme4. *Journal of Statistical Software*, 67(1):1–48, 2015. doi:10.18637/jss.v067.i01.
- R. E. Beard. Appendix: Note on some mathematical mortality models. In G. E. W. Wolstenholme and M. O'Connor, editors, *The Lifespan of Animals. Ciba Foundation Colloquium on Ageing*, pages 802–811, Boston, 1959. Little, Brown. doi:10.1002/9780470715253.app1.
- C. Bohk, R. Rau, and J. E. Cohen. Taylor’s power law in human mortality. *Demographic Research*, 33(21):589–610, 2015. doi:10.4054/DemRes.2015.33.21.
- G. Boole. *Calculus of finite differences*. Chelsea Publishing Company, New York, 4th edition, 1880.
- B. M. Casey, D. D. McIntire, and K. J. Leveno. The continuing value of the apgar score for the assessment of newborn infants. *New England Journal of Medicine*, 344(7):467–471, 2001. doi:10.1056/NEJM200102153440701.
- J. E. Cohen, M. Xu, and H. Brunborg. Taylor’s law applies to spatial variation in a human population. *Genus*, 69(1):25–60, 2013.
- J. E. Cohen, C. Bohk-Ewald, and R. Rau. Gompertz, Makeham, and Siler models explain Taylor’s law in human mortality data. *Demographic Research*, 38(29):773–841, 2018. doi:10.4054/DemRes.2018.38.29.
- F. Colchero and B. Y. Kiyakoglu. Beyond the proportional frailty model: Bayesian estimation of individual heterogeneity on mortality parameters. *Biometrical Journal*, pages 1–12, 2019. doi:10.1002/bimj.201800280.
- A. Gelman and J. Hill. *Data Analysis Using Regression and Multilevel/Hierarchical Models*. Analytical Methods for Social Research. Cambridge University Press, Cambridge, 2007. ISBN 978-0-511-26878-6. doi:10.1017/cbo9780511790942.
- J. M. Hoem. Identifiability in hazard models with unobserved heterogeneity: The compatibility of two apparently contradictory results. *Theoretical Population Biology*, 37(1):124–128, 1990. doi:10.1016/0040-5809(90)90030-y.
- P. Hougaard. Life table methods for heterogeneous populations: Distributions describing the heterogeneity. *Biometrika*, 71(1):75–83, 1984. doi:10.1093/biomet/71.1.75.
- P. Hougaard. Survival models for heterogeneous populations derived from stable distributions. *Biometrika*, 73(2):387–396, 1986. doi:10.1093/biomet/73.2.387.

- J. J. Hsieh. Construction of expanded infant life tables: A method based on a new mortality law. *Mathematical Biosciences*, 76(2):221–242, 1985. doi:10.1016/0025-5564(85)90006-9.
- E. M. Kitagawa. Components of a difference between two rates. *Journal of the American Statistical Association*, 50(272):1168–1194, 1955. doi:10.1080/01621459.1955.10501299.
- D. A. Levitis. Before senescence: the evolutionary demography of ontogenesis. *Proceedings of the Royal Society B*, 278(1707):801–809, 2011. doi:10.1098/rspb.2010.2190.
- D. A. Levitis and D. E. Martínez. The two halves of U-shaped mortality. *Frontiers in Genetics*, 4(31):1–6, 2013. doi:10.3389/fgene.2013.00031.
- T. I. Missov and J. W. Vaupel. Mortality implications of mortality plateaus. *SIAM Review*, 57(1):61–70, 2015. doi:10.1137/130912992.
- A. Naccarato and F. Benassi. On the relationship between mean and variance of world's human population density: A study using Taylor's power law. *Letters in Spatial and Resource Sciences*, 11(3):307–314, 2018. doi:10.1007/s12076-018-0214-5.
- National Center for Health Statistics. Birth cohort linked birth-infant death data files (U.S. data), 2016. URL ftp://ftp.cdc.gov/pub/Health_Statistics/NCHS/Datasets/DVS/cohortlinkedus/.
- J. H. Park, Y. S. Chang, S. Y. Ahn, S. I. Sung, and W. S. Park. Predicting mortality in extremely low birth weight infants: Comparison between gestational age, birth weight, Apgar score, CRIB II score, initial and lowest serum albumin levels. *PLoS ONE*, 13(2):1–10, 2018. doi:10.1371/journal.pone.0192232.
- M. M. Pollack, M. A. Koch, D. A. Bartel, I. Rapoport, R. Dhanireddy, A. A. E. El-Mohandes, K. Harkavy, and K. N. S. Subramanian. A comparison of neonatal mortality risk prediction models in very low birth weight infants. *Pediatrics*, 105(5):1051–1057, 2000. doi:10.1542/peds.105.5.1051.
- G. P. M. Poppe and C. M. J. Wijers. More efficient computation of the complex error function. *ACM Transactions on Mathematical Software (TOMS)*, 16(1):38–46, 1990.
- A. Remund. *Jeunesses vulnérables? Mesures, composantes et causes de la surmortalité des jeunes adultes*. PhD thesis, Université de Genève, 2015.
- D. R. Steinsaltz and K. W. Wachter. Understanding mortality rate deceleration and heterogeneity. *Mathematical Population Studies*, 13(1):19–37, 2006. doi:10.1080/08898480500452117.
- L. R. Taylor. Aggregation, variance and the mean. *Nature*, 189(4766):732–735, 1961. doi:doi.org/10.1038/2F189732a0.
- J. Trussell and T. Richards. Correcting for unmeasured heterogeneity in hazard models using the heckman-singer procedure. *Sociological Methodology*, 15:242–276, 1985. doi:10.2307/270852.

- J. W. Vaupel and J. R. Carey. Compositional interpretations of medfly mortality. *Science*, 260(5114):1666–1667, 1993. doi:10.1126/science.8503016.
- J. W. Vaupel and T. I. Missov. Unobserved population heterogeneity: A review of formal relationships. *Demographic Research*, 31(1):659–686, 2014. doi:10.4054/DemRes.2014.31.22.
- J. W. Vaupel and A. I. Yashin. The deviant dynamics of death in heterogeneous populations. Technical report, Laxenburg, Austria, 1983. URL <http://user.demogr.mpg.de/jwv/pdf/IIASA-83-001.pdf>.
- J. W. Vaupel and A. I. Yashin. Heterogeneity's ruses: Some surprising effects of selection on population dynamics. *The American Statistician*, 39(3):176–185, 1985. doi:10.2307/2683925.
- J. W. Vaupel and Z. Zhang. Attrition in heterogeneous cohorts. *Demographic Research*, 23(26):737–748, 2010. doi:10.4054/DemRes.2010.23.26.
- J. W. Vaupel, K. G. Manton, and E. Stallard. The impact of heterogeneity in individual frailty on the dynamics of mortality. *Demography*, 16(3):439–54, 1979. doi:10.2307/2061224.
- A. Wienke. *Frailty Models in Survival Analysis*. Biostatistics Series. Chapman and Hall, Boca Raton, 2011. ISBN 978-1-4200-7388-1. doi:10.1111/j.1541-0420.2012.01769.x.
- A. I. Yashin, I. A. Iachine, and A. S. Begun. Mortality modeling: A review. *Mathematical Population Studies*, 8(4):305–332, 2000. doi:10.1080/08898480009525489.

Chapter IV

The gestational age pattern of feto-infant mortality

The gestational age pattern of feto-infant mortality

Jonas Schöley*

1. Introduction

The different segments of a birth cohort's mortality trajectory have been thoroughly mapped starting with the sudden decline in the risk of death after a peak at birth (e.g., Bourgeois-Pichat 1951; Galley and Woods 1999; Berrut et al. 2016), the arrival at minimum risk in late childhood (Ebeling 2018), the "hump-shaped" excess mortality in adolescence (e.g., Thiele 1871; Goldstein 2011; Remund et al. 2018) and the exponential increase in the mortality hazard over much of the adult life (e.g., Gompertz 1825) which eventually flattens (e.g., Perks 1932; Vaupel 1997; Horiuchi and Wilmoth 1998) and then plateaus among the oldest-old (e.g., Gampe 2010; Barbi et al. 2018). Similar investigations have been made concerning the changing mortality risk of the unborn child over the age of a pregnancy (e.g., Shapiro et al. 1962; Bakkevig et al. 1978; Goldhaber and Fireman 1991; Carlson et al. 1999; Woods 2009).

Both survival scenarios, fetal and infant, meet at the point of birth but are nonetheless fundamentally separated by the use of different timescales. While prenatal mortality is indexed by gestational age, commonly measured as the weeks since the last menstrual period of the pregnant woman, the survival of those born alive is followed over chronological age, i.e., time since birth. Such a strict separation of populations along the dividing line of birth makes this critical transition invisible in the study of mortality, delegating to it either the role of a right censoring or a point of entry into the risk set. An alternative perspective allows bridging the feto-infant gap by situating birth within the lifecycle of a cohort of unborn children whose survival is tracked over the age of gestation into infancy. By marking the vital events of fetal death, birth and infant death on a common age scale the risky transition of birth becomes an event *within* the temporal observation horizon and its effect on the survival of a cohort on the onset of life can be studied by defining a feto-infant mortality trajectory: the combined risk of fetal or infant death among all members of a conception cohort still alive at a given week of gestation.

*Interdisciplinary Centre on Population Dynamics, University of Southern Denmark. Correspondence: jscholey@health.sdu.dk. During the writing of this article the author was a guest at the Max-Planck Institute for Demographic Research and funded by a grant from AXA Insurance.

Figure 1: The feto-infant mortality trajectory over gestational age for a U.S. cohort of fetuses conceived in 2009, surviving until fetal viability and followed over the next 52 weeks. The risk of feto-infant death among the survivors of the cohort declines exponentially over age interrupted only by a “birth hump.”

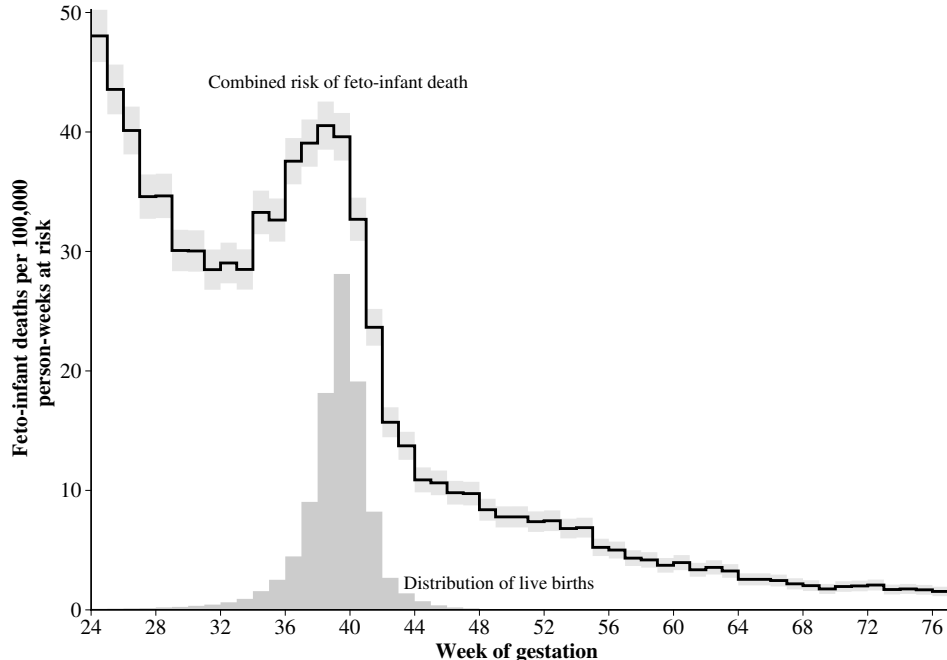


Figure 1 shows gestation specific mortality rates for a cohort of children conceived in 2009 and either born or registered as an infant or fetal death in the U.S. The denominator of the rate is based upon all members of the conception cohort alive (either as fetus or infant) during a given week of gestation whereas the numerator includes all fetal- and infant deaths within the same week. The feto-infant mortality trajectory constructed from these rates thus measures the changing risk of *any* adverse pregnancy outcome for the 52 weeks following gestational age 24, commonly defined as the “limit of viability” (Seri and Evans 2008). The trajectory may be interpreted as the changing hazard of death for a cohort as its members pass the tumultuous transition period from fetus to infant. An exponential decline in mortality characterizes this period, interrupted only by hump-shaped excess mortality associated with the age-distribution of deliveries.

In this paper, descriptive findings on the feto-infant mortality trajectory and the associated phenomenon of a “birth hump” are presented.

Mortality trajectories that stretch across the feto-infant gap have been proposed several times but never entirely realized. In his seminal work on “ontogenescence,” – the declining risk of death over age before maturity – Levitis (2011) considers the hazard of death on an age continuum from conception until adolescence with the event of birth acting as a “transitional shock.” By using a negative time scale before birth and positive after, Levitis

implicitly assumes all births to occur at the same time post-conception – a simplifying assumption which naturally leads to a spurious “birth spike” rather than a “birth hump.” Williamson and Woods (2003) and Woods (2009) model the cumulative risk of death of a cohort from conception until the first birthday and use weeks of gestation as time scale throughout the complete follow-up. As Williamson and Wood’s model is based on previously published disjoint fetal- and infant lifetables, they too assume all births to take place at full-term.

The joint consideration of fetal and infant death is perhaps most prominently expressed in the perinatal mortality rate, commonly defined as the sum of all fetal deaths and infant deaths during the first seven days of life over the number of births within a year (World Health Organization 2006). The necessity for such a measure arose from the uncertainty regarding the classification of a death as stillborn or infant due to both varying legal requirements and the subjective judgment of the pediatrician. Designed as a simple and therefore widely applicable indicator, the perinatal mortality rate does not consider the time dimension of pregnancy, nor does it permit a survival analytic interpretation as the denominator is not the population at risk.

Fetal lifetables add both a time dimension and a survival interpretation to the analysis of pregnancy outcomes via the introduction of an “ongoing pregnancies” denominator (e.g., Shapiro et al. 1962; French and Bierman 1962; Bakketeg et al. 1978; Goldhaber and Fireman 1991). These life-tables report the probability of fetal death among the intrauterine survivors to some week of gestation. In an influential article Yudkin et al. (1987) advertise the use of a “fetuses at risk” denominator for the analysis of perinatal mortality by gestational age leading to a range of age-specific mortality indices that include compound fetal- and infant death endpoints (Kristensen and Mac 1992; Smith 2001; Platt et al. 2004; Joseph 2004; Smith 2005; Joseph 2007). Kristensen and Mac (1992) follows a cohort of fetuses from week 31 of gestation into infancy until week 76 and calculates a corresponding survival curve. The ratio of fetal- and neonatal¹ deaths over fetuses at risk by week of gestation is advertised by Joseph (2007) as the proper “causal” framework to the study of perinatal mortality. Making a similar argument Platt et al. (2004) propose a Cox regression model over age of gestation featuring a combined feto-infant death endpoint.

This paper contributes to the aforementioned literature on survival analysis *around* the onset of life by studying the age pattern of mortality in a cohort of fetuses as they transition into infancy. A distinct phenomenon of this perinatal mortality trajectory is the “birth hump.” Via simple decomposition analysis, I show how fetal-, neonatal, and post-neonatal mortality and the probability of live birth all act together to form the “hump.” In a second step, I quantify the magnitude of the “hump” by proposing that the distinctive shape of feto-infant mortality on a cohort level is the result of two competing hazards: An “ontogenescent” hazard, due to causes with a declining incidence, and a “transitional” component, due to birth-related causes. I propose the probability of a fetus at 24 weeks of age to survive the following 12 months as a summary of the feto-infant mortality trajectory and ask how differences in this indicator across cohorts and between population strata are driven by changes in the shape of the gestational age pattern of feto-infant mortality.

¹ In this paper I use the term “neonatal” as referring to the first week of life.

2. Data and Methods

In this paper, I analyze U.S. fetal deaths, births, and infant deaths over the age of gestation. The data basis for this analysis consists of the birth certificates for the U.S. birth cohorts 1989/1990, 1999/2000, 2009/2010, the linked infant death certificates where applicable, and the fetal death certificates for the years 1989/1990, 1999/2000, and 2009/2010. Digitized versions of the certificates are provided by the National Center for Health Statistics in the form of the “Birth Cohort Linked Birth – Infant Death Data Files” (National Center for Health Statistics 2016a) and the “Fetal Death Data Files” (National Center for Health Statistics 2016b, see also Martin and Hoyert (2002) for an introduction).

To analyze the gestational age mortality trajectory of a cohort of fetuses as they transition into life, I construct three conception cohorts of all fetuses conceived during the years 1989, 1999, and 2009 respectively. The 2009 cohort is further stratified by sex and maternal origin, two characteristics which are available on most birth-, fetal- and infant death certificates and serve to show how the phenomenon of the birth hump and the ontogenescent feto-infant mortality decline compares across key demographics.

Only fetuses who survived until week 24 of gestation, commonly defined as the “age of viability,” are considered in this study. Reporting guidelines and practice for fetal death vary across states. A left-truncation age of 24 serves to rectify these differences. It is chosen because based on evidence that under-reporting drastically increases already at week 23 (Greb et al. 1987)². Furthermore, a relatively late left-truncation age serves to minimize the bias due to the unknown numbers of induced abortions.

The initial size of the fetal-cohort at the beginning of week 24 is calculated via the “extinct cohort” method (Bakketeig et al. 1978; Feldman 1992) by adding all life-births within a conception cohort to all fetal deaths at weeks 24+. This is due to the simple observation that a life-birth at week of gestation t was a fetus prior to t .

Using a multi-state lifetable, I follow the initial fetal population at week 24 for 52 weeks counting for each week t fetal deaths, neonatal deaths, post-neonatal deaths, and the corresponding population of survivors and their distribution across these three states. Distinguishing fetuses, newborns and infants who survived the first week of life then allows to decompose week-to-week changes in the combined feto-infant mortality rates $m_t = \frac{\# \text{fetal or infant deaths at week } t}{\text{Total feto-infant time at risk during week } t}$ into changes due to a shifting distribution of fetuses, vs. neonates vs. post-neonates, and changes due to declining or increasing mortality rates within each state. Such a decomposition explains the “birth hump” in terms of the perinatal population dynamics. The Kitagawa method (Kitagawa 1955) is used to perform the decomposition.

² While their study dates back to 1987 I found evidence for the continued under-registration of fetal deaths in the U.S. prior to week 24 in the form of declining fetal death rates going from week 23 to 20 which lacks a biological explanation.

Table 1: Parametric specification of the feto-infant mortality trajectory over age of gestation and derived quantities.

Ontogenetic component	Transitional component
<i>Ontogenetic hazard</i> The instantaneous risk of fetal or infant death at gestational age $t = x + 24$ due to causes with a continuously declining incidence.	<i>Transitional hazard</i> The instantaneous risk of fetal or infant death at gestational age x due to causes associated with the timing of onset of labor.
$h^O(x) = a_1 \exp(-bx)$	$h^T(x) = a_2 \exp\left(-\frac{(x - c)^2}{2\sigma^2}\right)$
<i>Cumulative ontogenetic hazard</i>	<i>Cumulative transitional hazard</i>
$H^O(x) = \int_0^x h^O(s) ds = \frac{a_1 - a_1 \exp(-bx)}{b}$	$H^T(x) = \int_0^x h^T(s) ds = a_2 \sigma \sqrt{\pi/2} [\text{erf}(A) + \text{erf}(B)],$ where $A = \frac{c}{\sqrt{2}\sigma}$, $B = \frac{x-c}{\sqrt{2}\sigma}$, and $\text{erf}(\cdot)$ is the Gaussian error function.
a_1 <i>Level of feto-infant mortality</i> The approximate hazard of feto-infant death at age of fetal viability.	a_2 <i>Magnitude of birth hump</i> The instantaneous risk of fetal or infant death contributed by the birth-hump component at its peak.
b <i>Rate of ontogenescence</i> The relative rate of feto-infant mortality decline over gestational age in absence of birth hump.	c <i>Location of birth hump</i> The gestational age $t = c + 24$ coinciding with the peak of the risk of fetal or infant death contributed by the birth-hump component.
	σ <i>Spread of transitional shock</i> The curvature of the risk of feto-infant death around its peak. Higher values flatten the birth hump.
Combined hazard	
<i>Hazard of feto-infant death</i> The instantaneous risk of fetal or infant death x weeks past fetal viability.	$h(x) = h^O(x) + h^T(x)$
<i>Feto-infant survival curve</i> The probability of surviving x weeks past fetal-viability.	$S(x) = \exp\left(-H^O(x) - H^T(x)\right)$
<i>Cumulative incidence of feto-infant death</i> Probability of fetal or infant death x weeks past fetal-viability.	$F(x) = 1 - S(x)$
Competing risks inference	
Cumulative incidence of feto-infant death due to causes associated with the timing of onset of labor.	$F^T(x) = \int_0^x S(s)h^T(s) ds$
Share of feto-infant deaths over x weeks following fetal viability contributed by the "birth hump".	$\rho(x) = \frac{F^T(x)}{F(x)}$

Assuming a competing risks model (Table 1) where death is either the result from causes which exhibit gradually declining incidence over gestation (e.g., extreme prematurity, in-utero fatalities due to congenital anomalies) or from causes increasing in incidence as full-term approaches (e.g., obstetric causes), I quantify the share of fetal- or infant deaths over the one-year follow-up from fetal viability which can be attributed to the “birth-hump.”

I define $F(52)$, the probability for a fetus alive at the 24th week of pregnancy to die in the following year, as a summary indicator of adverse pregnancy outcomes. In order to elucidate how the “shape” of the feto-infant hazard trajectory determines population differences in overall feto-infant death counts, I decompose differences in $F(52)$ between two populations into differences due to the initial magnitude of mortality at the age of fetal viability, differences due to the rate of mortality decline over gestational age, and differences due to the location, shape, and magnitude of the “birth hump” component. This decomposition is performed via the Horiuchi decomposition (Horiuchi et al. 2008) of the differences in $F(52)$ as predicted by the model outlined in Table 1.

3. Results

3.1 Feto-infant population dynamics over gestational age

The gestational age trajectory of feto-infant mortality as shown in Figure 2A may be segmented into a decline from week 24 to 33, a steep increase from week 33 to 39, a steep decrease from week 39 to 45, and a more gradual decrease over weeks 45 to 72. Throughout these four segments, the population composition shifts from a cohort of fetuses to a cohort with a substantial share of neonates to a cohort entirely composed of postneonates. Fetal mortality rates decline until week 32 and start to increase drastically into post-term, neonatal mortality declines until week 40, and then plateaus and post-neonatal mortality declines continuously over the entire observation period (Figure 2B). As shown by the Kitagawa decomposition in Table 2, the particular shape of the feto-infant mortality trajectory is the result of both the aforementioned changes in composition and rates.

Weeks 25 to 33: pre-term decline. Feto-infant mortality declines by 34.6 percent over the nine weeks following the age of fetal-viability. The overwhelming share of the decline can be attributed to the lessening burden of prematurity reflected in the 95.7% decline of neonatal mortality: Infants born at week 25 have a risk of death elevated by a factor of 654 compared to the fetal population at the same age whereas at week 33 this neonate penalty is reduced to a factor of 35.8. However, the increasing share of neonates from less than a percent to 1.9 percent counterbalances the effect of the reduction in neonatal mortality on the differential in feto-infant mortality.

Weeks 33 to 39: increase towards full-term. Approaching full-term, feto-infant mortality reverses its trend and increases by 38.9 percent. Part of this increase is due to the increase in fetal death rates by more than 144 percent, an effect that is, in turn, mediated by the declining share of the fetal population in the cohort by 51.7 percent. Neonatal mortality

rates continue to be higher compared to fetal mortality prior to week 39 (Figure 2C), and thus the rapidly increasing share of newborns contributes to the increase in combined feto-infant mortality.

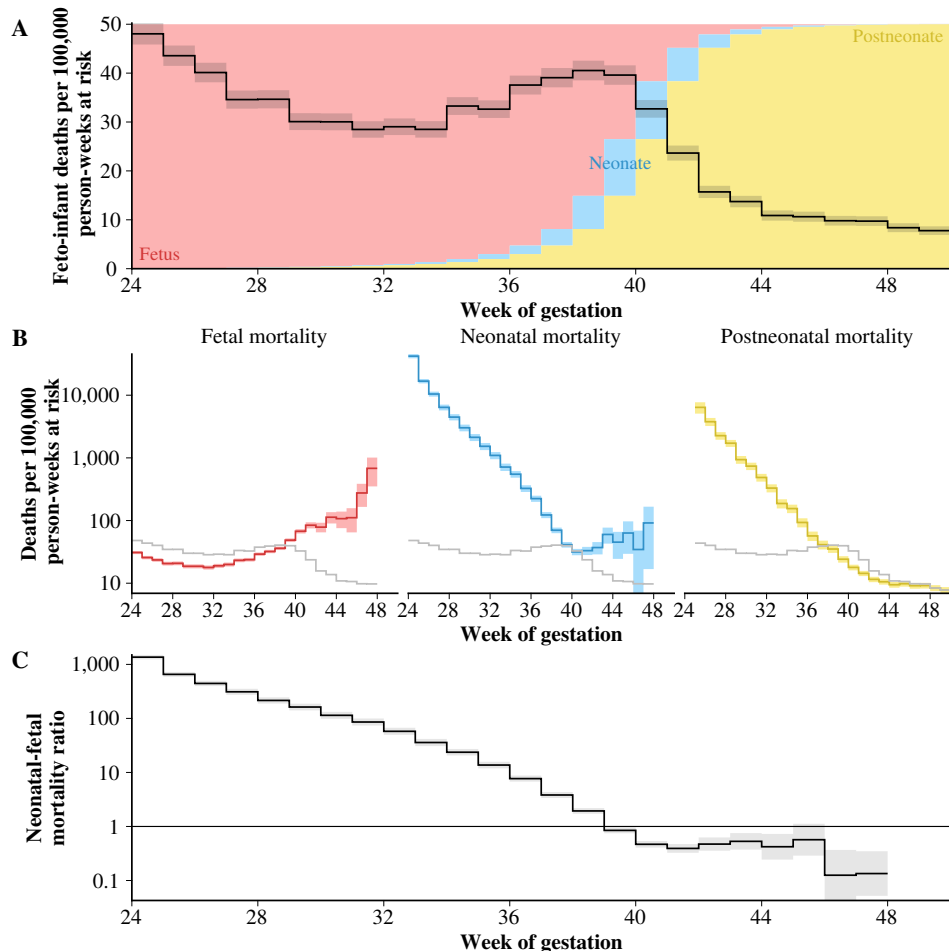
Weeks 39 to 45: post-term decline. While mortality increases post-term for both fetuses and neonates, it is the quickly vanishing share of both sub-populations that, along with declining rates of post-neonatal mortality, drives the steep decline in feto-infant mortality following full-term.

Weeks 45 to 72: post-neonatal decline. With no remaining fetuses or neonates in the population, the feto-infant mortality trajectory is completely determined by the declining mortality of the post-neonatal population.

Table 2: Decomposition of the change in combined feto-infant mortality over gestational age into contributions due to changing risk of death among fetuses, newborns, and post-neonates and the changing structure of the population along these dimensions. Percent relative change is given in parenthesis.

Week	25	→	33	→	39	→	45	→	72
Mortality by stratum in deaths per 100,000 person-weeks exposure									
Fetus	25.6	(-22.4)	19.9	(+144)	48.6	(+128)	111.1	.	.
Neonatal	16,774	(-95.7)	713	(-94.2)	41.2	(+53.5)	63.2	.	.
Postneonatal	6,392	(-97.1)	187	(-87.1)	24.1	(-59.3)	9.8	(-78.8)	2.1
Relative exposure by stratum									
Fetus	.998	(-2.6)	.973	(-51.7)	.470	(-98.9)	.005	(-100)	0
Neonatal	<.001	(+732)	.008	(+2901)	23.2	(-97.6)	.006	(-100)	0
Postneonatal	<.001	(+5,130)	.019	(+1443)	.298	(+232)	.989	(+1.1)	1
Combined feto-infant mortality									
	43.6	(-34.6)	28.5	(+38.9)	39.6	(-73.2)	10.6	(-80.4)	2.1
Absolute change in feto-infant mortality due to differences in									
Composition	+121.2		+96.7		-37.2		-0.39		
Rates	-136.3		-85.6		+8.2		-8.2		
Total Δ	-15.1		+11.1		-28.9		-8.6		

Figure 2: Rates of fetal death, neonatal death, and post-neonatal death over weeks of gestational age as calculated for the cohort of U.S. fetuses conceived in 2009. The shaded background shows the distribution of survivors among the three states.



3.2 Stratum-specific feto-infant mortality trajectories

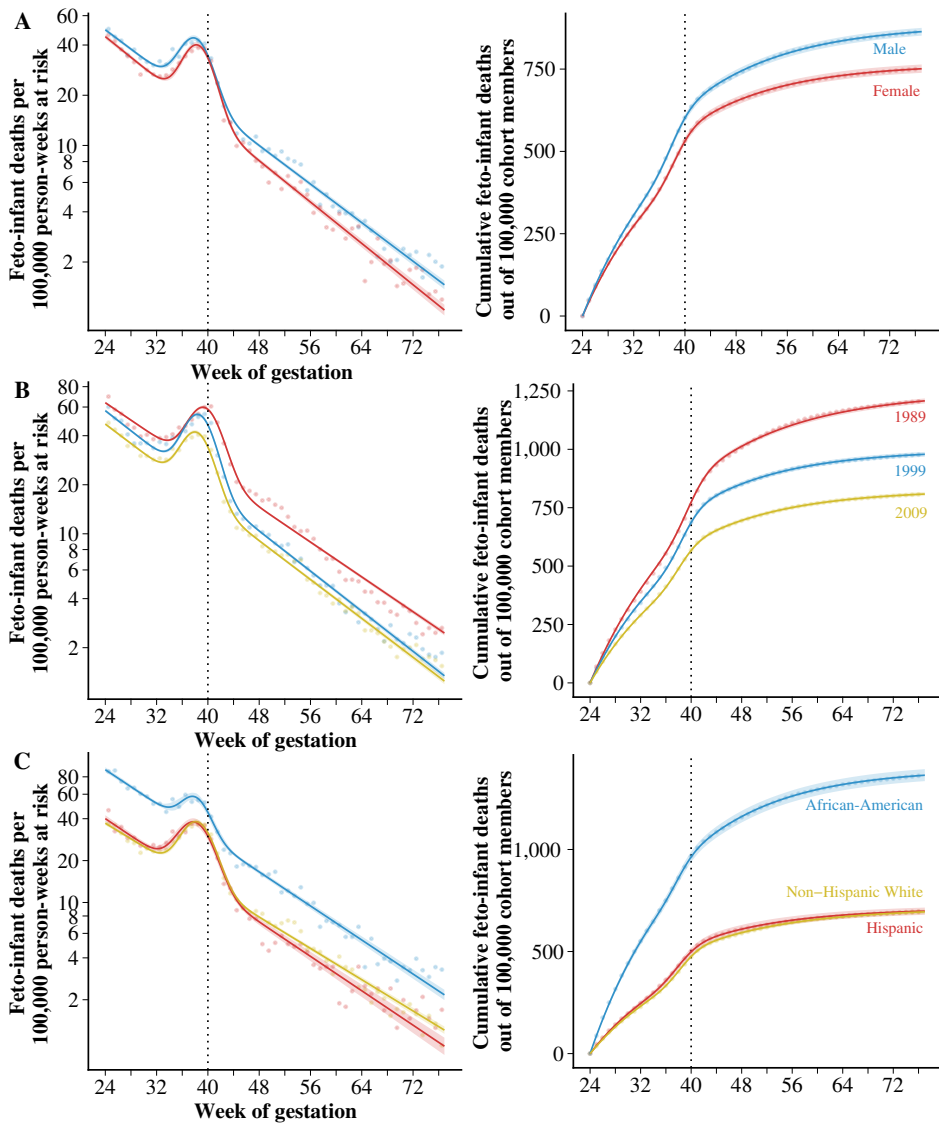
Males have a higher probability of death in the 52 weeks following fetal viability (Figure 3A). Out of 100,000 male fetuses of the 2009 U.S. conception cohort surviving until 24 weeks of gestation 851–878³ (one out of 114–116) will not survive the following year, compared to 739–763, (one out of 131–135) female deaths over the same period. Thus, the male probability of feto-infant death is 12.6–17.8 percent higher than that of females. Most of this difference in survival is explained by a higher hazard level in males as measured by the a_1 parameter: Ignoring the slightly earlier peak of the birth hump in males, the male hazard of feto-infant death is consistently higher across the 52 weeks of post-viability gestational age. The hazard of feto-infant death declines with a rate of 6.5–6.8 percent per additional week of gestation for males and 7.0–7.3 percent for females. The higher rate of ontogenescence among females substantially contributes to the sex-difference in one-year post-viability survival, while different magnitude and spread of the “birth hump” exhibit only a marginal and non-significant contribution. For additional parameter estimates see Tables 3 and 6.

Feto-infant survival improves considerably in the U.S. from 1989 to 2009. Out of 100,000 fetuses conceived in 1989 and reaching the age of viability 1,196–1,219 (one in 82–84), do not survive the following 52 weeks. This number drops to 969–990 (one in 101–103) deaths for the 1999 cohort and further down to 800–818 (one out of 122–125) deaths for conceptions in 2009. The 17.8–20.1 percent improvement in feto-infant survival between 1989 and 1999 is mainly explained by an increase in the rate of ontogenescence from approximately 6.1–6.2 percent per additional week of gestation to 7.0–7.2 percent and by a drop in the level of feto-infant mortality from 63–65 to 56–58 deaths per 100,000 person-weeks of exposure at fetal-viability. While the location of the peak “birth-hump” shifts into earlier gestation by about a week, neither magnitude nor spread of the hump change substantially between cohorts 1989 and 1999. Hence, the contribution of the transitional component to the overall improvement in one-year post-viability survival is small.

A different picture emerges for the 16.1–18.6 percent improvement in feto-infant survival between conception cohorts 1999 and 2009, which is primarily driven by a decline in the level of feto-infant mortality from 56–58 to 46–48 deaths per 100,000 person-weeks of exposure at fetal-viability. A substantial reduction in the magnitude of the birth hump from a peak value of 32–35 deaths per 100,000 person-weeks of exposure to 23–25 further contributes to the survival improvements while the rate of ontogenescence remains nearly constant.

³ I report the 95 percent prediction interval around the estimates.

Figure 3: Age trajectories of feto-infant survival A) by sex for the U.S. conception cohort 2009, B) by U.S. conception cohort, C) by maternal origin for the U.S. conception cohort 2009. Fitted (lines) versus lifetable estimates (points).



There are considerable differences in feto-infant survival by ethnicity of the mother with the hazard of feto-infant death for the cohort of African-American origin consistently being greater than the hazards for the cohort of Hispanic or Non-Hispanic White origin (Figure 3C). In the U.S. conception cohort 2009, out of 100,000 fetuses of African-American origin at pregnancy week 24 an estimated 1,332–1,399 (one in 71–75) either die in-utero or as infants in the following year compared to 679–719 (one in 139–147), and 684–705 (one in 142–146) for fetuses of Hispanic and non-Hispanic white origin respectively. Virtually all of the differences in feto-infant survival between the African-American stratum and the White/Hispanic origin strata are due to differences in the hazard level. Notably, the share of deaths attributable to the birth-hump is substantially lower in the African-American stratum (7.5–11.0 percent) compared to the Hispanic (18.7–24.4 percent) and non-Hispanic White (19.1–21.7 percent) strata. For further details see Tables 5 and 8.

4. Discussion

With the advent of modern obstetric practice, the distinction between fetus and infant stage became malleable and a question of optimal choice: Should we deliver early? Should we perform surgery in-utero? Should we try to prolong the pregnancy? Better and more widely employed prenatal diagnostics made the uterus almost transparent⁴. The feto-infant distinction lost relevance as available knowledge about the degree of maturity, and the presence of congenital disorders informed the future survival prospects of the child, in-utero or not. Isaacson (1996), in a historical study of obstetric texts, identified the “creation of the fetus-infant” – a being separate from the pregnant woman and endowed with a history that begins before birth. The consideration of the feto-infant mortality trajectory over age of gestation naturally arises from the continued blurring of lines that divide the stages of existence. But what does the feto-infant as a concept contribute to the study of mortality? 1. a more realistic quantification of undesired pregnancy outcomes, 2. the phenomenon of a “birth hump,” and on a related note, 3. the possibility to model the risk associated with the transition of birth.

Quantifying undesired pregnancy outcomes: A sole focus on rates of infant mortality, fetal mortality or perinatal mortality hides the true incidence of adverse pregnancy outcomes, and the incompatible definition of these measures prohibits to form a simple sum which more truthfully reflects on the loss of life within a pregnancy cohort. By employing the methods of survival analysis, I have calculated that one out of 73 African-American women who conceived in 2009 and continued their pregnancy to the 24th week of gestation are expected to lose their child in the following year. Not only shows this number the continued racial disparity in the prospects of survival at the onset of life when compared to the population average of one in 124; would pregnancy come with the same warnings as prescription drugs, feto-infant death past the age of fetal viability would have to be labeled as a “common” side effect according to the standards put forth in CIOMS Working Groups III and V (1999).

⁴ In quite a real sense if one considers the images generated from a 3D ultrasound.

The phenomenon of the “birth hump”: Former bio-demographic analyses and descriptions of the age trajectories of combined feto-infant mortality suffered either from a lack of data, the authors being forced to rely instead on rough assumptions and combinations of observations from various populations (Williamson and Woods 2003; Woods 2009; Levitis 2011; Berrut et al. 2016). The detailed micro-data on fetal deaths, births, and infant deaths in the U.S. allowed me to calculate the mortality trajectory of various fetal cohorts as they transition into infancy. Interestingly, the asymmetric sigmoid-shape for the cumulative distribution of feto-infant deaths around term, proposed by Williamson and Woods (2003) on the grounds of theoretical considerations, is supported by the data presented here and it can be derived from the assumption of an exponentially declining hazard component added to a hazard component with a Gaussian shape. Under a simple competing risks model, less than 20 percent of feto-infant deaths during the one-year follow-up from the age of fetal viability are contributed by the “birth hump.” Notably, among the conception cohort of African-American maternal origin, this contribution is only 9 percent, while the general level of feto-infant mortality is much higher among this stratum compared to the population average. This suggests that the “hump” is an additive phenomenon, which in turn implies an increasing share of deaths during or shortly after labor on all fetal and infant death as feto-infant mortality continues to decline.

Risks associated with the transition of birth: A formidable challenge for future research is to connect the aggregate phenomenon of the “birth-hump” to the transitional shock experienced by an individual as it moves from the intrauterine environment into infancy. In perinatal epidemiology, the same estimation problem is motivated by the desire to maximize the survival chances of an unborn child. Should labor be induced at a given age of gestation, or is it better to wait until labor sets in naturally? At heart lies the question of the risk of death prior to and after delivery, but such a change in risk can only ever be estimated indirectly as no one born alive ever died in utero. Current approaches to calculating the “risk of birth” thus are based on the strong assumption that children born in a given week of gestation t experienced the same risk of fetal death as the complete cohort of unborn children until t . But given that some fetal conditions are associated with a higher risk of stillbirth, pre-term birth, and infant death, this assumption must be deemed very crude, and instead, one would expect prematurely born infants to have had a higher risk of fetal death compared to infants born on full-term. Including exactly those information on fetal condition into the model, which are strongly associated with the timing of birth as well as fetal and infant death, would alleviate this issue and allow for a more precise estimate of the change in mortality across the feto-infant transition conditional on the timing of birth. The methodological framework for such an analysis could be given by the multi-timescale and multi-state approach to survival analysis, as proposed by Iacobelli and Carstensen (2013).

A. Description of methods

Determining gestational age

For the purposes of this paper, a key field on the birth and death certificates is the estimated age of gestation upon delivery as a proxy for the length of a pregnancy. This measure is subject to certain biases, which are crucial to keeping in mind when interpreting the results. Gestational age is defined as the weeks since the first day of the last menstrual period of the mother (LMP) and commonly measured by subtracting the date at LMP as reported by the women from the date of (still-)birth. This method suffers from recall bias, which may lead to digit preference in the reported dates. An alternative is to derive the age of a pregnancy from ultrasound measurements of the unborn child. While the ultrasound method generally allows for a more precise estimate of the date of life-birth, it can be systematically biased in cases where the fetus is growth restricted. As abnormal fetal growth is a risk factor for fetal death, the gestational age at stillbirth may be severely biased under the ultrasound method. Additionally, the age of gestation at fetal death is positively biased by the time-lag between intrauterine death and the delivery of the dead fetus, which in-part explains the observation of fetal deaths at the implausible gestational ages of 46 and 47 weeks. In analyzing the age pattern of feto-infant mortality, I will utilize the gestational ages at delivery as they are reported on the birth and fetal death certificates and point out the role of the aforementioned biases whenever they are relevant for the interpretation of the results.

Delineating conception cohorts

When considering the survival of fetuses into infancy, a straightforward definition of a cohort is all subjects who have been conceived during the same time period, i.e., a “conception cohort.” To determine the year of conception y for every single subject in the data I subtract the estimated weeks of gestation at delivery from the date at delivery and add two weeks to account for the average delay between the date of the last menstrual period of the mother (the time origin of the gestational age) and the date of fertilization. In this paper, I compare conception cohorts 1989, 1999, 2009.

Assembling the multi-state feto-infant life table

After delineating the conception cohorts y and determining N_{24}^F , the number of fetuses at risk at the start of observation, I calculate a multi-state feto-infant life table across the five states of fetus F , neonate N , post-neonate P , dead D and censored C . This requires the aggregation of transition counts T among states over age. For each single week of gestation let $T_t^{F \rightarrow D}$ denote the number of fetal deaths, $T_t^{F \rightarrow N}$ the number of births, $T_t^{N \rightarrow D}$ the number of neonatal deaths, $T_t^{N \rightarrow P}$ the number of recent survivors of the first week of life, $T_t^{P \rightarrow D}$ the number of post-neonatal deaths, and $T_t^{P \rightarrow C}$ the number of censorings

at week 77. The fetal, neonatal and post-neonatal population at risk at the beginning of gestational age t are then given by the recurrence equations

$$\begin{aligned} N_t^F &= N_{t-1}^F - T_{t-1}^{F \rightarrow D} - T_{t-1}^{F \rightarrow N}, \\ N_t^N &= N_{t-1}^N + T_{t-1}^{F \rightarrow N} - T_{t-1}^{N \rightarrow D} - T_{t-1}^{N \rightarrow P}, \\ N_t^P &= N_{t-1}^P + T_{t-1}^{N \rightarrow P} - T_{t-1}^{P \rightarrow D} - T_{t-1}^{P \rightarrow C}. \end{aligned}$$

To calculate the population exposures, I assume a uniform distribution of births and fetal deaths within each week of gestation where E_t^F is the total time spent in the fetal state over week of gestation t by the conception cohort under observation. The exposure times for the neonate and post-neonate state, E_t^N and E_t^P , are additionally informed by the chronological age of the infant at the time of transition measured in days.

Writing $S = \{F, N, P\}$ for the set of fetal, neonatal and post-neonatal states with $s \in S$ I calculate, for every week t , state-specific mortality rates $m_t^{s \rightarrow D} = \frac{T_t^{s \rightarrow D}}{E_t^s}$, total exposure times $E_t = \sum_S E_t^s$, state-specific relative exposures $p_t^s = \frac{E_t^s}{E_t}$, the combined feto-infant mortality rate $\bar{m}_t = \sum_s m_t^{s \rightarrow D}$. The empirical distribution of life-births given by $\pi_t^{F \rightarrow N} = \frac{T_t^{F \rightarrow N}}{\sum_t T_t^{F \rightarrow N}}$.

Expressing the combined feto-infant mortality rate at week of gestation t as a weighted average of fetal-, neonatal-, and post-neonatal mortality rates, $m_t = \sum_S p_t^s m_t^{s \rightarrow D}$ allows to explain the birth hump in terms of the shifting population proportions and mortality rates among the three groups over time. An application of the Kitagawa decomposition [Kitagawa 1955] to the difference in feto-infant mortality between weeks t_1 and t_2 yields

$$\Delta \bar{m}_{t_1, t_2} = \underbrace{\sum_S \frac{p_{t_1}^s + p_{t_2}^s}{2} \Delta m_{t_1, t_2}^s}_{\Delta r = \Delta r^F + \Delta r^N + \Delta r^P} + \underbrace{\sum_S \frac{m_{t_1}^s + m_{t_2}^s}{2} \Delta p_{t_1, t_2}^s}_{\Delta c = \Delta c^F + \Delta c^N + \Delta c^P}$$

The approach of further decomposing the rate component Δr and the compositional component Δc in their sub-population contributions Δr^F , Δr^N , Δr^P , and Δc^F , Δc^N , Δc^P has been proposed by (Chevan and Sutherland 2009).

A latent competing risks model of feto-infant mortality

In order to describe the shape and magnitude of the apparent “birth hump,” it is useful to separate the feto-infant hazard trajectory into two components: a monotonically declining “ontogenescent hazard” h^O and a hump-shaped “transitional hazard” h^T . Both sources of risk add up to

$$h(x) = h^O(x) + h^T(x), \quad (1)$$

the total hazard of feto-infant death at gestational age $t = x + 24$, where x measures the weeks since fetal viability. The primary purpose of model (1) is to facilitate comparisons

between populations by providing a parsimonious and informative parametrization of the feto-infant mortality trajectory, and to that end, I choose simple parametric expressions for both components. A negative-Gompertz hazard,

$$h^O(x) = a_1 \exp(-bx),$$

captures the overall trend of log-linearly declining feto-infant mortality over weeks of gestation with a_1 being the level of the ontogenetic hazard at fetal viability, and b the rate of ontogenescence, that is the relative rate of feto-infant mortality decline over the 52 weeks post-viability when any excess mortality contributed by the birth hump has been separated out.

The transitional hazard component reflecting the “birth hump” is specified to follow the kernel of a normal distribution resulting in the “Gaussian” hazard

$$h^T(t) = a_2 \exp\left(-\frac{(t - c)^2}{2\sigma^2}\right),$$

scaled by a_2 , which measures the mortality level at the mode of the hump at age $x = c$. The width of the hump is controlled via parameter σ with larger values resulting in flatter peaks.

The above decomposition of the overall hazard of feto-infant death into two components follows a long tradition of “competing risks” modeling of population mortality (Makeham1867, Siler1979, Heligman1980, Remund2018) where the overall risk of death is the sum of cause-specific hazards, each following a different age-trajectory. This begs the question about the nature of the risks competing with each other. The defining feature of the ontogenetic component is the continuous decline in hazard. Potential prenatal drivers of this decline are conditions that tend to lead to early fetal death such as severe congenital anomalies, e.g., anencephaly, or complications of fetal health that are all the more lethal, the earlier in pregnancy they occur, such as in-utero infection, placental dysfunction or abruption, abnormalities of the umbilical cord or rupture of the uterus. Correlated with these conditions is the risk of pre-term delivery, either induced in an attempt to save the fetus, or spontaneous. In either case, the survival chances of the pre-term child improve dramatically with the age of gestation. The post-term decline in the hazard of death may result from the continuing maturity of the cohort of infants and their increasing ability to resist the challenges posed by infection and accidents as well as the successful management of congenital malformations and chronic health conditions. Hazards due to complications of labor in late pre-term or term infants are captured by the transitional component and may be strictly birth-related such as intrapartum asphyxia or birth trauma or the consequence of severe fetal malformations that do not allow for survival outside of the uterus.

The feto-infant mortality trajectory informs about the development of a cohort's mortality risk, as its member's transition into life. Complementary to this risk perspective is the incidence of feto-infant death as measured by the probability of fetal- or infant death within x weeks following fetal-viability. The cumulative incidence of feto-infant death can be derived from the two hazard components via the well-known relationship

$$F(x) = 1 - \exp\left(-\int_0^x h(s) ds\right) = 1 - \exp\left(-\int_0^x h^O(s) + h^T(s) ds\right).$$

Level, ontogenescent and transition components of mortality differentials

Evaluating $F(x)$ at $x = 52$ gives the probability of fetal or infant death within one year of reaching the age of fetal viability, and thus $F(52)$ is a summary measure of adverse pregnancy outcomes combining fetal and infant deaths. The difference in $F(52)$ between two populations may be decomposed into three effects: 1) differences due to different levels of feto-infant mortality as measured by parameter a_1 , 2) ontogenescent differences due to different rates of mortality decline over age of gestation as measured by parameter b , and 3) transitional differences due to the different magnitude, location and shape of the birth hump as measured by parameters a_2 , c and σ . Given parameter vector $\theta = (a_1, b, a_2, c, \sigma)$, for populations A and B , I perform a Horiuchi decomposition (Horiuchi et al. 2008) to explain how the between-population difference in each parameter contributes to the overall difference $F(52, \theta_A) - F(52, \theta_B)$. The level and ontogenescent contributions to the difference in one-year survival are given by the a_1 and b parameter contributions respectively whereas the a_2 , c , and σ contributions sum up to the transitional contribution, e.g., the difference in one-year survival due to difference in the magnitude, location, and shape of the birth hump.

Competing risks inference

How many members of a cohort fail to overcome the “birth hump” on their way to infancy? Following the calculus of competing-risks, one can derive the share of infant deaths contributed by the transitional hazard. The cumulative probability of feto-infant death due to causes associated with the transitional component is $F^T(x) = \int_0^x S(s)h^T(s) ds$ which can be evaluated using numerical integration techniques. The share of deaths attributable to the transitional hazard up until post-viability age x then is $\rho(x) = F^T(x)/F(x)$.

Censored likelihood

I fit model (1) via maximum likelihood with the likelihood function constructed from the probability of observing D_j fetal or infant deaths in age group j given model parameters $\theta = (a_1, b, a_2, c, \sigma)$, written as $D_j[S(x_j|\theta) - S(x_{j+1}|\theta)]$, and the probability of observing C_j censored survivors at the end of age group j , $C_jS(x_j + 1|\theta)$, hence reflecting the fact

that observations are both interval-censored, as the timing of combined fetal and infant deaths is only known to lie within some week of gestation, and right-censored, because observation stops one year after fetal-viability when most members of a cohort are still alive. Taking the product over all age groups $j = 1 : J$ yields the likelihood function

$$L(\boldsymbol{\theta}|D_j, C_j) = \prod_j [S(x_j|\boldsymbol{\theta}) - S(x_{j+1}|\boldsymbol{\theta})]^{D_j} S(x_{j+1}|\boldsymbol{\theta})^{C_j},$$

with corresponding log-likelihood

$$\log L(\boldsymbol{\theta}|D_j, C_j) = \sum_j D_j \log [S(x_j|\boldsymbol{\theta}) - S(x_{j+1}|\boldsymbol{\theta})] + C_j \log S(x_{j+1}|\boldsymbol{\theta}).$$

B. The nosplit algorithm for memory-efficient aggregation of event history data

The state-of-the-art for aggregation of multi-state life history data into age-period and cohort intervals is the “split-aggregate” method, whereby first, the individual level data-set is expanded into a single row per individual per time interval visited. In a second step, transition counts and state occupancy times per time interval are calculated from this expanded data set. The split step expands an already large data set even further and thus can be extremely costly in memory usage and processor time.

I present an episode-split free method to aggregate multi-state life-history data into time intervals. The “nosplit-aggregate” method first produces three summary tables from the unaltered individual-level data set and then derives the interval and state-specific risk sets, exposure times, and transition counts via elementary calculations on the aggregated tables.

The code listing below gives an implementation of nosplit in the R language (R Core Team 2020).

```

1  # Aggregate Transitions Counts and Occupancy Times
2  #
3  # Episode-split-free Risk-set and Exposure Time Calculation
4  # from Event History Data
5  #
6  # @param df
7  #   A data frame.
8  # @param t_in
9  #   Entry time into state.
10 # @param d_in
11 #   State being entered.
12 # @param t_out
13 #   Exit time from state.
14 # @param d_out
15 #   State being exited into.
16 # @param breaks
17 #   A numeric vector of break points for time-scale.
18 # @param wide
19 #   Output table in wide format (default=TRUE)?
20 # @param closed_left
21 #   Time intervals closed to the left and open to the right (default=TRUE)?
22 # @param disable_input_checks
23 #   Should input checks be disabled (default=FALSE)?
24 #
25 # @return
26 #   A data frame with columns
27 #     orig: origin state
28 #     j:    age group index
29 #     x:    starting age of j
30 #     n:    width of j
31 #     Z:    number of entries into origin state during j
32 #     W:    number of exits from origin state during j
33 #     P:    population number in origin state at beginning of j
34 #     O:    total observation time of population visiting origin state in j
35 #   (if wide = FALSE)

```

```

36  #      dest: destination state
37  #      W_k: number of exits from origin state to destination state during j
38  #      (if wide = TRUE)
39  #      to_`: number of exits from origin state to state ` during j
40 AggregateStateTransitions <- function (
41   df,
42   t_in, d_in, t_out, d_out,
43   breaks,
44   wide = TRUE, drop0exp = TRUE,
45   closed_left = TRUE,
46   disable_input_checks = FALSE
47 ) {
48
49   require(tidyverse)
50
51   t_in = enquo(t_in); d_in = enquo(d_in);
52   t_out= enquo(t_out); d_out = enquo(d_out)
53
54   # input checks
55
56   if (identical(disable_input_checks, FALSE)) {
57     # check if all transition times are contained in
58     # range of breaks
59     t_range = c(min(pull(df, !!t_in)), max(pull(df, !!t_out)))
60     breaks_range = range(breaks)
61     if (identical(closed_left, TRUE) ) {
62       if (any(
63         t_range[1] < breaks_range[1] |
64         t_range[2] >= breaks_range[2]
65       )) {
66         stop(paste0(
67           'Transition time outside range of breaks. Ensure that all t_ >=',
68           breaks_range[1], ' and <', breaks_range[2]
69         ))
70       }
71     }
72     if (identical(closed_left, FALSE) ) {
73       if (any(
74         t_range[1] <= breaks_range[1] |
75         t_range[2] > breaks_range[2]
76       )) {
77         stop(paste0(
78           'Transition time outside range of breaks. Ensure that all t_ >',
79           breaks_range[1], ' and <=', breaks_range[2]
80         ))
81       }
82     }
83   }
84
85   # total number of age intervals
86   J_ = length(breaks)-1
87   # index of age intervals
88   j_ = 1:J_
89   # width of age intervals
90   n_j_ = diff(breaks)
91   # unique origin states

```

```

92   k_in_ = unique(pull(df, !d_in))
93   # unique destination states
94   k_out_ = unique(pull(df, !d_out))

95
96   # find the index of an interval defined by
97   # <breaks> each element in <x> is contained in
98   # returns NA if x outside breaks
99   FindIntervalJ <-
100   function(x, breaks, cl = closed_left) {
101     if (identical(cl, TRUE)) {
102       # [a, b)
103       right = FALSE; lowest = FALSE
104     } else {
105       # (a, b] with [a0, b0]
106       right = TRUE; lowest = TRUE
107     }
108     .bincode(
109       x = x, breaks = breaks,
110       right = right, include.lowest = lowest
111     )
112   }

113
114   # 1. Aggregation
115
116   # tabulate exits by age, origin and destination state
117   W_k_tab <-
118   df %>%
119   select(t_out = !!t_out, d_in = !!d_in, d_out = !!d_out) %>%
120   mutate(
121     # add age interval index to each exit
122     j = FindIntervalJ(pull(., t_out), breaks, closed_left),
123   ) %>%
124   # for each observed combination of
125   # age and
126   # origin state and
127   # destination state...
128   group_by(d_in, d_out, j) %>%
129   summarise(
130     # ...total number of exits
131     W_k = n(),
132     # total time lost in age due to exit
133     Lw_k = sum(breaks[j+1]-t_out)
134   ) %>%
135   ungroup()

136
137   # tabulate exits by age and origin state
138   # based on prior tabulation on destination specific exits
139   W_tab <-
140   W_k_tab %>%
141   # for each observed combination of
142   # age and
143   # origin state...
144   group_by(j, d_in) %>%
145   summarise(
146     # ...total exits
147     W = sum(W_k),

```

```

148  # ...total time lost in interval due to exit
149  Lw = sum(Lw_k)
150  ) %>%
151  ungroup() %>%
152  # add rows for missing combinations
153  # of age interval and origin state
154  complete(
155    d_in = k_in_, j = j_,
156    fill = list(W = 0, Lw = 0)
157  )
158
159  # tabulate entries by age and state entered into
160  Z_tab <-
161  df %>%
162  select(d_in = !!d_in, t_in = !!t_in) %>%
163  mutate(
164    j = FindIntervalJ(pull(., t_in), breaks, closed_left),
165  ) %>%
166  group_by(j, d_in) %>%
167  summarise(
168    # ...total entries
169    Z = n(),
170    # ...total entries right at start of interval
171    Z0 = sum(t_in==breaks[j]),
172    # ...total time lost in interval due to late-entry
173    Lz = sum(t_in-breaks[j])
174  ) %>%
175  ungroup() %>%
176  complete(
177    d_in = k_in_, j = j_,
178    fill = list(Z = 0, Z0 = 0, Lz = 0)
179  )
180
181  # tabulate concurrent entries and exits by interval
182  ZW_tab <-
183  df %>%
184  select(t_in = !!t_in, t_out = !!t_out, d_in = !!d_in) %>%
185  # aggregate individual level entry
186  # and exit times into predefined age groups
187  mutate(
188    # add interval index to each entry
189    j = FindIntervalJ(pull(., t_in), breaks, closed_left),
190    # are entries and exits in same interval?
191    zw = j == FindIntervalJ(pull(., t_out), breaks)
192  ) %>%
193  # for each combination of
194  # state and
195  # interval
196  group_by(d_in, j) %>%
197  summarise(
198    # ...total concurrent entries and exits
199    # there may be NAs in logic vector <zw> when
200    # and entry or exit falls outside the range
201    # of all intervals. as those cases don't have to
202    # be counted na.rm=TRUE is applied
203    ZW = sum(zw, na.rm = TRUE)

```

```

204 ) %>%
205 ungroup() %>%
206 complete(
207   d_in = k_in_, j = j_,
208   fill = list(ZW = 0)
209 )
210
211 # 2. Determine risk-sets and exposure times
212
213 # exit counts for all possible combinations
214 # of origin state, destination state and
215 # age interval
216 # intrastate transitions are 0 now
217 # but are added later
218 W_k_tab_complete <-
219   W_k_tab %>%
220   select(-Lw_k) %>%
221   complete(
222     d_in = k_in_, d_out = k_out_, j = j_,
223     fill = list(W_k = 0)
224 )
225
226 # occurrence-exposure table
227 oe_tab <-
228   bind_cols(W_tab, Z_tab[,-(1:2)], ZW_tab[,-(1:2)]) %>%
229   mutate(
230     x = breaks[j],
231     n = n_j_[j]
232   ) %>%
233   # for each entry state...
234   group_by(d_in) %>%
235   mutate(
236     # number of observations entering j via j-1
237     # R_(j+1) = R_j + Z_j - W_j
238     R = c(0, head(cumsum(Z) - cumsum(W), -1)),
239     # population at risk at x_j
240     P = R + Z0,
241     # number of observations in j that did neither start
242     # nor end during j
243     Q = R - W + ZW,
244     # number of observations entering j
245     # that do not end during j
246     U = Z - ZW,
247     # total observation time during j
248     O = Q*n + (Z + W - ZW)*n - Lz - Lw,
249     # number of intrastate transitions
250     I = Q + U,
251   ) %>%
252   ungroup() %>%
253   left_join(W_k_tab_complete, by = c('d_in', 'j')) %>%
254   # intrastate transitions
255   mutate(
256     W_k = ifelse(d_in == d_out, I, W_k)
257   ) %>%
258   select(orig = d_in, dest = d_out, j, x, n, Z, W, P, O, W_k)
259

```

```
260 # drop intervals with 0 exposure
261 if (identical(drop0exp, TRUE)) {
262   oe_tab <-
263   oe_tab %>%
264   filter(0 > 0)
265 }
266
267 # convert to wide format
268 if (identical(wide, TRUE)) {
269   oe_tab <-
270   oe_tab %>%
271   mutate(dest = paste0('to_', dest)) %>%
272   spread(key = dest, value = W_k)
273 }
274
275 return(oe_tab)
276
277 }
```

C. Tables of parameter estimates

Table 3: Table of estimated parameters of feto-infant hazard trajectory over gestational age by sex.

	Male	Female
a_1	4.9e-4 (4.8e-4, 5.1e-4)	4.5e-4 (4.3e-4, 4.6e-4)
b	6.7e-2 (6.5e-2, 6.8e-2)	7.1e-2 (7.0e-2, 7.3e-2)
a_2	2.5e-4 (2.3e-4, 2.6e-4)	2.4e-4 (2.2e-4, 2.6e-4)
c	1.4e+1 (1.4e+1, 1.4e+1)	1.4e+1 (1.4e+1, 1.5e+1)
σ	2.4e+0 (2.2e+0, 2.6e+0)	2.3e+0 (2.2e+0, 2.5e+0)
$F(52) \times 10e5$	864 (851, 878)	751 (739, 763)
$F(52)^{-1}$	116 (114, 118)	133 (131, 135)
$\rho(52)\%$	17.0 (15.9, 18.2)	18.4 (16.9, 19.7)

Table 4: Table of estimated parameters of feto-infant hazard trajectory over gestational age by conception cohort.

	1989	1999	2009
a_1	6.4e-4 (6.3e-4, 6.5e-4)	5.7e-4 (5.6e-4, 5.8e-4)	<!- 4.7e-4 (4.6e-4, 4.8e-4)
$\rightarrow b$	6.2e-2 (6.1e-2, 6.2e-2)	7.1e-2 (7.0e-2, 7.2e-2)	6.9e-2 (6.8e-2, 7.0e-2)
a_2	3.5e-4 (3.4e-4, 3.6e-4)	3.4e-4 (3.2e-4, 3.5e-4)	2.4e-4 (2.3e-4, 2.5e-4)
c	1.5e+1 (1.5e+1, 1.6e+1)	1.5e+1 (1.4e+1, 1.5e+1)	1.4e+1 (1.4e+1, 1.4e+1)
σ	2.5e+0 (2.4e+0, 2.6e+0)	2.3e+0 (2.3e+0, 2.4e+0)	2.4e+0 (2.2e+0, 2.5e+0)
$F(52) \times 10e5$	1,207 (1,196, 1,219)	979 (969, 990)	809 (800, 818)
$F(52)^{-1}$	82.8 (82.1, 83.6)	102 (101, 103)	124 (122, 125)
$\rho(52)\%$	18.0 (17.3, 18.7)	20.1 (19.2, 21.0)	17.6 (16.7, 18.5)

Table 5: Table of estimated parameters of feto-infant hazard trajectory over gestational age by maternal origin.

	African-American	Hispanic	Non-Hispanic White
a_1	9.0e-4 (8.7e-4, 9.4e-4)	4.0e-4 (3.8e-4, 4.2e-4)	3.7e-4 (3.6e-4, 3.8e-4)
b	7.0e-2 (6.8e-2, 7.3e-2)	7.1e-2 (6.8e-2, 7.4e-2)	6.5e-2 (6.3e-2, 6.6e-2)
a_2	2.4e-4 (2.1e-4, 2.8e-4)	2.3e-4 (2.0e-4, 2.6e-4)	2.3e-4 (2.2e-4, 2.5e-4)
c	1.4e+1 (1.4e+1, 1.4e+1)	1.4e+1 (1.4e+1, 1.4e+1)	1.4e+1 (1.4e+1, 1.5e+1)
σ	2.1e+0 (1.7e+0, 2.5e+0)	2.6e+0 (2.4e+0, 2.9e+0)	2.4e+0 (2.3e+0, 2.6e+0)
$F(52) \times 10e5$	1,364 (1,332, 1,399)	698 (679, 719)	695 (684, 705)
$F(52)^{-1}$	73.3 (71.5, 75.1)	143 (139, 147)	144 (142, 146)
$\rho(52)\%$	9.2 (7.5, 11.0)	21.5 (18.7, 24.4)	20.4 (19.1, 21.7)

Table 6: Shape decomposition of differences in $F(52)$ between the sexes.

	Male - Female
$\Delta F(52) \times 10e5$	113 [95.3, 131]
Level contribution	62.1 [33.9, 89.2]
Ontogenescent contribution	41.4 [20.9, 61.2]
Birth hump contribution	9.23 [-5.67, 23.7]
$\Delta F(52)\%$	15.0 [12.6, 17.8]

Table 7: Shape decomposition of differences in $F(52)$ between the conception cohorts.

	1989 - 1999	1999 - 2009
$\Delta F(52) \times 10e5$	-228 [-244, -213]	-170 [-183, -156]
Level contribution	-97 [-121, -74.2]	-136 [-156, -116]
Ontogenescent contribution	-109 [-126, -92]	20.1 [6.0, 34.2]
Birth hump contribution	-21 [-33.8, -9.2]	-54.0 [-65.1, -42.8]
$\Delta F(52)\%$	-18.9 [-20.1, -17.8]	-17.4 [-18.6, -16.1]

Table 8: Shape decomposition of differences in $F(52)$ between maternal ethnicities.

	African-American White	- Hispanic - White	Hispanic - African-American
$\Delta F(52) \times 10e5$	668 (637, 701)	3.3 (-18.6, 25.4)	-665 (-701, -630)
Level contribution	747 (704, 797)	41.7 (10.3, 75.8)	-680 (-738, -623)
Ontogenescent contribution	-63.5 (-92.9, -35.0)	-46.9 (-72.3, -20.5)	-8.8 (-50.6, 32.7)
Birth hump contribution	-15.2 (-40.5, 11.9)	8.5 (-12.7, 32.8)	23.7 (-8.2, 56.7)
$\Delta F(52)\%$	96.4 (91.2, 102)	0.04 (-2.7, 3.7)	-48.8 (-50.7, -47.0)

References

- L. S. Bakketeg, D. G. Seigel, and P. M. Sternthal. A fetal-infant life table based on single births in Norway, 1967–1973. *American Journal of Epidemiology*, 107(3):216–225, 1978. doi:10.1093/oxfordjournals.aje.a112528.
- E. Barbi, F. Lagona, M. Marsili, J. W. Vaupel, and K. W. Wachter. The plateau of human mortality: Demography of longevity pioneers. *Science*, 360(6396):1459–1461, 2018. doi:10.1126/science.aat3119.
- S. Berrut, V. Pouillard, P. Richmond, and B. M. Roehner. Deciphering infant mortality. *Physica A: Statistical Mechanics and its Applications*, 463:400–426, 2016. doi:10.1016/j.physa.2016.07.031.
- J. Bourgeois-Pichat. La mesure de la mortalité infantile. II. les causes de décès. *Population*, 6(3):459–480, 1951. doi:10.2307/1523958.
- E. Carlson, J. M. Hoem, and J. Rychtarikova. Trajectories of fetal loss in the czech republic. *Demography*, 36(3):327–37, 1999. doi:10.2307/2648056.
- A. Chevan and M. Sutherland. Revisiting Das Gupta: Refinement and extension of standardization and decomposition. *Demography*, 46(3):429–449, 2009. doi:10.1353/dem.0.0060.
- CIOMS Working Groups III and V. Guidelines for preparing core clinical-safety information on drugs. Technical report, Geneva, 1999.
- M. Ebeling. How has the lower boundary of human mortality evolved, and has it already stopped decreasing? *Demography*, 55(5):1887–1903, 2018. doi:10.1007/s13524-018-0698-z.
- G. B. Feldman. Prospective risk of stillbirth. *Obstetrics and Gynecology*, 79(4):547–553, 1992.
- F. E. French and J. M. Bierman. Probabilities of fetal mortality. *Public Health Reports*, 77(10):835–47, 1962. doi:10.2307/4591645.
- C. Galley and R. Woods. On the distribution of deaths during the first year of life. *Population*, 11(1):35–60, 1999.
- J. Gampe. Human mortality beyond age 110. In H. Maier, J. Gampe, B. Jeune, J.-M. Robine, and J. W. Vaupel, editors, *Supercentenarians*, Demographic Research Monographs, pages 219–230. Springer, Berlin, 2010. ISBN 978-3-642-11519-6. doi:10.1007/978-3-642-11520-2_13.
- M. K. Goldhaber and B. H. Fireman. The fetal life table revisited: Spontaneous abortion rates in three kaiser permanente cohorts. *Epidemiology*, 2(1):33–39, 1991. doi:10.1097/00001648-199101000-00006.
- J. R. Goldstein. A secular trend toward earlier male sexual maturity: evidence from shifting ages of male young adult mortality. *PloS one*, 6(8):e14826, 2011. doi:10.1371/journal.pone.0014826.

- B. Gompertz. On the nature of the function expressive of the law of human mortality, and on a new mode of determining the value of life contingencies. *Philosophical Transactions of the Royal Society of London*, 115:513–583, Dec. 1825. doi:10.1098/rstl.1825.0026.
- A. E. Greb, R. M. Pauli, and R. S. Kirby. Accuracy of fetal death reports: comparison with data from an independent stillbirth assessment program. *American Journal of Public Health*, 77(9):1202–1206, 1987. doi:10.2105/ajph.77.9.1202.
- S. Horiuchi and J. R. Wilmoth. Deceleration in the age pattern of mortality at older ages. *Demography*, 35:391, 1998. ISSN 0070-3370. doi:10.2307/3004009.
- S. Horiuchi, J. R. Wilmoth, and S. D. Pletcher. A decomposition method based on a model of continuous change. *Demography*, 45(4):785–801, 2008. doi:10.1353/dem.0.0033.
- S. Iacobelli and B. Carstensen. Multiple time scales in multi-state models. *Statistics in Medicine*, 32(30):5315–5327, 2013. doi:10.1002/sim.5976.
- N. Isaacson. The "fetus-infant": Changing classifications of in utero development in medical texts. *Sociological Forum*, 11(3):457–480, 1996. doi:10.1007/bf02408388.
- K. Joseph. Incidence-based measures of birth, growth restriction, and death can free perinatal epidemiology from erroneous concepts of risk. *Journal of Clinical Epidemiology*, 57(9):889–897, 2004. doi:10.1016/j.jclinepi.2003.11.018.
- K. S. Joseph. Theory of obstetrics: An epidemiologic framework for justifying medically indicated early delivery. *BMC Pregnancy and Childbirth*, 7(1), 2007. doi:10.1186/1471-2393-7-4.
- E. M. Kitagawa. Components of a difference between two rates. *Journal of the American Statistical Association*, 50(272):1168–1194, 1955. doi:10.1080/01621459.1955.10501299.
- F. B. Kristensen and F. Mac. Life table analysis of infant mortality and feto-infant mortality distributed on causes of death in Denmark 1983–1987. *International Journal of Epidemiology*, 21(2):320–3, 1992. doi:10.1093/ije/21.2.320.
- D. A. Levitis. Before senescence: the evolutionary demography of ontogenesis. *Proceedings of the Royal Society B*, 278(1707):801–809, 2011. doi:10.1098/rspb.2010.2190.
- J. A. Martin and D. L. Hoyert. The national fetal death file. *Seminars in Perinatology*, 26 (1):3–11, 2002. doi:10.1053/sper.2002.29834.
- National Center for Health Statistics. Birth cohort linked birth-infant death data files (U.S. data), 2016a. URL ftp://ftp.cdc.gov/pub/Health_Statistics/NCHS/Datasets/DVS/cohortlinkedus/.
- National Center for Health Statistics. Fetal death data files (U.S. data), 2016b. URL ftp://ftp.cdc.gov/pub/Health_Statistics/NCHS/Datasets/DVS/fetaldeathus/.
- W. Perks. On some experiments in the graduation of mortality statistics. *Journal of the Institute of Actuaries*, 63(1):12–57, 1932.

- R. W. Platt, K. S. Joseph, C. V. Ananth, J. Grondines, M. Abrahamowicz, and M. S. Kramer. A proportional hazards model with time-dependent covariates and time-varying effects for analysis of fetal and infant death. *American Journal of Epidemiology*, 160(3):199–206, 2004. doi:10.1093/aje/kwh201.
- R Core Team. *R: A Language and Environment for Statistical Computing*. R Foundation for Statistical Computing, Vienna, Austria, 2020. URL <https://www.R-project.org/>.
- A. Remund, C. G. Camarda, and T. Riffe. A cause-of-death decomposition of young adult excess mortality. *Demography*, 55(3):957–978, 2018. doi:10.1007/s13524-018-0680-9.
- I. Seri and J. Evans. Limits of viability: definition of the gray zone. *Journal of Perinatology*, 28:S4–S8, Apr. 2008. doi:10.1038/jp.2008.42.
- S. Shapiro, E. W. Jones, and P. M. Densen. A life table of pregnancy terminations and correlates of fetal loss. *The Milbank Memorial Fund Quarterly*, 40(1):7, 1962. doi:10.2307/3348609.
- G. C. S. Smith. Life-table analysis of the risk of perinatal death at term and post term in singleton pregnancies. *American Journal of Obstetrics and Gynecology*, 184(3):489–496, 2001. doi:10.1067/mob.2001.109735.
- G. C. S. Smith. Estimating risks of perinatal death. *American Journal of Obstetrics and Gynecology*, 192(1):17–22, 2005. doi:10.1016/j.ajog.2004.08.014.
- T. N. Thiele. On a mathematical formula to express the rate of mortality throughout the whole of life, tested by a series of observations made use of by the Danish Life Insurance Company of 1871. *Journal of the Institute of Actuaries*, 16(5):313–329, 1871. doi:10.1017/s2046167400043688.
- J. W. Vaupel. Trajectories of mortality at advanced ages. In K. W. Wachter and C. E. Finch, editors, *Between Zeus and the Salmon: The Biodemography of Longevity*, chapter 2, pages 17–37. National Academy Press, Washington D.C., 1997. ISBN 0-309-05787-6.
- P. Williamson and R. I. Woods. A note on the fetal-infant mortality problem. *Journal of Biosocial Science*, 35(2):201–212, 2003. doi:10.1017/S0021932003002013.
- R. Woods. *Death before Birth*. Oxford University Press, 2009. ISBN 978–0–19–954275–8. doi:10.1093/acprof:oso/9780199542758.001.0001.
- World Health Organization. *Neonatal and Perinatal Mortality: Country, Regional and Global Estimates*. World Health Organization, 2006. ISBN 9241563206.
- P. L. Yudkin, L. Wood, and C. W. G. Redman. Risk of unexplained stillbirth at different gestational ages. *The Lancet*, 329(8543):1192–1194, 1987. doi:10.1016/S0140-6736(87)92154-4.